Depositional environment and provenance of the Dina formation, Provost oil field, east central Alberta, and a discussion of hydrocarbon distribution within

Joseph Kidston

Submitted in partial fulfillment of the requirements
for the Degree of Bachelor of Science (Honours)
Department of Earth Sciences
Dalhousie University, Halifax, Nova Scotia

April 2003

Dalhousie University

Department of Earth Sciences
Halifax, Nova Scotia
Canada B3H 3J5
(902) 494-2358
FAX (902) 494-6889

DATE April 16, 2003

AUTHOR Joseph Kidston

TITLE Depositional environment and provenance of the Dina formation, Provost oil field, east central Alberta, and a discussion of hydrocarbon distribution within

Degree Honours BSc. Convocation May Year 2003

Permission is herewith granted to Dalhousie University to circulate and to have copied for non-commercial purposes, at its discretion, the above title upon the request of individuals or institutions.

[redacted]
Signature of Author

Depositional environment and provenance of the Dina formation, Provost oil field, east central Alberta, and a discussion of hydrocarbon distribution within

The Dina formation, late Barremian to late Aptian, is the basal unit of the Mannville Group in east-central Alberta, and the primary oil-producing unit of the Provost oil field. In Section 23, Township 36-6W4 (part of the Belshill Lake paleo-channel), well logs from two wells suggest the Dina formation is ~21 m thick. Physical and biogenic sedimentary structures preserved in cores from these two wells indicate the upper ~14 metres of the Dina formation were deposited in an estuarine environment, and lithofacies show an upwards increase in marine influence, grading upwards from marine-influenced channel deposits on the bottom (of the cored interval) to moderately burrowed tidal flat (and channel) deposits on top. Oil-stained sandstone beds in the two cores indicate oil-distribution in the Dina formation is lithofacies dependent, and concentrated within channel sands of the upper lithofacies. The presence of accessory zircon, muscovite, and feldspar grains suggest a Canadian Shield provenance for the Dina formation.

TABLE OF CONTENTS

TABLE OF FIGURES

TABLE OF TABLES

ACKNOWLEDGEMENTS

First and foremost, I would like to thank my wonderful parents, Arthur Glen and Lola-May Kidston, for their incredible support during my final year at Dalhousie University. They always expressed a keen interest in my work, and saved me dinner in the oven on countless long nights. In particular, I would like to dedicate this thesis to my father, who also studied Geology at Dalhousie University, and has since worked all over the world, being involved today with the exploration activity offshore Nova Scotia. *Gracias a mi madre*, who ultimately got me aboard my very first scientific cruise aboard the *C.C.G.S. Hudson*. To my beautiful sister, Daisy, thank you for blazing the trail here at Dalhousie with your Master's thesis, and for helping me celebrate in Québec City. To my best friend and always hilarious twin brother, Artie, thank you for the colourful 'origami countdown'!

I am extremely grateful to my thesis advisor, Dr. Grant Wach, who organised donation of the cores and well-logs from Calgary, and who took me on as an Honours student. Dr. Wach taught me a tremendous amount of information regarding trace fossils and core descriptions, and I am not only honoured to have worked with him, but also indebted to him for all the resources and opportunities with which he provided me. I would like to thank the Canadian Society of Petroleum Geologists (Calgary) for donating the cores, Petrel Robertson (Calgary) for donating the well logs, and Chevron-Texaco (Houston) for donating the X-ray diffraction equipment.

A long list of thank-you's to Dr. Yawooz Kettanah for his much-appreciated help with the transmitted and reflected light microscopy (and with the XRD equipment too!), Gordon Brown for the polished thin sections, Keith Taylor for teaching me how to use the X-ray diffraction machines (and for the hammer!), Dr. Reynolds and Charlie Walls for providing and calibrating the spectrometers and scintillometer, Dr. Becky Jamieson and Adam Layman for the thin section photos, Tom Duffett for his idea on how to draft my core description sheets, and Mike Rygel for the crash course on 'figure-drawing'.

A big hurrah to my fellow classmates, Matt Harrington, Camilla Melrose, Adam Layman, and Mark Barry, with whom I spent *many* a long night in the computer lab with typing and printing away. Matt, I'll see you out on the boat, and Adam, I will miss

singing the Beach Boys with you! Finally, a very special thank you to Ms. Melanie Purves, who taught me a lot about writing (have you seen the McConnell Thrust yet Melanie?), but most of all, helped inspire me to pursue an Honours degree.

CHAPTER 1 : INTRODUCTION

1.1 Objectives

The primary objective of this thesis is to determine depositional environment(s) of the Dina formation in east central Alberta. To accomplish this, cores from two wells are described and interpreted. This thesis also determines provenance of the Dina formation, and discusses the distribution of oil within.

1.2 Geologic setting

1.2.1 Western Canada Sedimentary Basin (WCSB)

Figure 1A shows the study area of this thesis, which lies within the Western Canada Sedimentary Basin (WCSB). The WCSB is a large sedimentary basin extending over all of Alberta and parts of Saskatchewan, Manitoba, and British Columbia. Mossop & Shetsen (1994) summarise the WCSB as a large wedge of undeformed Phanerozoic sedimentary rocks resting on top of Precambrian crystalline basement. To the west, the WCSB is bound by allochthonous terranes of the Cordillera, and to the east, by an erosional zero-edge along the Canadian Shield (Wright *et al.*, 1994; Price, 1994). The northern and southern boundaries of the WCSB are often defined by ~61°N (just north of the Alberta-NWT border) and 49°N (the Canada-USA border), but these boundaries are somewhat arbitrary, and do not define the true basin boundaries. As Leckie & Reinson (1993) explain, the WCSB is actually part of a much larger basin, the Western Interior Basin. The Western Interior Basin spans the continent of North America, from the Arctic coast in the north, to the Gulf of Mexico in the south (Leckie & Reinson, 1993).

1.2.2 East-central Alberta

As Figure 1A shows, the study area lies within the Provost oil field of east central Alberta. Figure 1B is a close-up map of the study area, and shows the location of Wells 3B- and 4A-23-36-6W4. These two wells are in adjacent Legal Subdivisions (3B and 4A) of Section 23, Township 36, and Range 6W4, and lie ~230 km southeast of the city of Edmonton, Alberta, and ~80 km west of the Alberta-Saskatchewan border. (Please refer to Appendix C for an explanation of the Dominion Land Survey numbering system used to locate the wells.) It is not established where exactly within Legal

A)

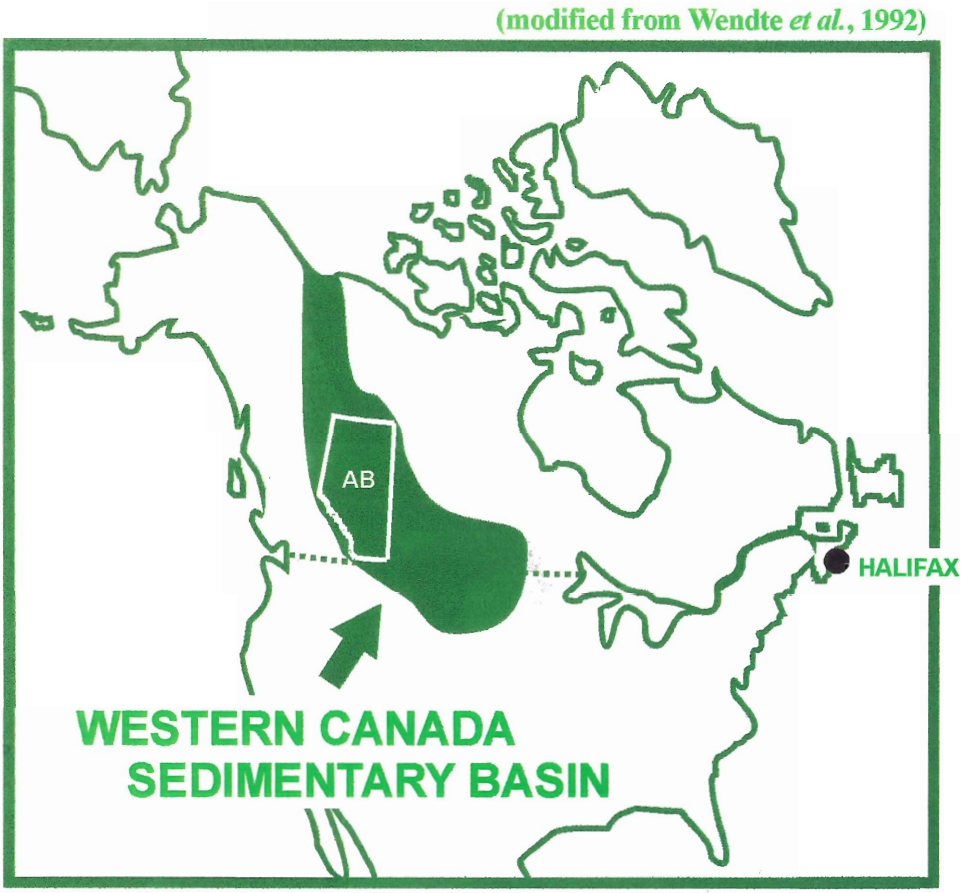

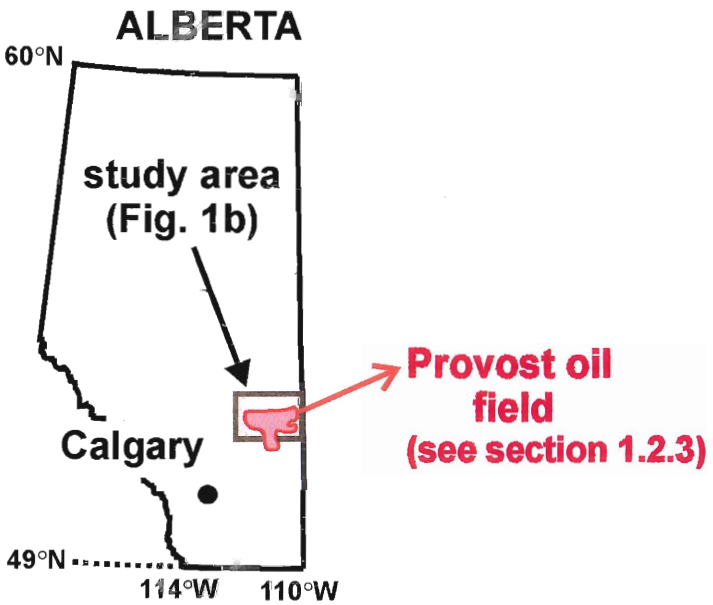

Figure 1 - Maps showing the study area of this thesis, and the locations of Wells 3B- and 4A-23-36-6W4. A) (*this page*) East central Alberta, the Provost oil field, and the Western Canada Sedimentary Basin. B) (*following page*) Map of the study area. The maximum distance separating Wells 3B- and 4A-23-36-6W4 is less than 500 m.

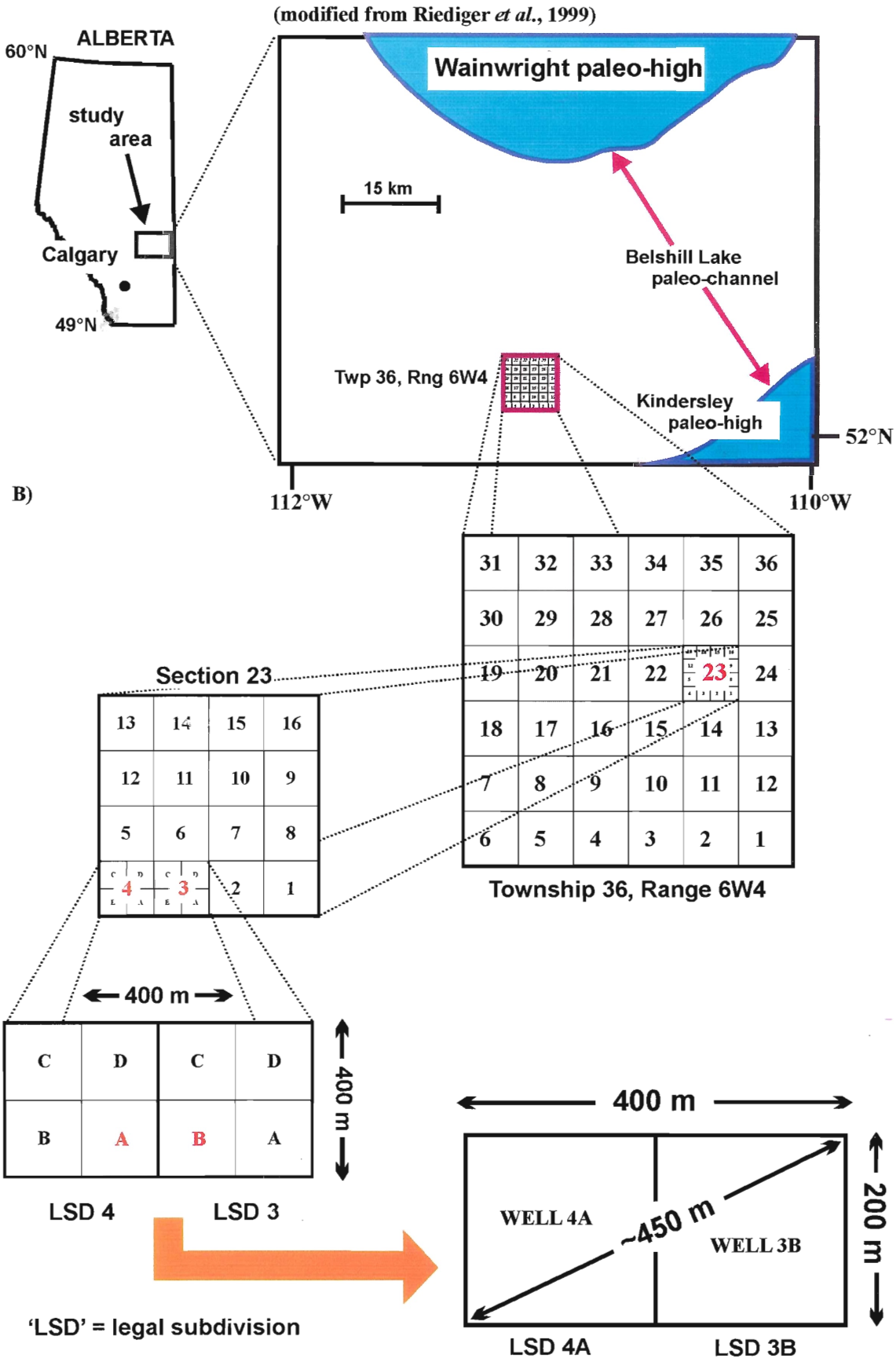
(modified from Riediger *et al.*, 1999)
ALBERTA
60°N
study area
Calgary
49°N
Wainwright paleo-high
15 km
Belshill Lake paleo-channel
Twp 36, Rng 6W4
Kindersley paleo-high
52°N
B)
112°W
110°W
31 32 33 34 35 36
30 29 28 27 26 25
19 20 21 22 23 24
18 17 16 15 14 13
7 8 9 10 11 12
6 5 4 3 2 1
Township 36, Range 6W4
Section 23
13 14 15 16
12 11 10 9
5 6 7 8
4 3 2 1
400 m
C D C D
B A B A
400 m
LSD 4
LSD 3
'LSD' = legal subdivision
400 m
WELL 4A
~450 m
WELL 3B
200 m
LSD 4A
LSD 3B

Subdivisions 3B and 4A the two wells are located, but as Figure 1B illustrates, the maximum distance conceivably separating the two cores is ~450 m. The two cores, therefore, are less than 0.5 km apart.

1.2.3 Provost oil field

According to Hayes *et al.* (1994), the Provost oil field (Figure 1A) was discovered in 1956 and is the second largest oil field in the Western Canada Sedimentary Basin (in terms of initial established recoverable oil reserves, with 11.9 x 10^6 m^3 or 71.4 MMBbls). The Dina formation is the major producing unit of the Provost oil field (Hayes *et al.*, 1994), and evidence for its oil-bearing nature is observed in cores from Wells 3B- and 4A-23-36-6W4, where oil-stained sandstone beds appear dark brown in colour and are often odiferous with hydrocarbons.

According to Riediger *et al.* (1999), two families of oil (families D and EQ) are recognised in the Dina reservoir of the Provost oil field. As Riediger *et al.* (1999) explain, family D oil is a light, thermally mature, low-sulphur crude oil which migrated up-dip into the Dina reservoir from the west, and whose source is the Devonian Duvernay Formation (which is part of the Woodbend Group; Podruski *et al.*, 1987). The family EQ oils, which are less thermally mature than the family D oils, comprise non-degraded, moderate- to high-sulphur oils which originated from the Devonian/Mississippian Exshaw Formation to the south, and the Early Cretaceous Ostracode zone to the southwest (Riediger *et al.*, 1999).

1.3 Local and regional stratigraphy

1.3.1 Regional stratigraphy of the Western Canada Sedimentary Basin

Undeformed strata of the WCSB (i.e. east of the Cordillera) are defined by two major successions of sedimentary rocks (Mossop & Shetsen, 1994). According to Mossop & Shetsen (1994), the Paleozoic to Jurassic strata (the platformal succession) comprise carbonates deposited on the stable North American craton next to a dominantly passive continental margin in the west. The mid-Jurassic to Paleocene strata (the foreland basin succession) overlie the platformal succession and are dominated by clastics deposited during active orogenic evolution of the Cordillera in the west (Mossop & Shetsen, 1994). In the study area, the Dina formation represents the base of the

younger foreland basin succession, and underlying Devonian carbonates represent eroded strata of the underlying platformal succession. These two successions are separated by a large-scale regional unconformity, which is discussed below.

1.3.2 Stratigraphy of the study area

Figure 2 is a stratigraphic column for the study area spanning the Late Devonian to Early Cretaceous. The Dina formation is Early Cretaceous (late Barremian to late Aptian) and forms the basal unit of the Mannville Group (late Barremian to middle Albian). As Figure 2 shows, the Dina formation is overlain by the Ostracode zone (late Aptian) and the Cummings formation (late Aptian to early Albian), both which are part of the Mannville Group.

The Dina formation defines the basal unit of the Mannville Group in *east central Alberta*, while other names are assigned to the basal unit of the Mannville Group in different regions of the WCSB. Examples include the Ellerslie (central Alberta), McMurray (northeastern Alberta), and Cadomin/Gething (northeastern British Columbia) formations, and the McCloud member in southwestern Saskatchewan (Hayes *et al.*, 1994).

The Dina formation was deposited in a series of paleo-valleys cut into much older rocks underlying a regional unconformity (Hayes *et al.*, 1994). According to Cant & Abrahamson (1996), this sub-Cretaceous regional unconformity constitutes a 2^{nd}-order sequence boundary in the classification scheme of Vail *et al.* (1977), and represents a major change in the tectonic regime of the WCSB (which changed from a period of uplift and erosion to a period of basin-wide subsidence and sedimentation; Hayes *et al.*, 1994). The rocks underlying this unconformity in the study area comprise Devonian to Mississippian strata (Figure 2), and Hayes *et al.* (1994) suggest that these rocks in the study area are defined by Devonian carbonates, although it is unclear if these carbonates are of the Woodbend Group, Winterburn Group, or both. Hayes *et al.* (1994) suggest the Dina formation in the study area is less than ~20 m thick.

As Figure 3 shows, the Dina formation is part of a transgressive systems tract (Cant & Abrahamson, 1996) deposited during Aptian transgression, when the Boreal Sea to the north advanced southwards across the North American craton (discussed later).

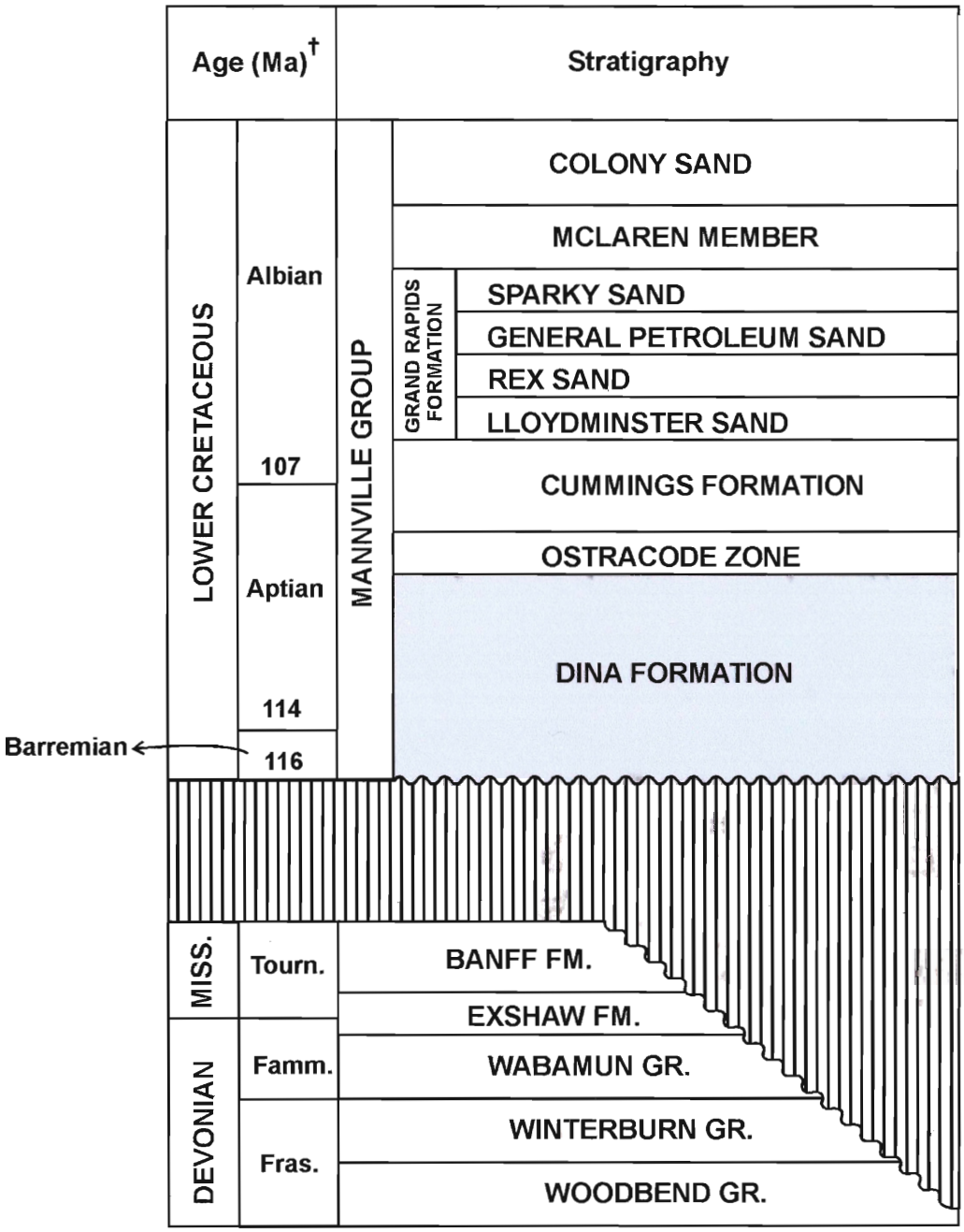

† stages (and exact ages) for the Cretaceous taken from Smith (1994), and for the Mississippian and Devonian from Wendte *et al.* (1992)

Figure 2 - Stratigraphic column of the study area (modified from Riediger *et al.*, 1999).

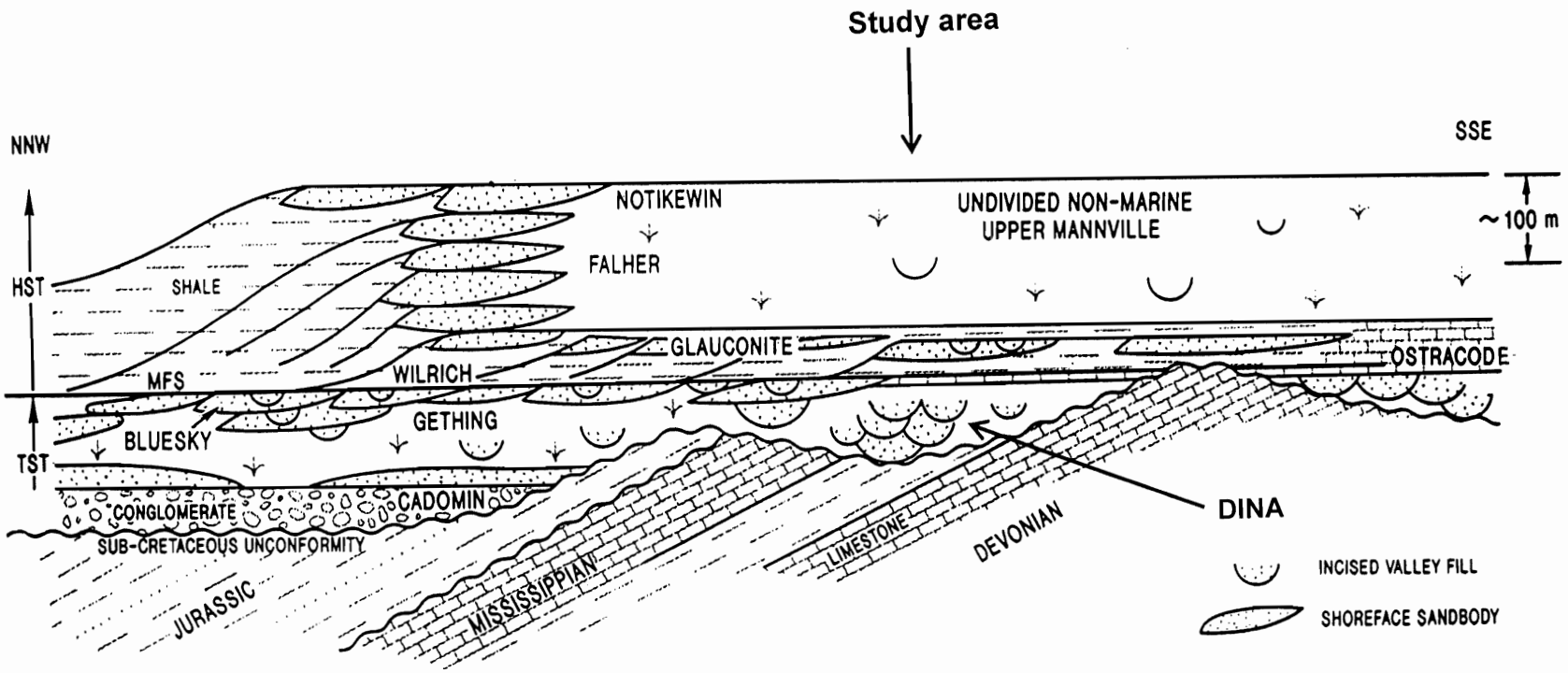

Figure 3 – Longitudinal stratigraphic cross-section of the Mannville Group across the WCSB, from northeastern British Columbia (NNW) to southern Alberta (SSE). An arrow at top locates the study area relative to the transect. The Dina formation comprises incised valley fill overlying the sub-Cretaceous unconformity (modified from Cant & Abrahamson, 1996).

The maximum flooding surface is defined by Cant & Abrahamson (1996) as the base or middle of the Ostracode zone, which correlates to the base of the Wilrich Shale in the west, and to the base of the Clearwater Shale in the east (not shown on Figure 3).

1.4 Post-Jurassic evolution of the WCSB

1.4.1 The rising Cordillera and migrating foreland basin

Beginning in the middle Jurassic, the continent of North America began to drift westwards as the Atlantic Ocean opened (Mossop & Shetsen, 1994). As it drifted, the continent of North America collided with several large oceanic terranes that were eventually accreted onto the western margin of the continent (Mossop & Shetsen, 1994). Collision and accretion resulted in compressional tectonism along the western margin of North America and as a result, platformal rocks were thrust, from west to east, in a series of imbricate sheets to form the Canadian Rocky Mountains and Rocky Mountain Foothills of the Cordillera (Mossop & Shetsen, 1994).

The weight of these thickened supracrustal rocks in the foreland thrust and fold belt of the Cordillera resulted in isostatic flexure of the North American continental lithosphere (Price, 1994), and created a subsiding foredeep which migrated eastwards (Mossop & Shetsen, 1994) as the Cordillera continued to rise. This migrating foredeep acted as a trap for sediments shed from both the rising Cordillera in the west (Mossop & Shetsen, 1994), and the Precambrian Canadian Shield to the east (Hayes *et al.*, 1994). Hayes *et al.* (1994) and Jackson (1984) suggest that sediments shed from the Canadian Shield were restricted to the eastern margin of the migrating foreland basin.

1.4.2 Aptian transgression

According to Smith (1994), a relative rise in sea level during the early Aptian allowed marine waters to transgress southwards (from the Boreal Sea to the north; Jackson, 1984) over low-lying parts of the WCSB. This relative rise in sea level was the result of subsidence of the foreland basin in response to the rising Cordillera (Leckie & Reinson, 1993), which as Stott (1984) explains, experienced a pulse of renewed thrusting and loading starting around the late Barremian and spanning the Aptian, Albian, and early Cenomanian. As transgression continued during the Aptian, a marine influence spread over much of the WCSB, including over the study area (Smith, 1994). By the middle

Albian (or early Albian; Smith, 1994), a global eustatic rise in sea level induced further transgression over the WCSB, and by the late Albian, culminated in formation of the Western Interior Seaway, an epeiric ocean covering the entire length of the Western Interior Basin, from the Arctic Ocean to the Gulf of Mexico (Leckie & Reinson, 1993; Smith, 1994).

1.5 Paleo-environment of the study area

Figures 4A and 4B are paleo-geographic maps of Alberta spanning the Aptian which show the increase in marine influence over the region attributed to Aptian transgression. In the study area, the Dina formation was deposited in a broad paleovalley called the Belshill Lake Channel, which lay between two paleo-topographic highs (Figure 1B) called the Wainwright and Kindersley Highlands (Riediger *et al.*, 1999). The paleo-geographic maps of Figure 4 show how the paleo-environment of the Belshill Lake Channel (and the study area) changed during the Aptian from a fluvial setting (early Aptian) to a brackish-water one (late Aptian) during transgression from the north. According to Hayes *et al.* (1994), tidal regimes significantly influenced sedimentation in these brackish-water environments.

1.6 Provenance

The exact provenance of the Dina formation in the study area is unclear. Hayes *et al.* (1994) report that lower Mannville Group strata, which cover nearly the entire WCSB, comprise sediments derived primarily from the Cordillera in the west, but that the Canadian Shield supplied quartzose sediments to a series of paleo-valleys restricted along the eastern margin of the WCSB. It is not clear if the Belshill Lake Channel was part of this paleo-valley network draining off of the Canadian Shield. Jackson (1984) describes a similar series of paleo-valleys draining off of the Canadian Shield into the basin, but limits these to the northeastern realm of the WCSB. Jackson (1984) also suggests that the Dina formation deposited in the Belshill Lake Channel includes sediments derived from Mississippian to Jurassic strata of the Pembina High (situated ~300 km northwest of the Belshill Lake Channel), as well as Jurassic strata of other prominent paleo-topographical highs of the WCSB. Smith (1994) reports that during deposition of the Dina formation,

Figure 4 (*following two pages*) – Paleo-geographic maps of Alberta during Aptian transgression of the WCSB (modified from Smith, 1994). A) The early to late Aptian. B) The late Aptian.

A) LATE BARREMIAN TO LATE APTIAN (i.e. LOWER DINA)

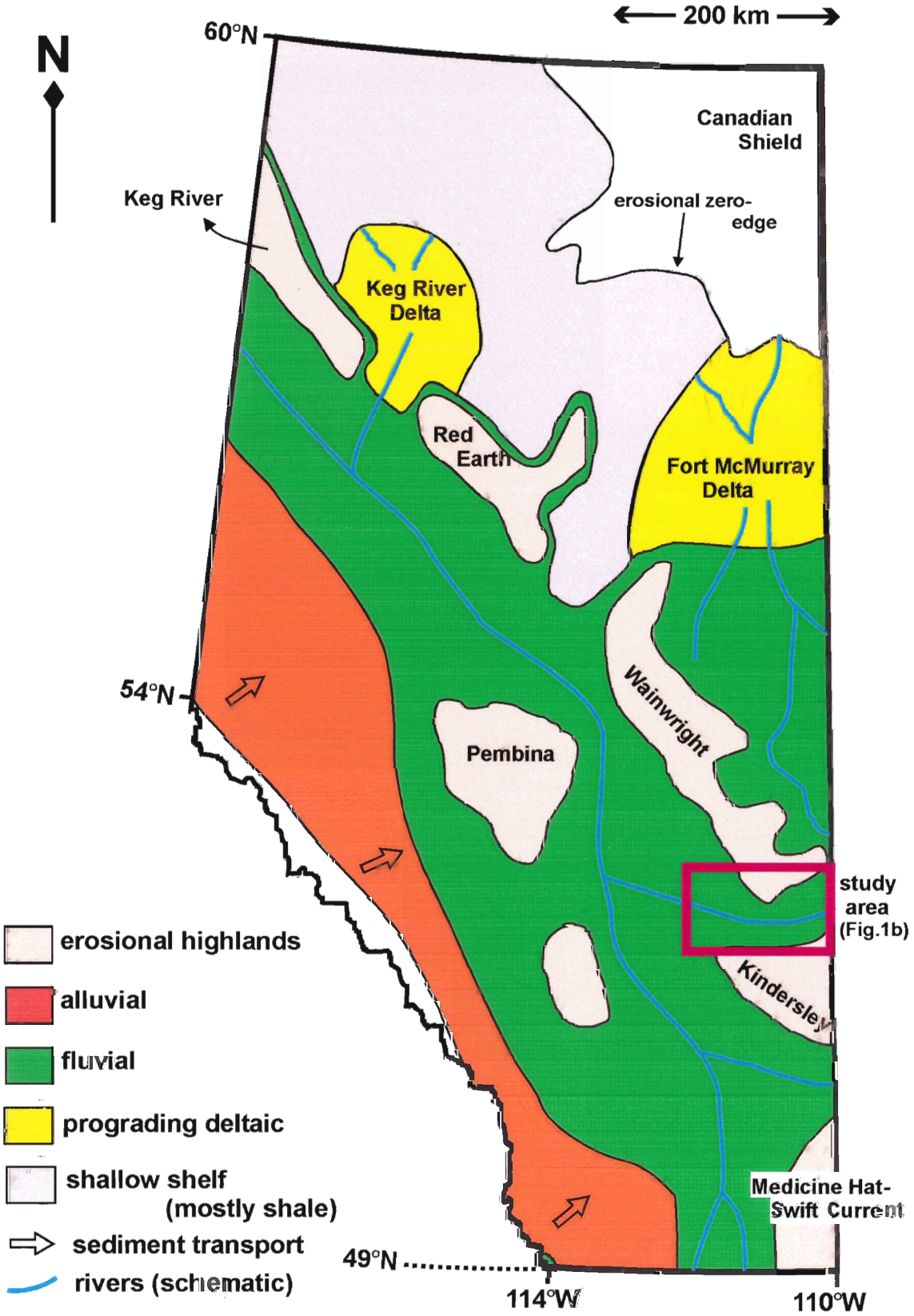

B) LATE APTIAN (i.e. UPPER DINA)

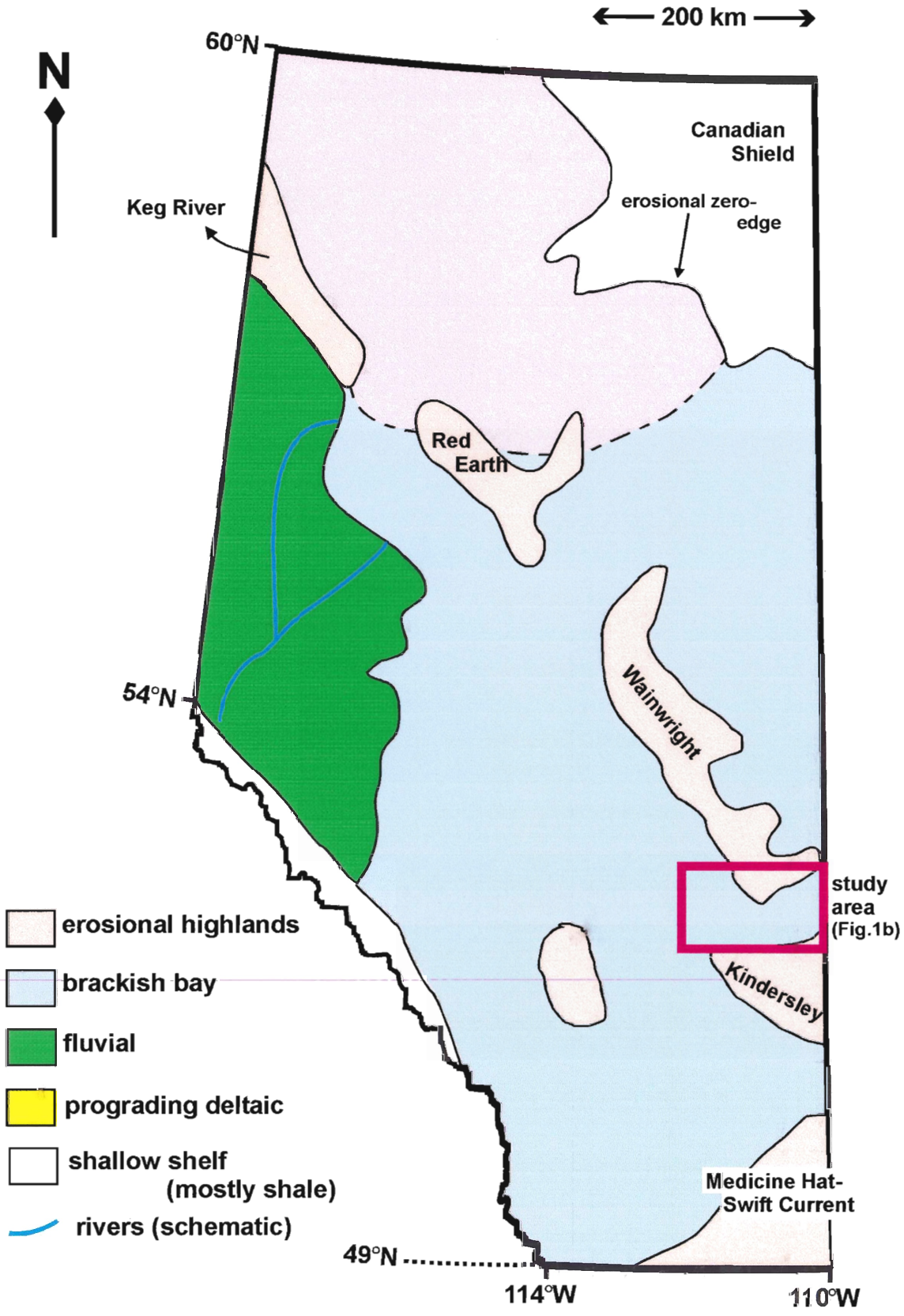

(i.e. Aptian time), the Pembina High comprised Jurassic strata (defined by clastics; Hayes *et al.*, 1994), the Wainwright High comprised Devonian strata (defined by carbonates; Hayes *et al.*, 1994), and the Kindersley High was composed of both of these rock types (Jurassic clastics and Devonian carbonates).

Although it is unclear how to recognise sediments derived from these paleo-topographic highs in sediments of the Dina formation (as suggested by Jackson, 1984), Cant (1989) provides a method of differentiating between Cordilleran and Canadian Shield provenance. According to Cant (1989), sandstone of Canadian Shield provenance is highly quartzose (80-95% quartz), while sandstone of Cordilleran provenance is relatively rich in lithics (25-40%), chert, and may contain volcanic fragments derived from the accreted terranes in the Cordillera. Hopkins (1981) adds that accessory muscovite and feldspar also suggest derivation from crystalline rocks of the Canadian Shield, and Williams (1963) suggests the same for detrital zircon grains. Sandstone units in the two cores discussed in this thesis provide a chance to determine provenance of the Dina formation.

1.7 Previous Work

According to Riediger *et al.* (1999), the Dina formation was described and interpreted in the study area by M. Sherwin and R. W. MacDonald, in studies which were not published. They describe the Dina formation as a series of fining-upward, normally-graded channel deposits which grade from coarse, basal lag deposits to planar and trough cross-bedded, fine grained sandstones containing significant amounts of quartz and light and dark chert. (The presence of chert fragments suggests derivation from the Cordillera in the west.) They conclude that the channel deposits exhibit a gradual increase in marine influence, changing from fresh-water meandering channel deposits on the bottom to estuarine channel complexes on top. M. Sherwin and R. W. MacDonald also describe and interpret the overlying Ostracode zone in the study area. They describe the Ostracode zone as comprising interbedded limestone and calcareous, fossiliferous shale deposited in a shallow, restricted, brackish-water embayment during transgression of the Boreal Sea from the north.

Sedimentary structures and ichnological features characteristic of brackish-water environments are described and compiled by Wightman *et al.* (1987), and are useful in

evaluating some of the sedimentary and ichnological features observed in the two cores described and interpreted in this thesis.

Several authors discuss depositional environment and/or provenance of the basal unit of the Mannville group (i.e. correlative with the Dina formation) in central and northeastern Alberta. For example, Hayes *et al.* (1994) briefly describe the depositional environment of the Ellerslie formation (central Alberta) as characterised by a tidal influence and brackish-water conditions, and Hopkins (1981) concludes Canadian Shield provenance for the Ellerslie formation. Cant (1989) suggests Canadian Shield provenance for the McMurray formation of eastern Alberta as well.

CHAPTER 2 : METHODS

2.1 Methods

2.1.1 Core descriptions

Two cores from Wells 3B- and 4A-23-36-6W4 are described in this thesis: Core 2 from Well 3B, and Core 1 from Well 4A. In this thesis, these cores are referred to as Core 3B and Core 4A respectively. Each core is ~15 m long (7 boxes), for a total of ~30 m of core and 14 boxes (each box holds up to ~2.4 m of core). From bottom to top, both cores comprise the upper ~14 m of the Dina formation, ~1 m of the Ostracode zone, and less than 1 m of the overlying Cummings formation. (These rock formations and their approximate boundaries are identified according to lithological descriptions by M. Sherwin and R. W. MacDonald, see Riediger *et al.*, 1999, and section 1.7). Only the Dina formation is described and discussed in this thesis. Cores 3B and 4A were donated to Dalhousie University by the Canadian Society of Petroleum Geologists (CSPG) in Calgary, Alberta. These two cores were cut by Suncor Inc. in January and February of 1989, and are 3" slabs with flat surfaces. Both cores are in fairly good shape, although are broken and cut (previously sampled) in some places.

Cores 3B and 4A are very similar in appearance, and are described together in section 3.1. Core summaries are shown in Figure 5. The core description sheets used to log the two cores are included in Appendix E, where a legend defining the symbols is also included. Each sheet describes up to two metres of core, with a maximum resolution of 1 cm. There are 8 sheets for each core, for a total of 16 core description sheets in Appendix E. The core description sheets record grain size, sedimentary structures, laminae geometry, surface boundary descriptions, bioturbation, oil stain, trace fossils, and interpretations of ichnofacies, lithofacies, and depositional environment(s). The bioturbation index on the core description sheets ranges from 0 (no bioturbation) through to 4 (heavily bioturbated and/or churned), and the oil stain index (OSI, created by the author) is a qualitative, visual observation of the *colour* of an oil-stained sandstone bed (0-no oil stain, 1-light brown, 2-darker brown, and 3-very dark brown). The colour of an oil-stained sandstone bed is assumed directly proportional to the amount of oil present inside the rock.

Photos of the two cores, including detailed photos of important sedimentary structures, were taken using a digital camera (courtesy of Dr. Grant Wach). The core photos are included in Appendix A, and the detailed photos are presented in Chapter 3, Figure 6, Plates 1-10.

2.1.2 Scintillometer and spectrometers

Three different gamma-ray detectors were used in several attempts to generate higher-resolution gamma-ray logs of the cores at 10 cm resolution (about 10 times the vertical resolution of standard well logs), but neither device was sensitive enough to differentiate between background radiation and gamma rays emitted from the cores. The first device used was a hand-held scintillometer, the second a hand-held spectrometer, and the third a much larger spectrometer with a larger sodium iodide crystal. All three devices are designed for use on the outcrop, however, and are not sensitive enough for use on core cuttings, which represent much smaller volumes of rock relative to the outcrop scale. According to A. Ruffell (2003, personal communication), there is, in fact, a hand-held Scintrex device which rests on the ends of core boxes and is sensitive enough to record gamma ray counts from core of any size, loose or consolidated.

2.1.3 Transmitted- and reflected-light microscopy

Three polished thin sections (standard size, approx. 20 x 46 mm) were made from Core 3B in order to analyse mineralogy of the Dina formation: thin section #1 from 933.10 m, thin section #2 from 926.66 m, and thin section #3 from 924.27 m. Blue dye was added to stain for porosity. Mineralogy of the three polished thin sections was observed under the transmitted- and reflected-light microscopes at Dalhousie University, and the results are presented in section 3.2, and summarised in Table 3.

2.1.4 X-ray diffraction analysis

Four samples from Core 3B were analysed using X-ray diffraction (XRD), in order to determine clay mineralogy and to confirm observations made under the transmitted- and reflected light microscopes. The XRD analyses were carried out using the Philips XRG 3100 X-ray generator and Philips APD 3720 console at Dalhousie University, both which of which were recently donated by Chevron-Texaco in Houston, Texas. The four samples analysed in this thesis are the first batch of samples analysed

using these machines at Dalhousie University. Three of the samples came from pieces of Core 3B left over from thin section preparation (933.10, 926.66, and 924.27 m), and the fourth sample was taken from a pyrite-rich unit of Core 3B (923.84 m). The four samples were ground up using a mortar and pestle into clay-sized grains, prepared as dry mounts, and analysed using the newly-acquired machines, which are capable of automatically loading and analysing large sample batches. Results from the XRD analyses are presented in section 3.3 (Figure 10), and summarised in Table 3. The raw data generated during the analyses are included in Appendix F.

2.1.5 Well Logs

Photocopies of the well logs for Cores 3B and 4A were donated by Petrel Robertson in Calgary, Alberta, and are included in the back inside cover of this thesis, in Appendix G. Small comments written in the margins of these well logs (i.e. regarding formation boundaries) are not those of the author, and came with the original well log copies donated from Calgary. Background information regarding well-logs and their interpretation are included in Appendix D, and summarised in Figure 12. These well logs are correlated in section 4.5 (Figure 13).

CHAPTER 3 : RESULTS

3.1 Core descriptions

Cores 3B and 4A are described from the bottom of the cored intervals upwards to the formation boundary between the Dina formation and Ostracode zone (defined at 919.91 m in Core 3B, and 923.55 m in Core 4A). The distribution and abundance of sedimentary structures within the two cores are very similar, and each core comprises the same two lithofacies (referred to in this thesis as 'lower' and 'upper'). Core summaries are shown in Figure 5, and the detailed core description sheets (16 in total) are included in Appendix E. Table 1 defines the cored intervals for each of the 14 core boxes, and also defines the location of formation boundaries and cumulative thicknesses. The detailed photographs of important sedimentary structures are presented at the end of this chapter in Figure 6, Plates 1 through 10. (These plates are generally ordered from the bottom of the cored intervals upwards.) Appendix B provides reference diagrams and descriptions of the trace fossils described below, and also defines some of the terminology used when discussing ichnofacies and biogenic sedimentary structures.

3.1.1 Lower lithofacies

lightly burrowed, calcareous-cemented, silty sandstone, very fine (upper) to fine (upper), Core 3B: 933.25-932.55 m, Core 4A: 937.60-933.59 m

This lithofacies is characterised by brown sandstone with grey, calcareous cement and minor silty material. Grain size generally ranges from very fine (upper) to fine (upper). The silty material is defined by silty laminae (rare), silt rip-up clasts (rare to common), and the silty linings of trace fossils (rare to common). The silty laminae (932.70 and 933.20 m in Core 3B, and 935.42 m in Core 4A) are less than 1 cm thick, have scoured and uneven upper surfaces, and alternate with sandstone beds up to ~0.4 m thick in Core 3B, ~0.6 m in Core 4A. The silt rip-up clasts (Figure 6, Plate 2 for an example) are sub-angular to rounded, less than ~3 cm wide, and 'suspended' in the sandstone (i.e. matrix-supported). The silty linings of the trace fossils are discussed later.

Many of the sandstone beds in this lithofacies are rippled. Centimetre-scale, millimeter-scale, and climbing ripple lamination are all observed. The cm-scale ripple cross-lamination, defined by superimposed laminae $\leq$1.5 cm thick, is observed

Figure 5 – Core summaries for Cores 3B and 4A. Detailed core descriptions are included in Appendix E.

LEGEND**

- planar, parallel bedding
- current ripples
- climbing ripples
- scour
- burrowed
- churned
- pyrite
- organic material
- silt rip-up clast
- stylolite
- fossil
- HCl reacts to HCl (10%)
- F fining-upwards sequence

** extracted from legend included in Appendix E

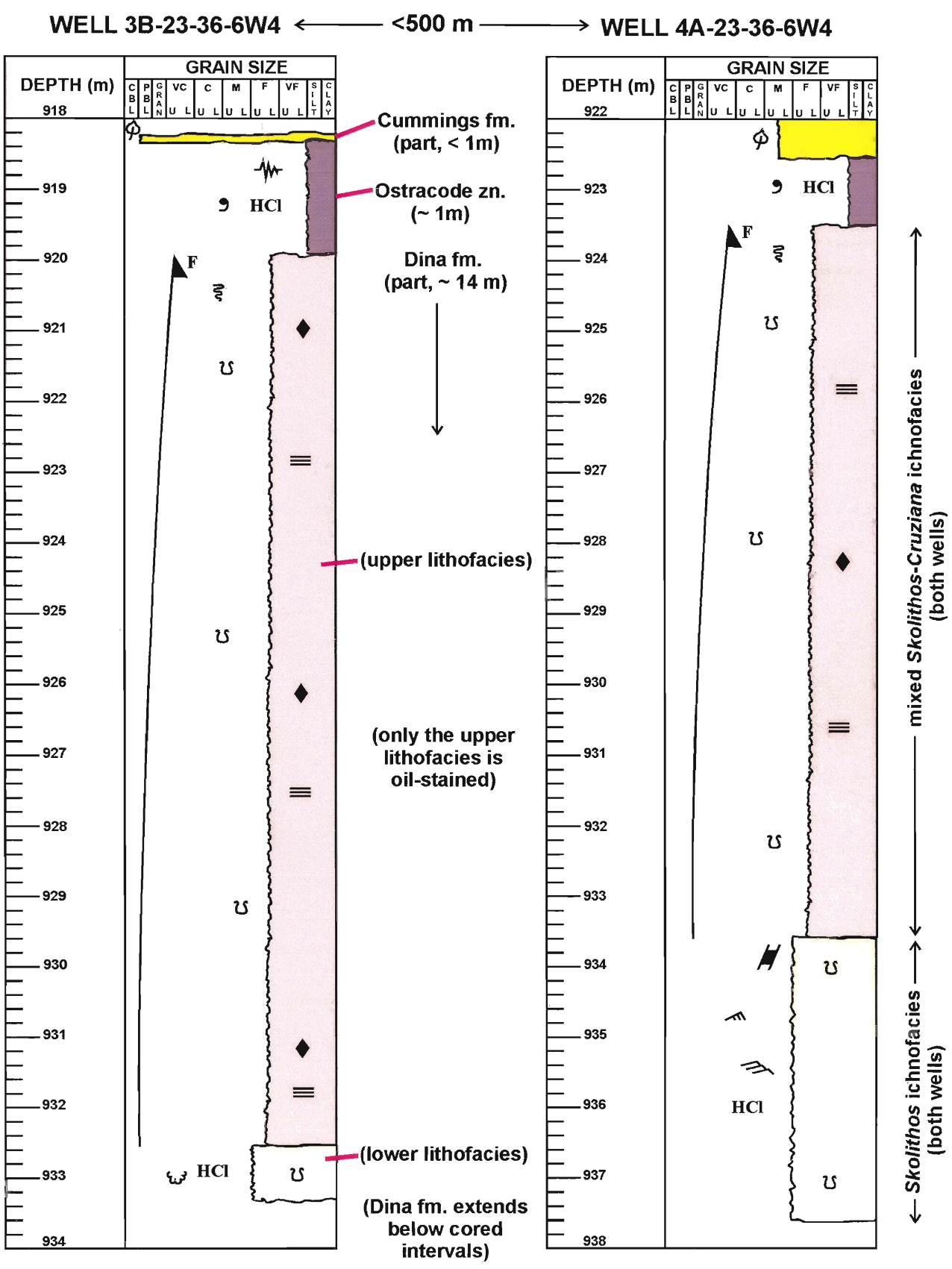
WELL 3B-23-36-6W4
<500 m
WELL 4A-23-36-6W4
DEPTH (m)
GRAIN SIZE
CBL
PBL
GRAN
VC
C
M
F
VF
SILT
CLAY
U L
Cummings fm.
(part, < 1m)
Ostracode zn.
(~ 1m)
Dina fm.
(part, ~ 14 m)
(upper lithofacies)
(only the upper lithofacies is oil-stained)
(lower lithofacies)
(Dina fm. extends below cored intervals)
HCl
mixed Skolithos-Cruziana ichnofacies (both wells)
Skolithos ichnofacies (both wells)

Table 1 - Cored intervals and formation boundaries for Cores 3B and 4A. The two cores are separated by a distance of <500 m.

				Cumulative thickness (in core)
CORE 3B (918.25 - 933.25 m)	Box 1	918.25-920.59 m	Cummings fm. (918.25 - 918.33 m)*	0.08 m (part)*
	Box 2	920.59-922.83 m		
	Box 3	922.83-925.18 m	Ostracode zn. (918.33 - 919.91 m)	1.58 m
	Box 4	925.18-927.42 m		
	Box 5	927.42-929.67 m	Dina fm. (919.91 - 933.25 m)**	13.34 m (part)**
	Box 6	929.67-931.79 m		
	Box 7	931.79-933.25 m		
CORE 4A (922.00 - 937.60 m)	Box 1	922.00-924.45 m	Cummings fm. (922.00 - 922.61 m)*	0.61 m (part)*
	Box 2	924.45-926.90 m		
	Box 3	926.90-929.35 m	Ostracode zn. (922.61 - 923.40 m)	0.79 m
	Box 4	929.35-931.80 m		
	Box 5	931.80-934.25 m	Dina fm. (923.40 - 937.60 m)**	14.20 m (part)**
	Box 6	934.25-936.70 m		
	Box 7	936.70-937.60 m		

* the Cummings formation extends above the cored intervals
** the Dina formation extends below the cored intervals

throughout this lithofacies in Core 3B (dipping by ~5°), and near 936.15 m and 936.65 m in Core 4A (dipping by ~15-20°). The mm-scale ripple cross-lamination (observed near 934.45, 935.16, and 936.32 m in Core 4A) is defined by laminae sets (less than ~2 cm thick) of ripple foreset laminae up to ~4 mm thick, and generally dipping by ~20°. Their small size makes the mm-scale ripple foreset laminae difficult to see. Many of the larger, cm-scale ripple cross-laminations are themselves obscured by calcareous cement. The climbing ripple lamination is observed from 935.50-60 m in Core 4A (Plate 3), and is defined by several parallel, superimposed sandstone beds (up to ~1 cm thick, each dipping by ~14°), each composed of stacked laminae sets of ripple foreset laminae up to ~7 mm thick, and dipping by ~10°. The climbing ripple lamination is obscured by the calcareous cement, and is a little difficult to make out in Plate 3. A schematic diagram of climbing ripple lamination is shown in Figure 7.

The degree of cementation in this lithofacies varies considerably, but generally increases towards the bottom of the cored interval. This cement reacts vigourously with 10% HCl (aq). In some spots the sandstone is completely cemented and looks bluish-grey, and in other sections appears brown with 'patches' of grey cement.

Pyrite is rare in this lithofacies, although there is a large patch of microcrystalline pyrite ~6 cm wide at approximately 935.00 m in Core 4A.

Biogenic sedimentary structures in this lithofacies include trace fossils associated with the *Skolithos* ichnofacies, including *Skolithos* (rare, Plate 1) and *Palaeophycus* (rare and questionable, Plate 1). These trace fossils are rare to common in Core 4A, and rare in Core 3B. In Core 3B, the trace fossils are restricted to the thin, silty laminae (and directly below them). The *Skolithos* traces are distinctly lined by black, silty material (Plate 1), as are the *Palaeophycus* traces, and the importance of this is discussed later, in section 4.1.1. The questionable *Palaeophycus* traces are observed in Core 4A only, and are questionable because they are rare and look very similar to the more common *Skolithos* traces (both are lined). The trace fossils in this lithofacies are generally <1 cm long (or wide).

The top of this lithofacies is defined by the gradual disappearance of the calcium carbonate cement, and this contact is gradational over approximately 10 cm in Core 3B

(~932.50-.60 m) and gradational in Core 4A over approximately 15 cm (~933.45-.60 m). The nature of this boundary is discussed in section 4.1.3.

3.1.2 Upper lithofacies

oil-stained, interbedded sandstone and siltstone, moderately to heavily burrowed, silt to fine (lower), Core 3B : 932.55-919.91 m, Core 4A : 933.45-923.55 m

This lithofacies is characterised by interbedded, brown sandstone and black siltstone layers (defined by beds and laminae generally 1 mm to 4 cm thick). Grain size ranges from silt to fine (lower), and gradually fines upwards along this lithofacies as silt content increases.

Interbedded sandstone and siltstone layers define most of the bedding in this lithofacies (examples of this are shown in Plates 5 and 6). Interbedded sandstone and siltstone layers are observed over approximately 80% of this lithofacies in Core 3B, and over approximately 60% of this lithofacies in Core 4A. Flaser, wavy, and lenticular bedding are all common, with flaser bedding relatively abundant on the bottom. This flaser bedding gradually grades upwards along this lithofacies (as silt content increases) into wavy and lenticular bedding.

Interspersed throughout this lithofacies, and 'alternating' with intervals (up to ~1.3 m thick) of interbedded sandstone and siltstone units, are relatively clean sandstone beds ranging from approximately 2-35 cm thick (Plate 7 for two examples). These sandstone beds account for the remaining ~20% of this lithofacies in Core 3B, but are more abundant in Core 4A, accounting for ~40% of this lithofacies. These relatively clean sandstone beds exhibit sedimentary structures similar to those observed in sandstone beds of the underlying lithofacies, in that many are rippled (with mm-scale ripple cross-lamination), some have sharp bottom contacts (scoured in some cases), and one sandstone bed contains silt rip-up clasts (~925.57 m in Core 4A). The mm-scale ripple cross lamination is generally defined by laminae sets ($\leq$2 cm thick) of ripple foreset laminae 2-5 mm thick, and dipping by ~20° (examples include 925.66 m in Core 3B, and 926.55, 928.26, and 928.65 m in Core 4A). Questionable wave-ripple cross lamination is observed in two of the relatively clean sandstone beds of Core 4A (approximately 928.55 and 928.95 m), and is defined by stacked ripple foreset laminae

(up to ~6 mm wide), which dip from approximately 0-10°. These ripple laminae are heavily obscured by dark oil stains, and are difficult to photograph. Figure 8 provides a schematic diagram of wave-ripple cross lamination. The 'bundled upbuilding' and 'variable modes of lamination' shown in Figure 8 are observed in the two examples of wave-ripple cross lamination observed in Core 4A (and described above).

It is important to mention the core description sheets here. The relatively clean sandstone beds observed in this lithofacies are not always easy to pick out on the core description sheets in Appendix E, because many have minor silty material and, therefore, comprise the same grain size range as the interbedded sandstone and siltstone units (silt to fine (lower)). Some of the relatively clean sandstone beds, however, comprise only sandstone (i.e. at 921.30-.35 m in Core 3B, and 929.30-.56 m in Core 4A) and are easy to see on the core description sheets because of their relatively coarse grain size range (very fine (upper) to fine (lower)). Some of the relatively clean sandstone beds are also identified on the core description sheets by the symbol for ripple cross-lamination.

Many of the sandstone beds in this lithofacies are oil-stained (Plates 7 and 10). Table 2 lists all of the oil-stained sandstone beds and 'intervals' (i.e. multiple layers of interbedded siltstone and oil-stained sandstone) in descending order from top to bottom, and also lists their thickness, oil-stain index (OSI), and under- and overlying rock lithology. The OSI index (created by the author) is a visual assessment of the *colour* of an oil-stained sandstone bed (0-no oil stain, 1-light brown, 2-darker brown, and 3-very dark brown, see legend in Appendix E), which is assumed directly proportional to the amount of oil stain present. The distribution of oil-stained sandstone beds in this lithofacies (Table 1) is discussed more in section 4.4.

There is a syneresis crack observed in Core 3B at approximately 929.30 m (Plate 4), which is ~3 cm long, ~3 mm wide, crenulated, and filled with sandy material. This syneresis crack is significant and is discussed later.

Table 2 : Oil-stained sandstone beds in Cores 3B and 4A, listed from top to bottom along the cores (GR = gradational, CB = core break)

Interval (m)	Oil Stain Index (OSI)	Thickness (cm)	Directly overlain by : (contact, lithology)	Directly underlain by : (contact, lithology)
			CORE 3B	
921.30-921.35	1.0	5	GR, ~1 cm slightly sandy siltstone	CB, >1 cm slightly sandy siltstone
924.09-924.13	1.0	4	GR, >1 cm sandy siltstone	CB, >1 cm silty sandstone (rubble)
924.51-924.53	0.5	2	CB, >1 cm wavy-bedded siltstone	CB, >1 cm wavy-bedded siltstone
925.43-925.46	0.5	3	GR, >1 cm sandy siltstone	CB, >1 cm sandy siltstone
925.49-925.54	0.5	5	GR, >1 cm sandy siltstone	CB, >1 cm slightly sandy siltstone
925.58-925.69	2.0	11	GR, >1 cm slightly sandy siltstone	CB, >1 cm sandstone
925.69-925.74	3.0	5	CB, >1 cm sandstone	CB, >1 cm slightly sandy siltstone (rubble)
926.01-926.14	0.5	13	GR, ~2 cm slightly sandy siltstone	CB, >1 cm sandy siltstone
926.76-926.85	1.0	9	GR, ~3 mm slightly sandy siltstone	GR, ~5 mm sandy siltstone
926.87-926.96	2.5	9	CB, ~2 cm wavy-bedded sandstone	CB, >1 cm slightly sandy siltstone
927.14-927.19	0.5	5	GR, >1 cm silty sandstone	GR, >1 cm slightly sandy siltstone
927.28-927.34	1.0	6	GR, > 1 cm sandy siltstone	GR, >1 cm slightly silty sandstone
927.34-927.39	1.5	5	GR, >1 cm sandy siltstone	CB, ~1 cm slightly sandy siltstone
			CORE 4A	
924.28-924.31	2.5	3	CB, >1 cm sandstone (rubble)	CB, >1 cm sandy siltstone
924.45-924.49	1.0	4	CB, >1 cm sandy siltstone	CB, ~0.5 cm slightly sandy siltstone (rubble)
924.71-924.92	1.0	21	CB, >1 cm slightly sandy siltstone	CB, >1 cm siltstone
925.11-925.30	2.5	19	GR, >1 cm sandy siltstone	CB, >1 cm sandy siltstone
925.33-925.42	2.5	9	CB, >1 cm sandy siltstone	CB, >1 cm sandstone
925.54-925.90	2.5	36	CB, >1 cm sandstone	CB, ~0.5 cm sandy siltstone
925.90-925.94	0.5	4	GR, ~0.5 cm sandy siltstone	CB, ~3 mm sandy siltstone
926.07-926.30	2.5	23	CB, >1 cm slightly silty sandstone	CB, >1 cm sandstone
926.40-926.45	0.5	5	CB, >1 cm sandstone	CB, >1 cm sandstone
926.57-926.59	2.5	2	CB, >1 cm sandstone	CB, >1 cm sandstone
926.69-926.72	2.5	3	CB, >1 cm sandstone	CB, >1 cm wavy-bedded sandstone
926.83-926.86	2.5	3	CB, >1 cm very sandy siltstone	CB, >1 cm sandy siltstone
926.92-926.99	2.0	7	GR, >1 cm very slightly sandy siltstone	CB, >1 cm sandstone
927.08-927.14	1.5	6	GR, ~1 cm sandy siltstone	GR, >1 cm sandy siltstone

Table 2 (cont.).

Interval (m)	Oil Stain Index (OSI)	Thickness (cm)	Directly overlain by : (contact, lithology)	Directly underlain by : (contact, lithology)
			CORE 4A	
927.14-927.43	3.0	29	GR, >1 cm slightly siltstone	CB, >1 cm very slightly silty sandstone
927.64-927.88	2.0	24	GR, >1 cm sandy siltstone	CB, ~2 mm sandy siltstone
928.00-928.03	2.5	3	CB, > 1 cm sandstone	GR, >1 cm sandy siltstone
928.03-928.05	1.5	2	GR, >1 cm silty sandstone	GR, ~3 mm sandy siltstone
928.05-928.16	3.0	11	CB, ~3 mm sandy siltstone	CB, >1 cm sandstone
928.23-928.41	3.0	18	CB, > 1 cm sandstone	CB, ~2 cm sandy siltstone
928.43-928.66	3.0	23	CB, ~2 cm sandy siltstone	CB, ~1 cm very sandy siltstone
928.85-929.03	3.0	18	CB, >1 cm sandstone	CB, >1 cm sandy siltstone
929.30-929.56	3.0	26	CB, ~1 cm silty sandstone	CB, >1 cm slightly silty sandstone (rubble)
929.56-929.91	1.0	35	CB, >1 cm sandstone rubble	CB, >1 cm wavy-bedded sandstone
930.09-930.31	3.0	22	CB, >1 cm silty sandstone	CB, ~1 cm sandy siltstone
930.58-930.70	0.5	12	CB, >1 cm very sandy siltstone	CB, >1 cm sandstone
930.70-930.74	2.0	4	CB, ~1 cm silty sandstone	CB, >1 cm wavy-bedded sandstone
930.82-930.93	0.5	11	CB, >1 cm silty sandstone	CB, >1 cm very silty sandstone
931.11-931.28	3.0	17	GR, ~2 mm sandy siltstone	CB, >1 cm sandstone
931.54-931.60	2.5	6	CB, > 1 cm silty sandstone	CB, >1 cm sandstone
931.60-931.70	2.0	10	GR, ~1.5 cm sandy siltstone	GR, ~1 cm sandy siltstone
931.80-931.96	3.0	16	CB, >1 cm silty sandstone	CB, >1 cm silty sandstone
932.05-932.13	3.0	8	CB, >1 cm silty sandstone	CB, >1 cm sandstone
932.13-932.20	1.0	7	CB, >1 cm sandstone	CB, >1 cm sandstone
932.20-932.30	2.5	10	CB, >1 cm sandstone	CB, >1 cm sandstone
932.30-932.32	1.0	2	CB, >1 cm sandstone	CB, >1 cm sandstone

Dark brown patches of micro-crystalline pyrite are abundant in Core 3B (observed throughout this lithofacies, predominantly in the siltier units) but rare in Core 4A (one example at 930.05 m in Core 4A).

Biogenic sedimentary structures in this lithofacies comprise a low-diversity, mixed *Skolithos-Cruziana* assemblage of trace fossils dominated by *Planolites* (Plates 5 and 6), *Chondrites* (Plates 5 and 6), and *Skolithos* (Plate 7), with rare *Cylindrichnus* traces (Plate 8), and questionable trace fossils of *Zoophycos* (Plate 9). Nearly all of the trace fossils in this lithofacies are less than 2 cm long or wide, although some of the *Skolithos* burrows are as long as ~3 cm, and one of the *Cylindrichnus* traces is ~7 cm long (Plate 8).

Trace fossil abundance and bioturbation in this lithofacies both increase upwards. At the bottom of this lithofacies, where silt content is low and sand content high, *Skolithos* is rare to common and *Planolites* and *Chondrites* rare. As silt content gradually increases upwards, *Planolites* and *Chondrites* increase in abundance while *Skolithos* decreases in abundance, observed almost exclusively within the relatively clean sandstone beds. (*Skolithos* is more abundant in Well 4A, which has more sandstone.) Near the top of this lithofacies, where silt content is relatively high and sand content low, *Skolithos* is very rare, *Planolites* and *Chondrites* are abundant, and bioturbation high. Bioturbation is highest at the very top of the Dina formation, where the sediments are mixed and churned (919.91 - 922.11 m in Core 3B; 923.90 - 924.16 m in Core 4A).

Faunal diversity in this lithofacies also increases upwards. Nearly all of the questionable and rare trace fossils identified in this lithofacies are observed near the top, where silt content is relatively highest. The two *Cylindrichnus* burrows are observed near the middle of the lithofacies in very silty sandstone of Core 3B at approximately 926.28 and 923.65 m. The questionable *Zoophycos* traces are observed near the top of this lithofacies in sandy siltstone at approximately 923.60 m in Core 4A, and 922.55-923.32 m in Core 3B.

The contact between this lithofacies and the overlying shales and limestones of the Ostracode zone is gradational over approximately 9 cm in Core 3B (919.91-920.00 m), and defined by a core break and missing core in Core 4A (923.40-.55 m).

3.2 Thin section mineralogy

Observations made using the transmitted- and reflected-light microscopes are described below. Table 3 (included at the end of this chapter) is a summary of these observations, and includes observations made during the XRD analyses as well. Pictures of minerals from thin sections #1 and #2 are shown in Figure 9, and are discussed later regarding provenance of the Dina formation. The three polished thin sections are from Core 3B: #1-933.10 m, carbonate-cemented sandstone; #2-926.66 m, interbedded siltstone and sandstone; and #3-924.27 m, interbedded siltstone and sandstone (much higher silt content than #2).

3.2.1 Transmitted-light microscope observations

thin section #1 (933.10 m) - Angular to rounded quartz grains (≤0.2 mm wide, max ~0.3 mm wide) support each other, and their interstices are filled with calcite cement. Quartz and calcite make up about 95% of this thin section (50% quartz, 45% calcite), although some of the cement (less than 1%) is actually dolomite (identified by its characteristic rhombohedral shape; Nesse, 1991). Disregarding the calcite cement, quartz makes up ~90% of this thin section, with the remaining minerals comprising ~5% clay minerals, and ~1% opaques. Accessory zircon (Figure 9A) is also observed, approximately 0.2 mm long. The quartz grains in Figure 9 (A-E) have slightly elevated interference colours (as high as 1° red) due to the polished nature of the thin section.

thin section #2 (926.66 m) - Thin layers (less than ~1 cm thick) of angular to rounded quartz grains (≤0.1 mm wide, max ~0.2 mm wide) alternate with thin layers (less than ~1 cm thick) of clay minerals. Accessory muscovite (Figures 9B and 9E) is defined by elongated laths or 'filaments' generally ≤0.2 mm long, max ~0.3 mm long, and accessory feldspar (exhibiting both microcline and albite twins, Figures 9C and 9D) is defined by sub-angular to sub-rounded grains ≤0.1 mm wide. The quartzose layers in this thin section (i.e. the sandstone layers) are over 90% quartz, ~4% clay minerals, and ~1% opaques.

thin section #3 (924.27 m) - This thin section is similar to #2, but contains much more clay material, and the quartz grains are smaller in size. Thin layers (less than ~0.4 cm thick) of angular to sub-angular quartz grains (≤0.1 mm wide, max ~0.1 mm wide) alternate with thin layers (less than ~0.4 cm thick) of clay minerals. The relatively

quartzose layers comprise ~50% clay minerals, ~45% quartz, and ~2% opaques. Accessory muscovite filaments are also observed (≤0.2 mm long), but not included in Figure 9.

3.2.2 Reflected-light microscope observations

thin section #1 (933.10 m) - The opaques in this thin section are defined by pyrite crystals (≤0.2 mm wide, max ~0.3 mm wide, irregularly shaped) with accessory magnetite (≤0.2 mm wide, round).

thin section #2 (926.66 m) - The opaques in this thin section are defined by pyrite crystals (≤0.1 mm wide, euhedral to irregularly shaped) with accessory magnetite (≤0.2 mm wide, round) and marcasite (≤0.2 mm wide, irregularly shaped).

thin section #3 (924.27 m) - The opaques in this thin section are defined by pyrite crystals (≤0.1 mm wide, euhedral to irregularly shaped) with accessory magnetite (≤0.1 mm wide, round).

3.3 X-ray diffraction results

The results from the X-ray diffraction analyses are summarised in Table 3. The raw data generated during the analyses are included in Appendix F. Figure 10 (at the end of this chapter) includes four spectral plots for each sample. Samples #1391, #999, and #1379 are from the same locations on Core 3B as thin sections #1, #2, and #3 respectively (i.e. 933.10, 926.66, and 924.27 m), while the fourth sample, #1392, is from a pyrite-rich interval (923.84 m) on Core 3B.

XRD sample #1391 (933.10 m) - Quartz and calcite are identified (Figure 10, first page), which agrees with observations made under the transmitted-light microscope. Quartz and calcite account for nearly all of the peaks, except for one relatively small but well-defined peak at ~33.0° (2θ). Neither dolomite nor zircon account for this peak. This well-defined peak at ~33.0° (2θ) is observed in the spectral plots for the next two samples as well (#999 and #1379), and is present as a much larger peak on the spectral plot for the last sample, #1392.

XRD sample #999 (926.66 m) - Quartz and kaolinite are identified (Figure 10, second page), and these two minerals account for nearly all of the peaks in the spectral

plot. As with the previous sample, there is a relatively well-defined peak at ~33.0° (2θ) which is unaccounted for.

XRD sample #1379 (924.27 m) - Quartz, kaolinite, and lepidolite are identified (Figure 10, third page), and account for nearly all of the peaks in the spectral plot. (Lepidolite is a mica with essentially the same structure as muscovite; Nesse, 1991.) As with the previous two samples, there is a relatively well-defined but small peak at ~33.0° (2θ) which is unaccounted for.

XRD sample #1392 (923.84 m) - Quartz, pyrite, and marcasite are identified in this sample (Figure 10, fourth page). According to Nesse (1991), marcasite is the orthorhombic dimorph of pyrite (FeS_2). On the spectral plot for this sample, there are very well-defined peaks at ~33.0° (2θ) and ~56.1° (2θ) which pyrite accounts for. The relatively well-defined but small peaks at ~33.0° (2θ) seen in the spectral plots for the previous three samples, therefore, suggest that pyrite is present (in minor amounts) in the previous three samples.

3.4 Well Logs

Well-logs from Wells 3B- and 4A-23-36-6W4 are included in Appendix G. These well logs arrived from Calgary with notes written in the margins (regarding formation boundaries), and the reader is reminded that these are not those of the author. The well logs are scaled in metres, and extend from ~650-950 metres depth. They include the gamma ray (GR), spontaneous potential (SP), induction (ILM, ILD), spherically focused induction (SFLU), density porosity (DPHI), and neutron porosity (NPHI) logs. There are a total of four well logs in Appendix G, two for each well: one set shows the GR, DPHI, and NPHI logs, while the other set shows the SP, ILM, ILD, and SFLU logs. These well logs are correlated and discussed later in section 4.5 (Figure 13).

Figure 6 – Close-up photos (Plates 1 to 10) of sedimentary structures in Cores 3B and 4A.

Plate 1 – lined *Skolithos* traces, lower lithofacies

Plate 2 – silt rip-up clasts, lower lithofacies

Plate 3 – climbing ripple lamination, lower lithofacies

Plate 4 – syneresis crack, upper lithofacies

Plate 5 – interbedded sandstone and siltstone layers, with *Planolites* and *Chondrites*, upper lithofacies

Plate 6 – " "

Plate 7 – oil-stained sandstone beds, upper lithofacies, with *Skolithos* traces

Plate 8 – *Cylindrichnus* trace, upper lithofacies

Plate 9 – questionable *Zoophycos* traces, upper lithofacies

Plate 10 – abrupt change in oil stain, upper lithofacies

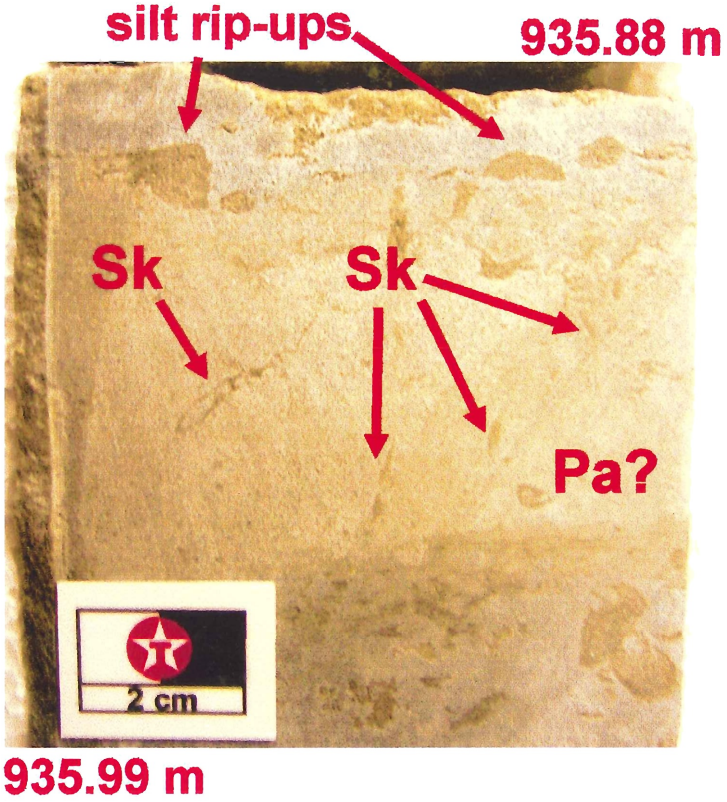

Plate 1 – Lined *Skolithos* (Sk) traces in sandstone, lower lithofacies, Core 4A. Note the questionable *Palaeophycus* trace (Pa, rare in this lithofacies), and the silt rip-up clasts.

Plate 2 – Silt rip-up clasts suspended in sandstone, lower lithofacies, Core 4A. Calcareous cementation of the sandstone gives it the grey-blue colour seen in the photo.

Plate 3 – Climbing ripple lamination in sandstone, lower lithofacies, Core 4A.
The lower figure is a trace of the laminae sets and individual laminae (compare with schematic diagram of climbing ripple lamination, Figure 7). Calcareous cementation of the sandstone gives it the grey-blue colour seen in the photo.

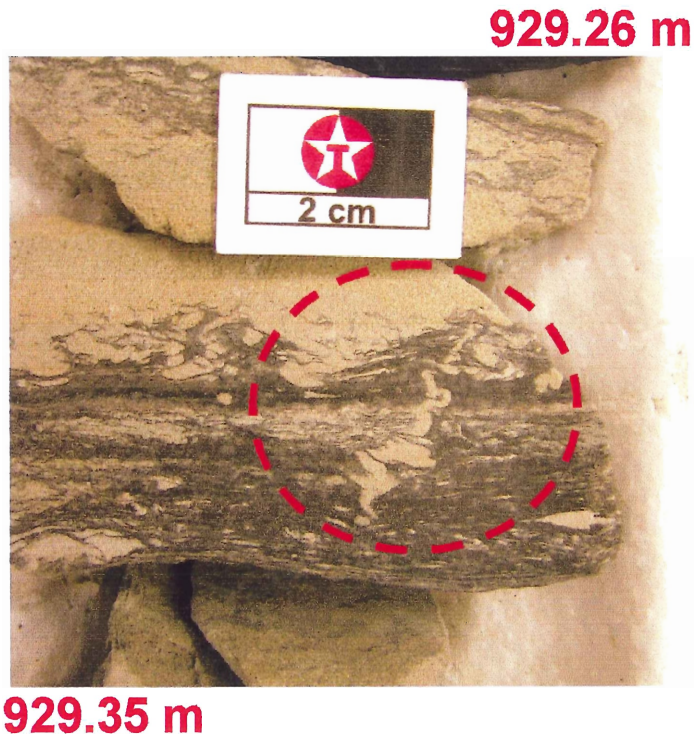

Plate 4 – Syneresis crack in sandy siltstone, upper lithofacies, Core 3B. Note the crenulated shape and infill by sandy sediments.

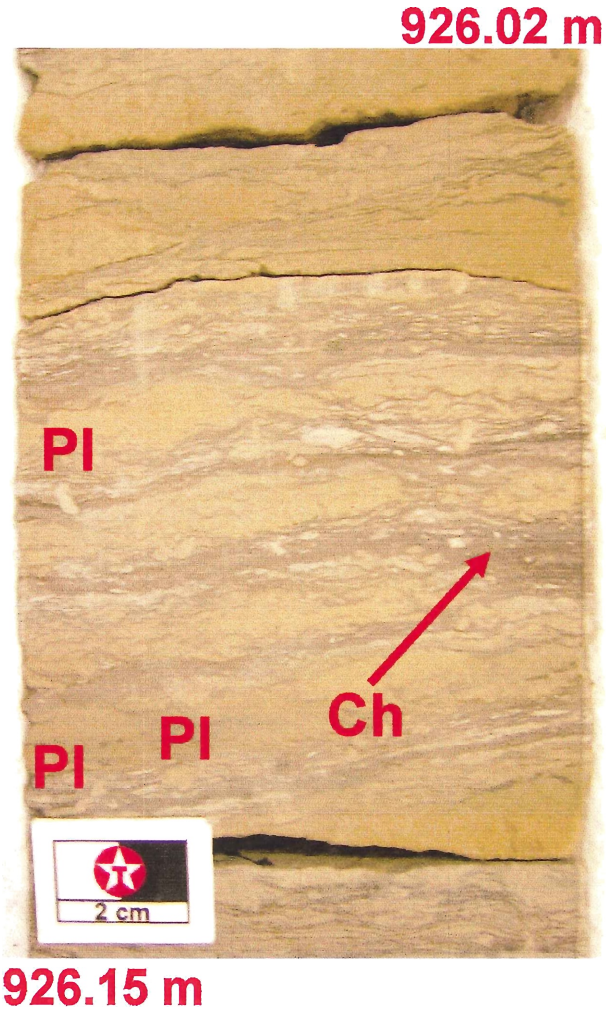

Plate 5 – Interbedded sandstone and siltstone layers, upper lithofacies, Core 3B. Observe the fairly equal sand versus silt content. This style of bedding accounts for ~80% of the upper lithofacies in Core 3B, and ~60% in Core 4A. Pl – *Planolites*, Ch – *Chondrites*.

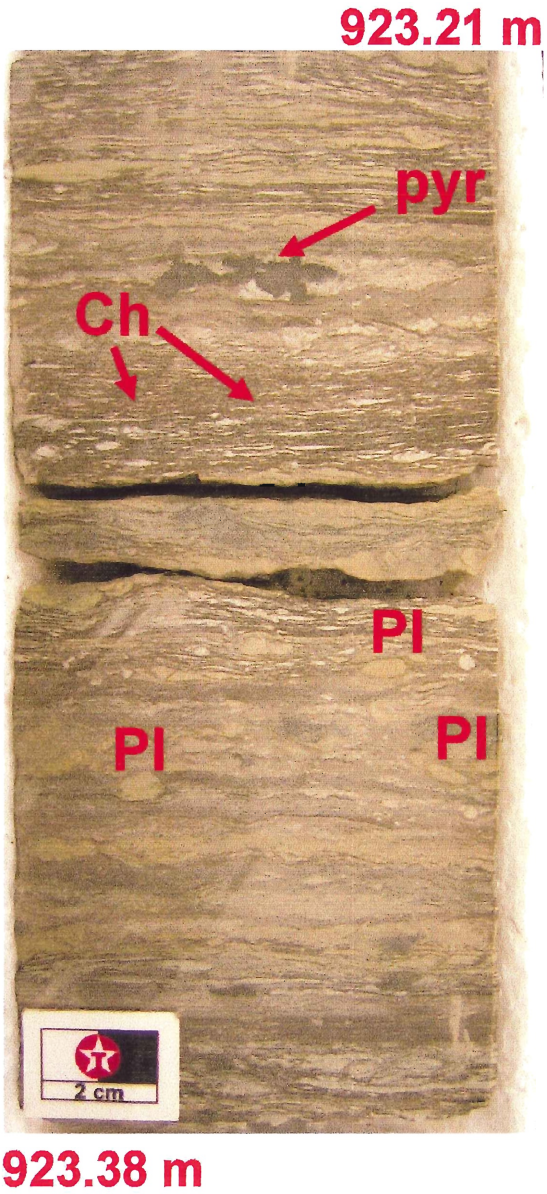

Plate 6 – Interbedded sandstone and siltstone layers showing wavy and lenticular bedding, upper lithofacies, Core 3B. Note the increased silt content (compare with Plate 4) and the micro-crystalline 'patch' of pyrite (pyr on photo). Pl – *Planolites*, Ch – *Chondrites*.

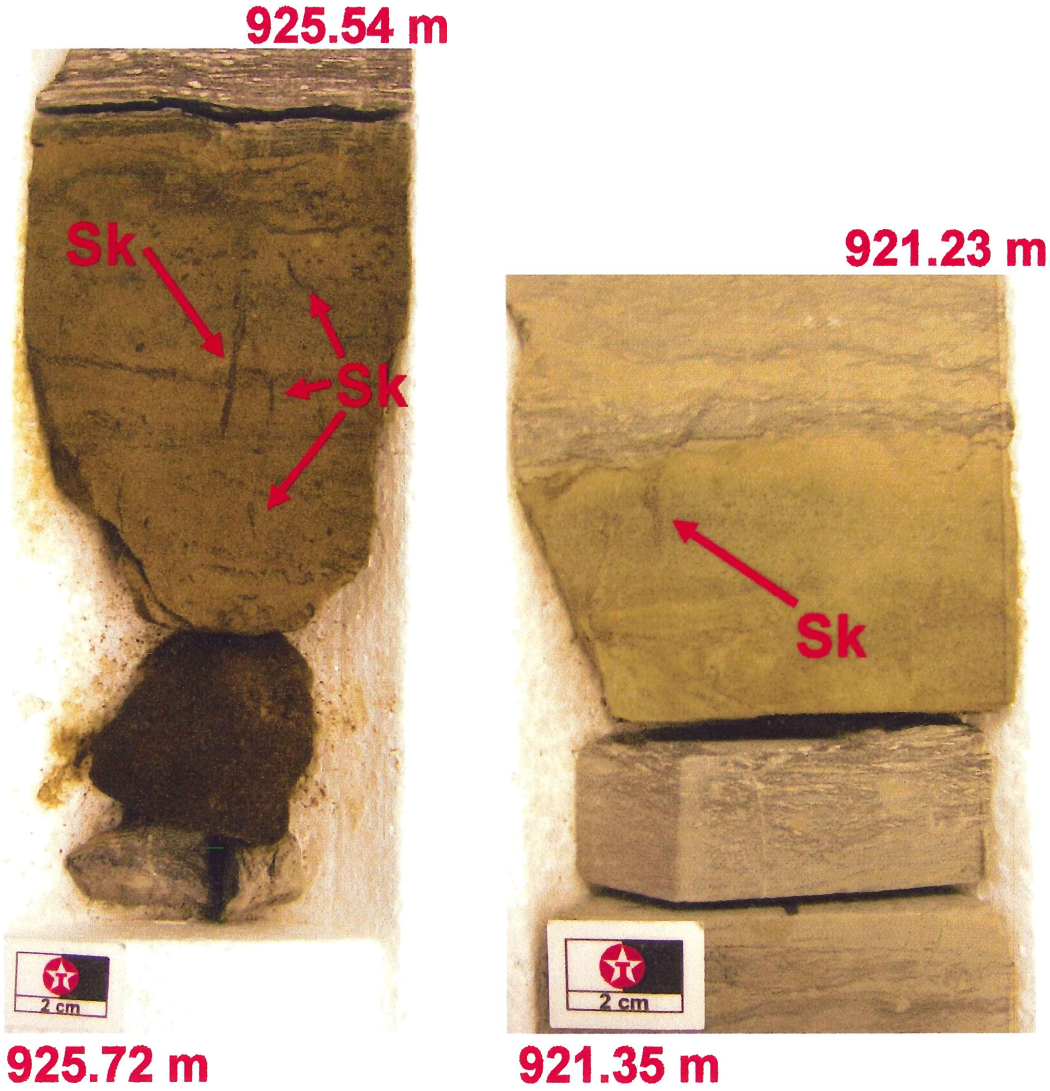

Plate 7 – Relatively clean sandstone beds, upper lithofacies, Core 3B. Many of these sandstone beds are burrowed by *Skolithos* (Sk in photo) and are rippled (with mm-scale ripple cross-lamination). Some of these sandstone beds, like the two shown above, are also oil-stained.

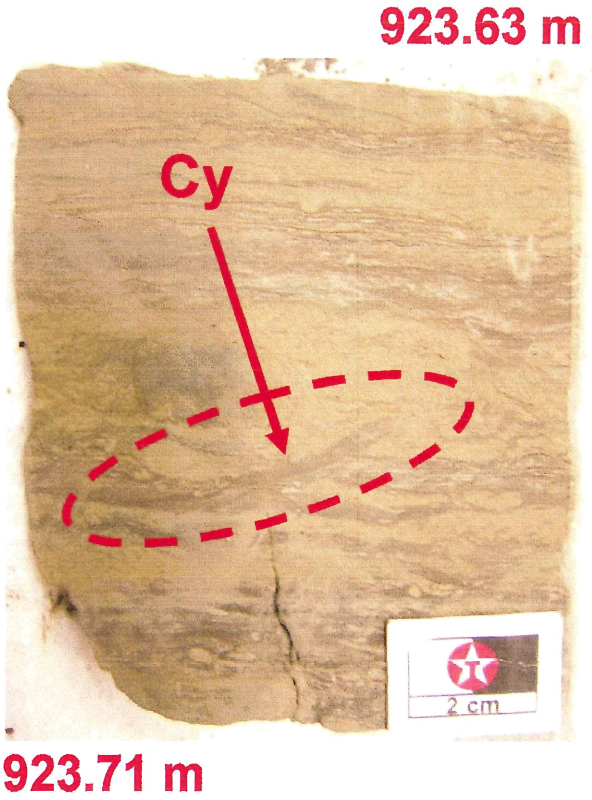

Plate 8 – *Cylindrichnus* trace (Cy in photo) in wavy-bedded sandstone/siltstone, upper lithofacies, Core 3B. Note the inclined orientation and relatively large size (~7 cm long).

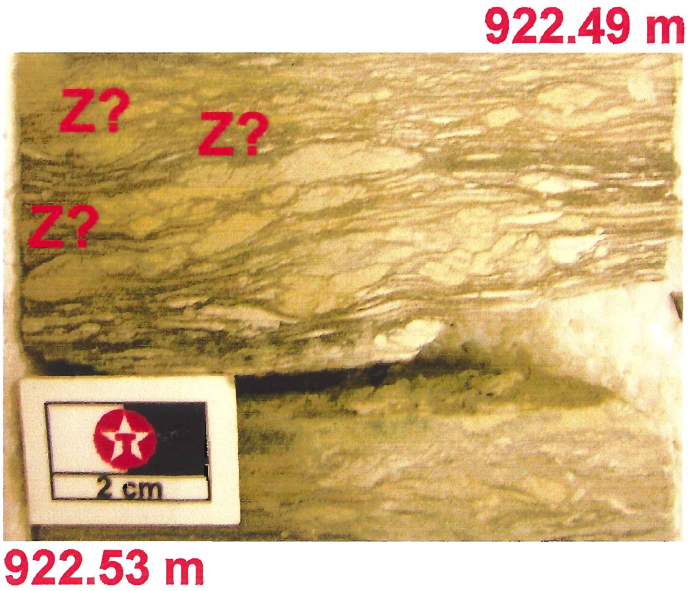

Plate 9 – Questionable *Zoophycos* traces in lenticular-bedded siltstone, upper lithofacies, Core 3B. Note their flat and slightly curved orientations, and the multiple burrow tunnels (spreite). These questionable *Zoophycos* traces are rare, restricted to the siltier (upper) portion of this lithofacies.

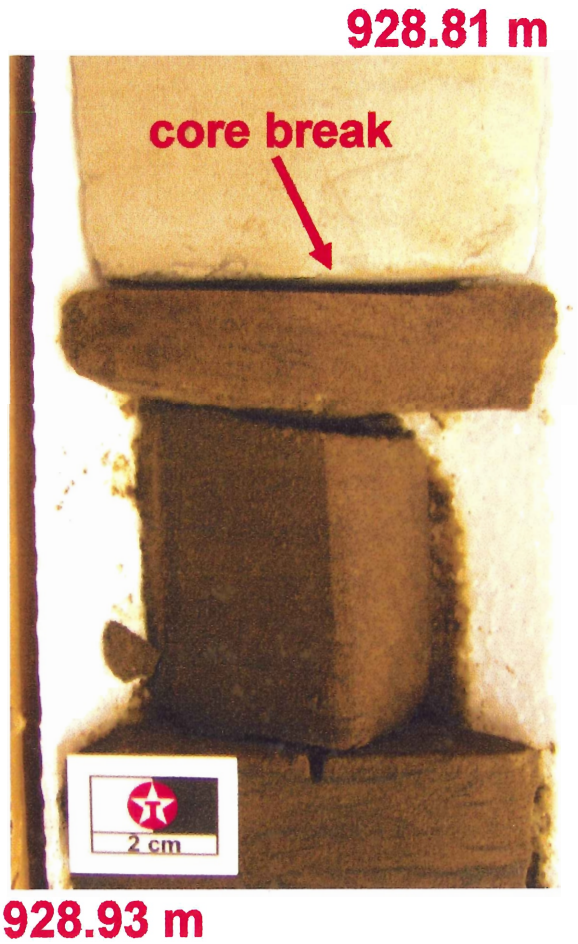

Plate 10 – Heavily oil-stained sandstone bed and its upper contact (core break) with non oil-stained sandstone, upper lithofacies, Core 4A. Note the abrupt change in oil stain across the core break, from heavy (OSI=3) below, to none (OSI=0) above.

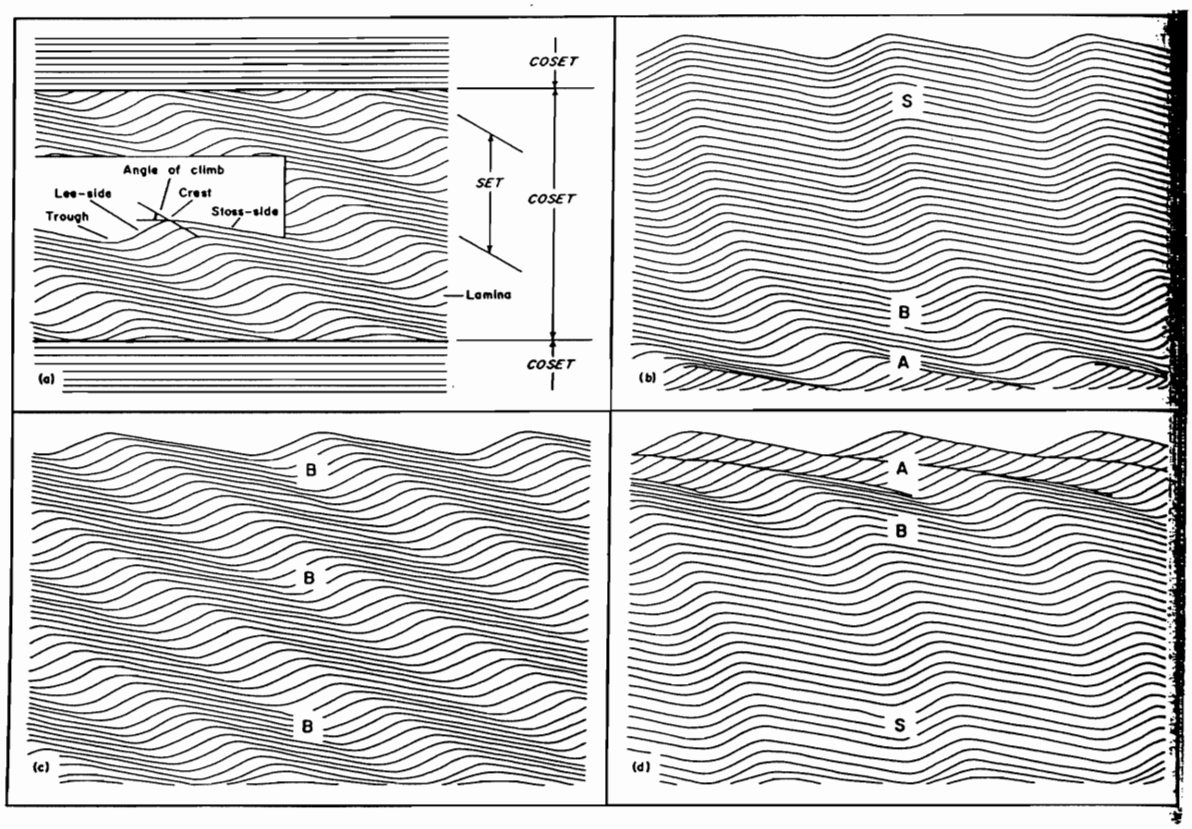

Figure 7 – Schematic diagram of climbing ripple lamination showing three different types (from Reineck & Singh, 1986). A) Ripple foreset terminology. B) Upwards increase in climbing angle. C) No upwards change in climbing angle. D) Upwards decrease in climbing angle. The climbing ripple lamination observed in Core 4A (see Figure 6, Plate 3) resembles type C.

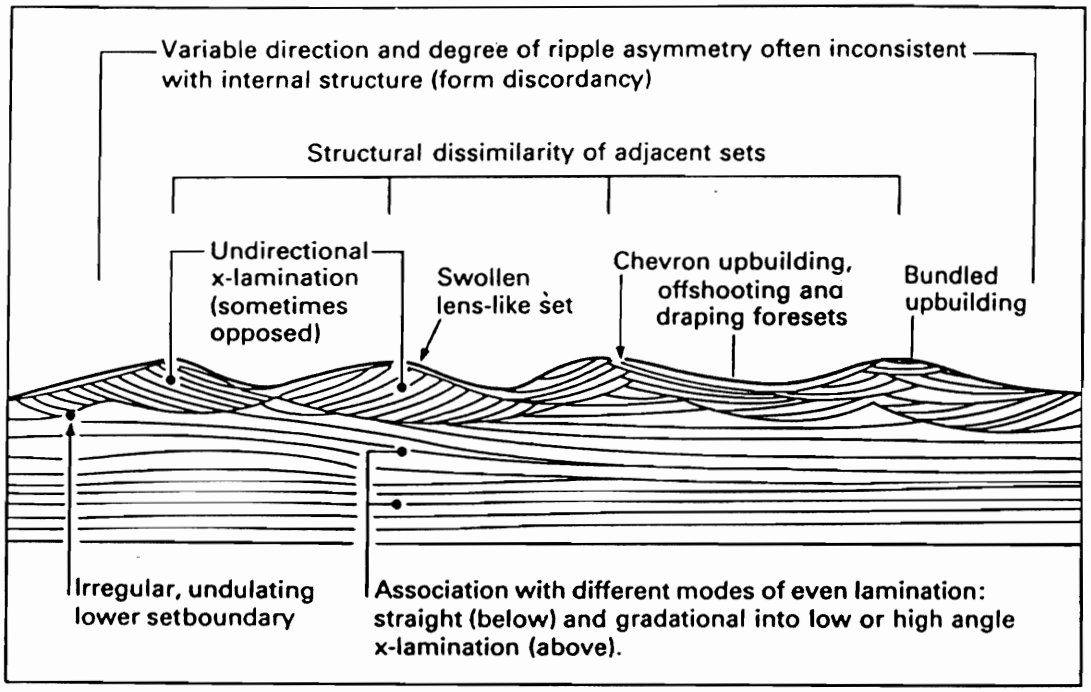

Figure 8 – Schematic diagram of wave-ripple cross lamination (from Johnson & Baldwin, 1986).

Figure 9 – Photographs of accessory minerals observed under the transmitted light microscope in sandy units of Core 3B (thin sections #1 and #2). Interference colours are slightly elevated due to the polished nature of the thin sections. Quartz grains, therefore, which define most of the mineral grains observed, display interference colours as high as 1° red. From left to right:

A) Detrital zircon (Z), thin section #1. Calcite cement (cal) occupies pore space between quartz grains (colourless to 1° red);

B) Accessory muscovite (Ms), thin section #2;

C) Accessory feldspar (Fsp, with cross-hatched microcline twins), thin section #2;

D) Accessory feldspar (with albite twinning), thin section #2; and

E) Accessory muscovite, thin section #2.

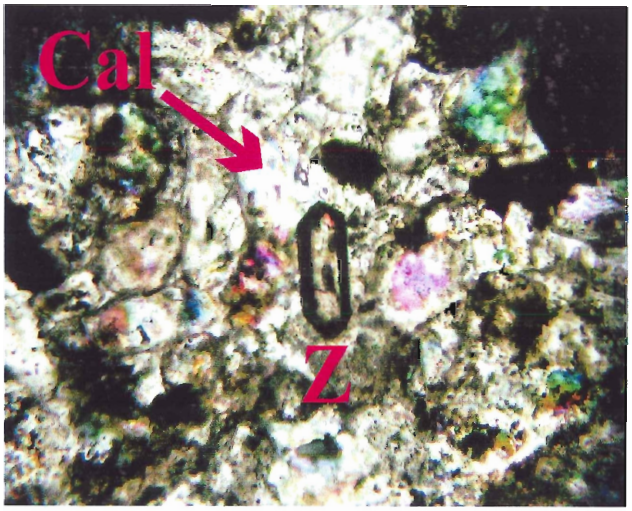

A) 0.2 mm

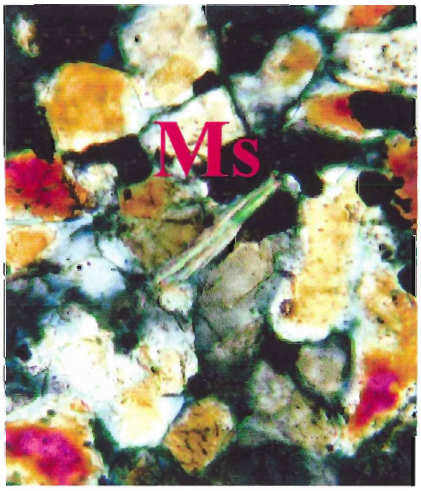

B) 0.1 mm

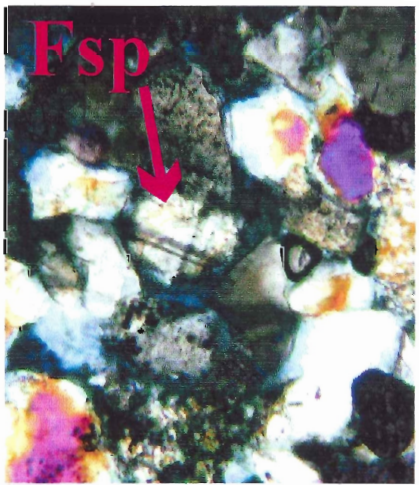

C) 0.1 mm

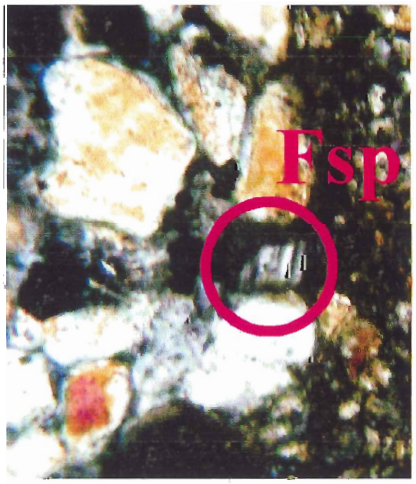

D) 0.1 mm

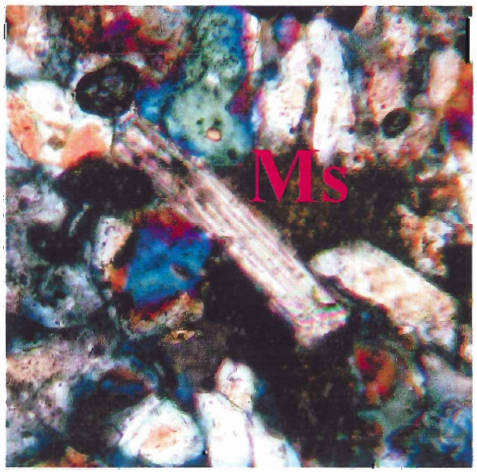

E) 0.1 mm

Table 3 : Summary of minerals observed in thin sections #1-3, Core 3B, using microscopy and XRD analysis.

	Minerals identified using :			
Location on Core 3B	**Transmitted-light microscope**	**Reflected-light microscope**	**X-ray diffraction analysis**	**Bulk Mineralogy**
933.10 m (thin section #1, XRD sample #1391)	quartz grains (cemented by calcite and dolomite), accessory zircon, no chert	pyrite, accessory magnetite	quartz and calcite	quartz, calcite, pyrite, accessory zircon and magnetite, no chert
926.66 m (thin section #2, XRD sample #999)	quartz grains, accessory muscovite and plagioclase, no chert	pyrite, accessory magnetite and marcasite	quartz and kaolinite	quartz, kaolinite, pyrite, accessory muscovite, feldspar, magnetite, and marcasite, no chert
924.27 m (thin section #3, XRD sample #1379)	quartz grains, accessory muscovite and zircon, no chert	pyrite, accessory magnetite	quartz, kaolinite, and lepidolite	quartz, kaolinite, lepidolite, accessory muscovite, zircon, and magnetite, no chert
923.84 m (no thin section, XRD sample #1392)	← (no thin section) →		quartz, pyrite, and marcasite	quartz, pyrite, and marcasite

Figure 10 (*following four pages*) – Spectral plots from XRD analyses of four samples from Core 3B. Minerals identified as positive matches are listed (abbreviated) below each spectral plot. The spectral plots are ordered from the bottom of the cored interval upwards (i.e. #1391, #999, #1379, #1392). Raw data generated during XRD analyses are included in Appendix F.

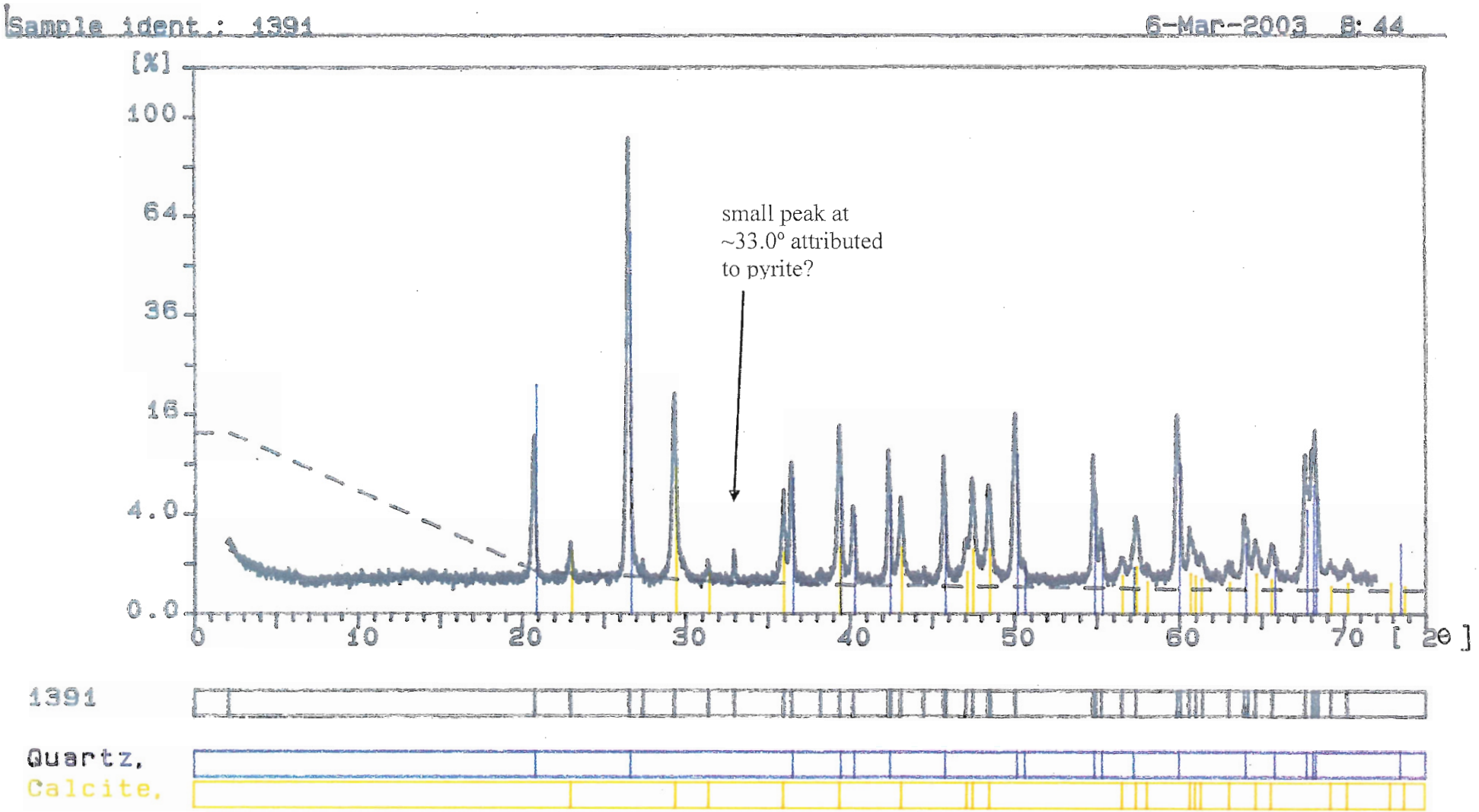
Sample ident.: 1391
6-Mar-2003 8:44
[%]
100
64
36
16
4.0
0.0
0
10
20
30
40
50
60
70
[2θ]
small peak at
~33.0° attributed
to pyrite?
1391
Quartz,
Calcite,

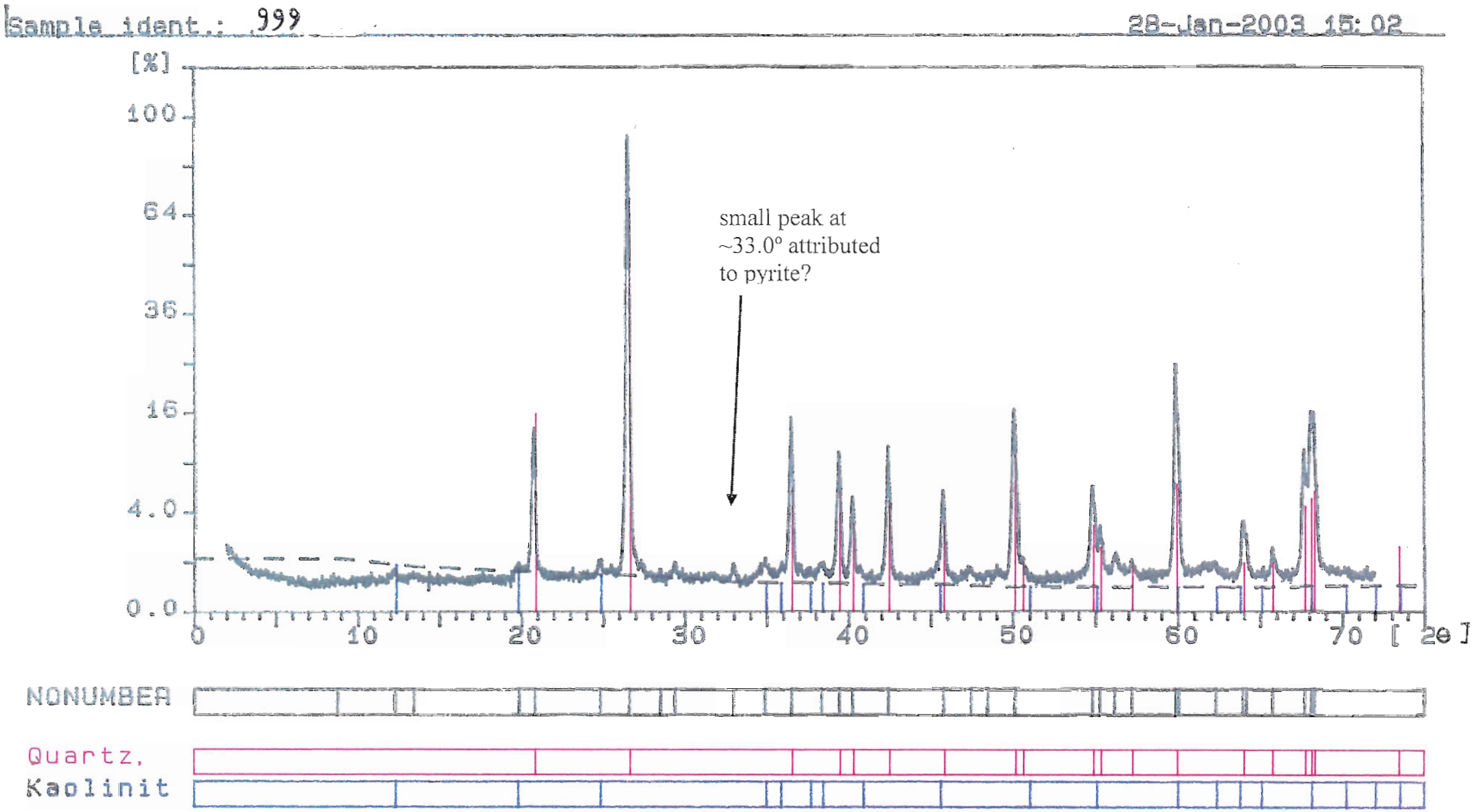
Sample ident.: 999
28-Jan-2003 15:02
[%]
100
64
36
16
4.0
0.0
0
10
20
30
40
50
60
70
[2θ]
small peak at
~33.0° attributed
to pyrite?
NONUMBER
Quartz,
Kaolinit

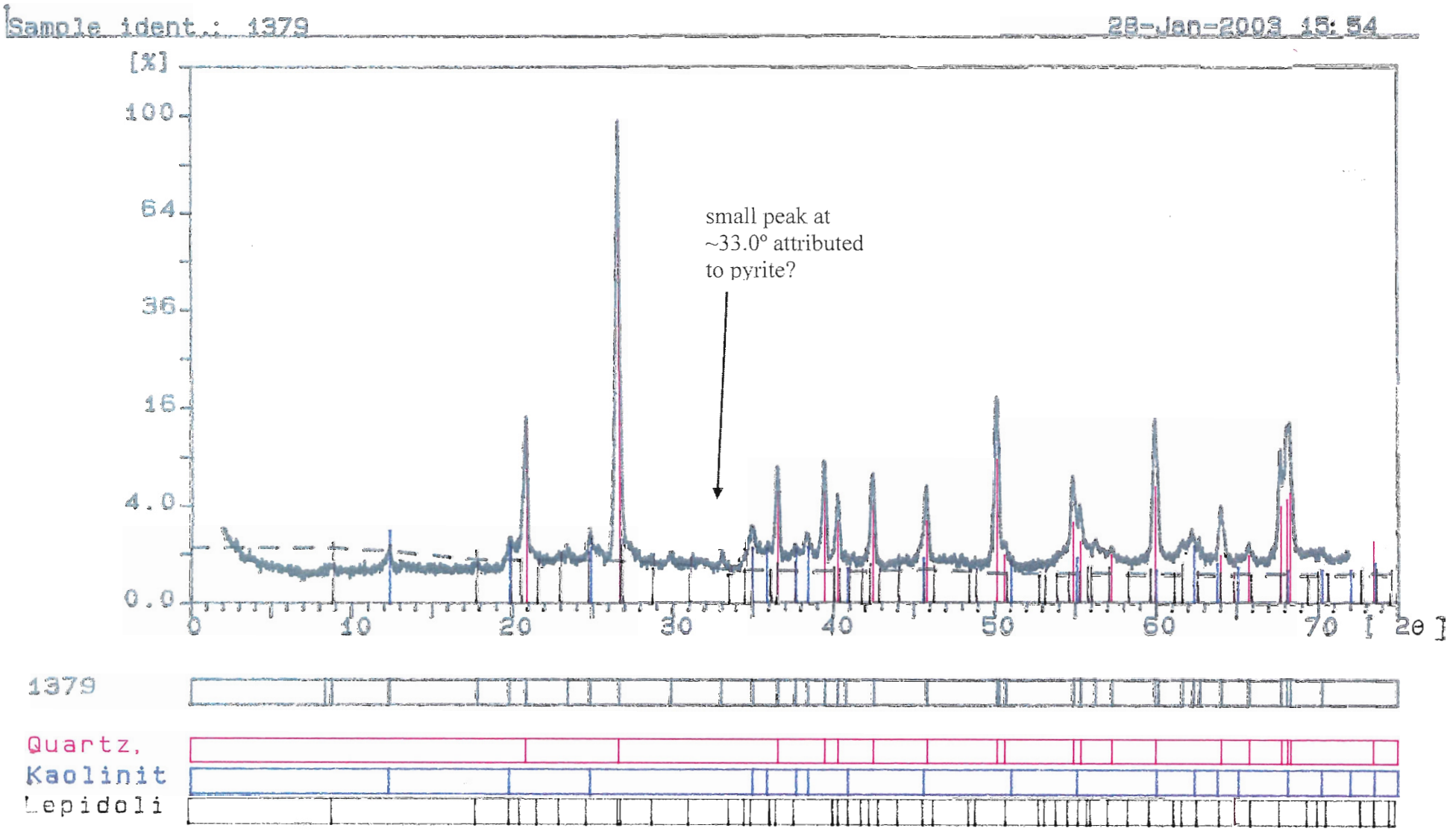
Sample ident.: 1379
28-Jan-2003 15:54
[%]
100
64
36
16
4.0
0.0
0
10
20
30
40
50
60
70
[2θ]
small peak at
~33.0° attributed
to pyrite?
1379
Quartz,
Kaolinit
Lepidoli

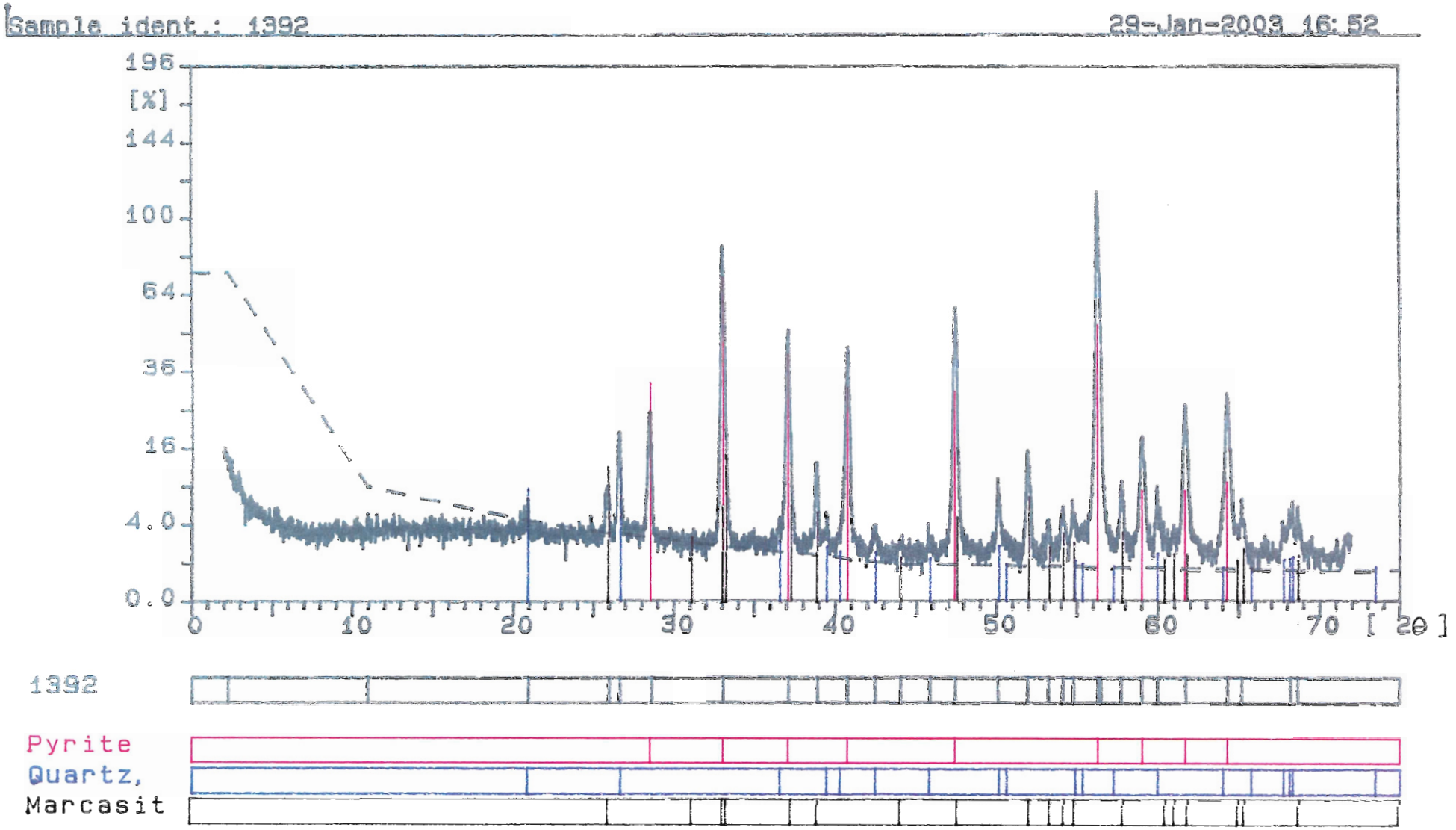
Sample ident.: 1392
29-Jan-2003 16:52
196
[%]
144
100
64
36
16
4.0
0.0
0
10
20
30
40
50
60
70
[2θ]
1392
Pyrite
Quartz,
Marcasit

CHAPTER 4 : INTERPRETATION AND DISCUSSION

4.1 Depositional environment of the Dina formation

4.1.1 Lower lithofacies

The lower lithofacies of Cores 3B and 4A is interpreted as marine-influenced channel deposits. The physical and biogenic sedimentary structures in this lithofacies indicate relatively high-energy, marine-influenced channel deposition, which an estuarine environment describes well (Figure 11). Elliott (1986) defines estuaries as semi-enclosed, coastal bodies of water which are in direct communication with the open ocean *and* fresh-water streams or rivers.

That there is a marine influence in this lithofacies is evident from the *Skolithos* trace fossils, which have black, silty linings. According to Wightman *et al.* (1987), only *Skolithos* burrows formed in marine-influenced environments are lined, and non-marine *Skolithos* burrows are unlined. The *Skolithos* trace fossil assemblage also indicates relatively high-energy conditions as well (Frey & Pemberton, 1984), which are viable in or alongside a channel in an estuarine setting.

Bedding in this lithofacies resembles descriptions of channel deposits in estuarine settings by Reineck & Singh (1986). They describe bedding in these types of deposits as comprising sandstone beds alternating with muddy beds, and the muddy beds generally have scoured top surfaces. This type of bedding is observed in this lithofacies. Reineck & Singh (1986) also describe silt rip-up clasts, ripple cross lamination, and erosional surfaces as common elements of channel deposits, and all of these sedimentary structures are observed in this lithofacies.

The climbing ripple lamination observed in this lithofacies agrees with the interpretation of this lithofacies as comprising channel deposits. Climbing ripple lamination (Figure 7) forms by the lateral migration and aggradation of ripples (by current or wave action) in waters carrying a *high sediment load* (Reineck & Singh, 1986), and implies *rapid sedimentation* (Collinson, 1986). Relatively high sedimentation rates are associated with subaqueous channels of estuarine environments, where sediment-laden waters entering the ocean flare out, slow down, and rapidly deposit their load (Reineck & Singh, 1986). These conditions are conducive to the formation of climbing

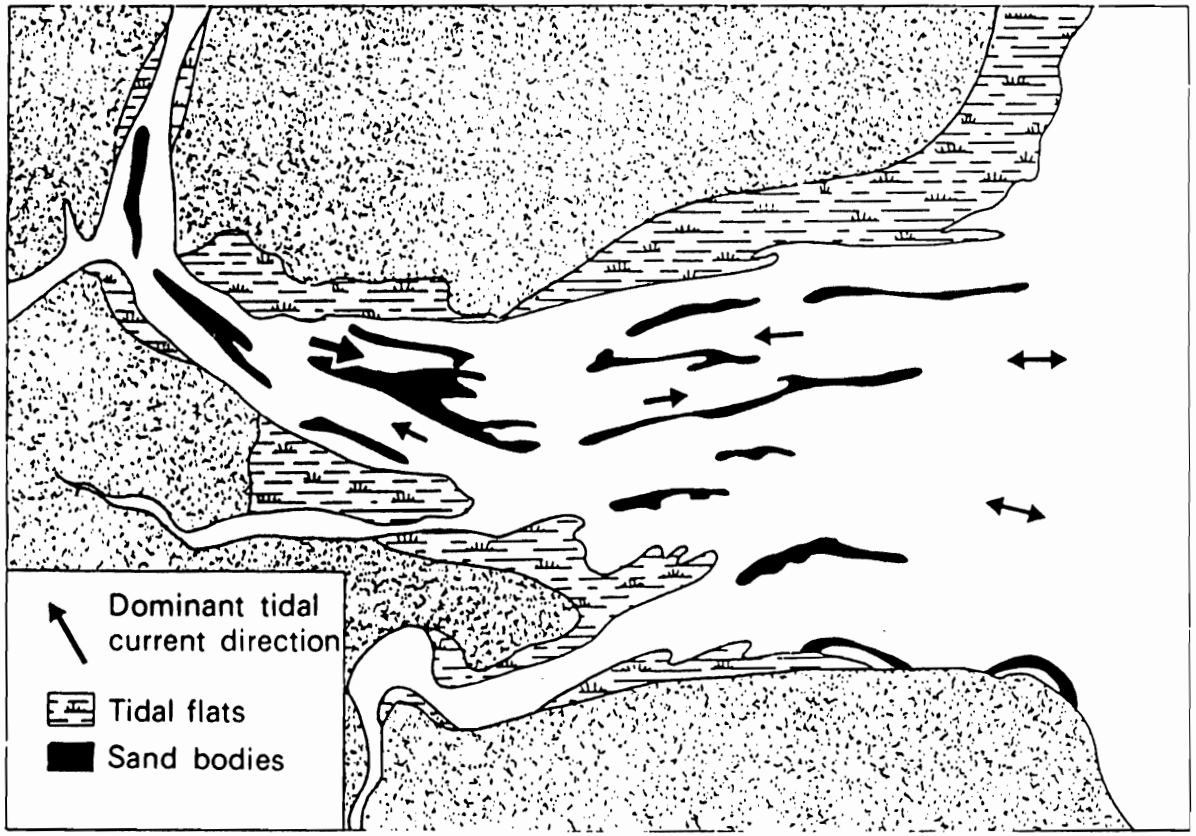

Figure 11 – Schematic diagram of an estuary (from Elliott, 1986).

ripple lamination. It is important to emphasize, however, that climbing ripple lamination is indicative of rapid sedimentation, but is not unique to channel deposits in estuarine environments (as described above). According to Reineck & Singh (1986), climbing ripple lamination forms in environments characterised by rapid sedimentation. It is a common sedimentary structure in subaqueous channel levees, fluvio-lacrustrine lakes, and turbidites (Reineck & Singh, 1986).

The calcium carbonate cement in this lithofacies is interpreted as diagenetic. Results from XRD analysis of sample #1391, together with observations of thin section #1 under the transmitted-light microscope, indicate that the cement is calcite (with accessory dolomite). According to Prothero & Schwab (1996), calcium carbonate (calcite) cement is common in sandstones, and forms during diagenesis by the precipitation of calcium carbonate out of groundwater and into pore spaces as it percolates through. Hopkins (1981) describes calcium carbonate cement in ripple cross-laminated sandstones of the Ellerslie formation (the basal unit of the Mannville Group in central Alberta, correlative with the Dina formation), which suggests that the calcium carbonate cement is a regional diagenetic feature of the basal Mannville Group strata.

4.1.2 Upper lithofacies

The upper lithofacies of the cored intervals in Cores 3B and 4A is interpreted as comprising estuarine tidal flat *and* channel deposits (i.e. subaqueous channel deposits). As with the lower lithofacies, an estuarine setting (Figure 11) explains well the bedding and sedimentary structures observed in this lithofacies. There is also evidence for tidal influence. According to Elliott (1986), tidal effects are associated with estuarine environments, affecting sediment deposition and transport within the estuary, and creating tidal flats along the flanks of the channel mouths. Brackish water is also characteristic of estuaries, and evidence for brackish-water conditions is observed in this lithofacies (discussed below). Estuaries comprise brackish water due to the influx and mixing of terrestrial fresh water with marine waters (Elliott, 1986; Wightman *et al.*, 1987).

The interbedded sandstone and siltstone layers (generally ~1 mm to ~4 cm thick, and including the flaser-, wavy- and lenticular bedding) which dominate this lithofacies are interpreted as tidal flat deposits (probably subtidal). According to Reineck & Singh

(1986), interbedded sandstone and siltstone layers indicate deposition under fluctuating current and wave activity, such as ascribed to tidal flats. Sandy layers (in this case, very fine (upper) to fine (lower)) are deposited during periods of relatively high wave and current activity (higher energy conditions), while the silty-/clay-rich layers are deposited during periods of slack water (Reineck & Singh, 1986).

Flaser bedding is defined as streaks of fine-grained sediment (i.e. mud) preserved within rippled sand, where the 'muddy' streaks do not form continuous laminae (Reineck & Singh, 1986). Lenticular bedding is the opposite, defined as lenses of sandy sediment embedded within muddy (finer-grained) sediment (Reineck & Singh ,1986). Wavy bedding is in the middle, between flaser and lenticular, and is defined as alternating, interbedded, and continuous layers of both sandy and finer-grained sediments (Reineck & Singh, 1986). According to Reineck & Singh (1986), flaser bedding is generally associated with higher-energy tidal environments where the deposition and preservation of sandy sediment is more likely than for finer-grained (muddier) sediment; the opposite holds for lenticular bedding. The gradual increase in silt content upwards through this lithofacies, and the corresponding upwards transition from flaser bedding through to wavy and lenticular bedding, therefore, represent a gradual decrease in energy regime upwards through this lithofacies.

The low-diversity, mixed *Skolithos-Cruziana* trace fossil assemblage described in this lithofacies suggests brackish-water settings (Wightman *et al.*, 1987). Of the trace fossils observed in this lithofacies, those associated with the *Skolithos* ichnofacies include *Skolithos* and *Cylindrichnus* (see Appendix B), and those associated with the *Cruziana* ichnofacies include *Chondrites* and *Zoophycos (*Appendix B*)*. The trace fossils observed in this lithofacies are of low diversity, and dominated by *Planolites* and *Chondrites*, with *Skolithos* rare to common. All other trace fossils are rare and/or questionable. For example, only two *Cylindrichnus* burrows are observed in this lithofacies. As Wightman *et al.* (1987) and Pemberton *et al.* (1992) explain, reduced salinity and salinity fluctuations in brackish-water environments create stressful conditions for marine faunae, resulting in reduced faunal diversity, and a low-diversity trace fossil assemblage. The slight increase in faunal diversity upwards along this lithofacies, therefore, suggests a

slight decrease in stress (i.e. an increase in salinity associated with more marine conditions).

As with the low-diversity trace fossil assemblage, the syneresis crack observed in this lithofacies at ~929.30 m in Core 3B (see Figure 6, Plate 4) also suggests brackish-water conditions. Although there is only one syneresis crack observed, Wightman *et al.* (1987) explain that syneresis cracks are extremely important diagnostic sedimentary structures of brackish-water environments. According to Wightman *et al.* (1987), syneresis cracks are identified by their irregular shape (desiccation cracks are V-shaped in profile; Reineck & Singh, 1986), and form near the sediment-water interface (or substratally) due to fluctuations in water salinity, which induce contraction of some of the crystal lattices in the flocculated clay minerals. The crenulated shape of the syneresis crack indicates that the crack formed *before* significant compaction of the sediments (Wightman *et al.*, 1987), and suggests that this syneresis crack formed at or near the sediment-water interface. The fluctuations in salinity required to form syneresis cracks require large volumes of fresh water discharged into the sea (Wightman *et al.*, 1987), which is a characteristic feature of estuarine environments (Elliott, 1986).

The relatively clean sandstone beds (less than ~35 cm thick) interspersed throughout this lithofacies are interpreted as channel sands deposited on the tidal flat (i.e. subaqueous channel deposits). Very similar sandstone beds are described by Rennie (1987), who describes relatively clean sandstone beds interbedded with tidal flat deposits in the McMurray formation of eastern Alberta (which is correlative with the Dina formation). Rennie (1987) describes these sandstone beds as relatively clean, planar-bedded, generally less than ~30 cm thick, and alternating with intervals of muddy and burrowed tidal flat deposits up to ~0.8 m thick. He interprets these sandstone beds as channel sands deposited on a tidal flat, and concludes that they were deposited under relatively higher energy conditions than the tidal flat deposits. Rennie (1987) suggests these channel sands were deposited during periodic storm and flooding events, when channels emptying into the estuary discharged sediments further seaward than usual, and out onto the tidal flats. The relatively clean sandstone beds in this upper lithofacies (described in section 3.1.2) are very similar to the channel sands described by Rennie (1987), and are interpreted as such. Evidence to support that they too were deposited

under relatively high-energy conditions include their relatively clean sand content, their sharp bottom contacts (scoured in some cases) with underlying silty laminae, and silt rip-up clasts suspended within some of the sandstone beds.

The interpretation of this lithofacies as comprising estuarine tidal flat and channel deposits is supported by the evidence above. There is also evidence in this lithofacies for Aptian transgression. The upwards decrease in energy regime (as interpreted earlier in this section from the upwards increase in silt content), and the upwards increase in water salinity (as interpreted earlier in this section from the upwards increase in faunal diversity), together suggest an increase in marine influence and ocean water depth with time, which is attributed to Aptian transgression through the Belshill Lake Channel.

4.1.3 Discussion of the boundary separating the two lithofacies

In this thesis, the boundary between the two lithofacies is defined by the disappearance of calcium carbonate cement from the sandstone, which is interpreted as diagenetic. Comparison of the sedimentary structures and bedding above and below the top of the 'cement' boundary shows that this boundary works well (in the study area) as the lithofacies boundary. For example, climbing ripple lamination is observed below, and the interbedded sandstone and siltstone layers above. It is unclear, however, as to why the calcium carbonate cement is present in only the lower lithofacies, and not the upper one as well.

Perhaps the silty laminae and increased silt content of the upper lithofacies acted as a barrier to water flow during diagenesis, and prevented groundwater from percolating through. Evidence to support this comes from Box 7, Core 3B (at approximately 932.55 m), where the calcium carbonate cement disappears rapidly (over an interval of ~10 cm) directly above a nearly continuous, silty lamina (less than ~1 cm thick). Directly below this silty layer, cementation of the sandstone is very high. This suggests the silty layer acted as a barrier preventing carbonate-bearing groundwater from moving upwards into the overlying sediments. In Core 4A, however, the cement abruptly disappears over a core break (at 933.45 m) between two clean sandstones with no silty laminae seen nearby, and it is difficult, therefore, to explain why the cement suddenly disappears there.

Hopkins (1981) describes calcium carbonate cement in ripple cross-laminated sandstones of the Ellerslie formation (the basal unit of the Mannville Group in central

Alberta, correlative with the Dina formation). This suggests the calcium carbonate cement is a regional diagenetic feature of the basal Mannville Group strata. The Wainwright and Kindersley paleo-topographic highs, which flanked the Belshill Lake Channel during deposition of the Dina formation, are a possible source of $CaCO_3$ for the groundwater, because according to Smith (1994) and Hayes *et al.* (1994), both paleo-topographic highs comprised Devonian carbonates.

4.3 Provenance of the Dina formation

Mineralogy of the sandstone in the Dina formation precludes a Cordilleran provenance, and suggests derivation from the Canadian Shield. Mineral grains such as chert fragments and volcanic lithics, which are diagnostic of Cordilleran provenance (Cant, 1989; Jackson, 1984), are not observed in sandstones of the Dina formation (Table 3). Instead, the sandstone is highly quartzose (greater than 90% quartz), and contains accessory zircon, muscovite, and feldspar grains (see Table 3 and Figure 9), all of which suggest derivation from the Canadian Shield to the east (Cant, 1989; Hopkins, 1981; Williams, 1963, see section 1.6). This suggests the Belshill Lake Channel and the Dina formation were part of the eastern paleo-valley system described by Hayes *et al.* (1994), which drained off of the Canadian Shield into the basin.

It is unclear, however, whether the paleo-topographical highs of the WCSB (such as the Pembina High) contributed sediments to the Dina formation. As Figures 1B and 4 show, the Dina formation was deposited in a valley (the Belshill Lake Channel) between two paleo-topographical highs, the Kindersley and Wainwright. As Figure 4 shows, the Pembina paleo-high was situated ~300 km northwest of the Belshill Lake Channel. During deposition of the Dina formation (Aptian time), the Pembina paleo-high comprised Jurassic clastics, the Wainwright comprised Devonian carbonates, and the Kindersley was composed of both Jurassic clastics and Devonian carbonates (Smith, 1994 and Hayes *et al.*, 1994). Jackson (1984) describes sediments derived from Jurassic strata of some of the paleo-highs in the WCSB as mature and quartzose, and, therefore, it is possible that some of the quartz grains in the Dina formation represent sediments derived from Jurassic strata of the Pembina and Kindersley paleo-highs.

4.4 Distribution of the oil-stained sandstone beds in the Dina formation

The distribution of oil-stained sandstone beds in Cores 3B and 4A indicates that oil distribution in the Dina formation is lithofacies-dependent, and restricted to the upper lithofacies. All of the oil-stained sandstone beds are observed in the upper lithofacies. Seals for many of these oil-stained sandstone beds are defined by silty laminae of tidal flat deposits. As Table 2 shows, however, many of the oil-stained sandstone beds are directly overlain by a core break, followed by sandstone (which is clean and not oil-stained, see Plate 10 of Figure 6 for an example). In these cases, it is unclear as to what seals the oil within the sandstone bed below the core break, and the core breaks may represent small gaps of missing core (i.e. the missing silty 'seal' layers).

There are two possible scenarios which explain why the oil is restricted to the upper lithofacies. The first scenario is that precipitation of calcareous cement in the lower lithofacies *before* emplacement of oil within the Dina formation reduced porosity and inhibited migration of oil into the lower lithofacies. If this scenario is correct, and oil migrated into the Dina formation *after* precipitation of the calcareous cement in the lower lithofacies, then it is difficult to explain why relatively porous intervals of the lower lithofacies (i.e. less cement) are not occupied by oil as well. The second scenario is that the lithofacies boundary (defined by the disappearance of calcium carbonate cement in the sandstone) defines the paleo oil-water contact, in which case the oil is restricted to the upper lithofacies because of buoyancy and density effects (oil floats on water). If this scenario is true, then the calcium carbonate cement precipitated out into only the lower lithofacies because it was flushed with groundwater, while the upper lithofacies filled with oil.

It is evident from Table 2 that thickness of the oil-stained bed or 'interval' (i.e. multiple layers of interbedded siltstone and oil-stained sandstone) does not determine the OSI value. For example, channel sandstone beds greater than 30 cm thick in Core 4A have OSI values ranging from 1.0 to 3.0, while oil-stained intervals of tidal flat deposits 5 cm thick in Core 3B have OSI values ranging from 0.5 to 3.0 (Table 2).

Table 4 is a modified version of Table 2, and provides further insight into the distribution of oil within the Dina formation. Table 4 lists the oil-stained sandstone beds according to their OSI value, in descending order, and also lists (using the interpretations

made in section 4.2.1) whether the oil-stained sandstone beds are a tidal flat deposit (T) or a channel sand (C). Brief notes useful in making this interpretation are included in Table 4 as well (i.e. flaser bedding suggests a tidal flat deposit).

The most important feature of Table 4 is that most of the oil-stained sandstone beds are channel sands. These also generally have higher OSI values than the tidal flat deposits (Table 4). The channel sands make better reservoir rock because they are relatively cleaner than the tidal flat deposits and, therefore, have higher porosity.

4.5 Well log correlation and interpretation

The well logs for the cored intervals in Cores 3B and 4A are correlated and interpreted in Figure 13. Figure 12 is a useful and brief summary of well log interpretation, and Appendix D provides more detailed background information regarding individual log responses (i.e. gamma ray versus spontaneous potential, deep induction versus spherically focused induction). In Figure 13, the stratigraphic datum used to hang the sections is defined by the Ostracode zone (the maximum flooding surface; Cant & Abrahamson, 1996), which in both cores comprises ~1 m of interbedded calcareous shales and limestones. According to Jackson (1984), the Ostracode zone is often used as a datum in the WCSB because it is easily identified on well logs and regionally extensive in central and southern Alberta. The cored intervals for Cores 3B and 4A are highlighted in black alongside the well logs in Figure 13, and formation boundaries of the Ostracode zone and Dina formation are also included to facilitate correlation.

The Dina formation exhibits very similar log responses in both wells, and correlates very nicely. The important features of the well log correlation are discussed next, beginning at the bottom of the cored intervals. At the bottom of the cored intervals, there is a spike in resistivity which begins below the lower limit of the cored intervals, and extends up to ~934 m in both cores. All three induction logs (ILM, ILD, and SFLU) record this resistivity spike, although it shows up best on the SFLU log (solid line). This resistivity spike represents the calcium carbonate cemented sandstone of the lower lithofacies. The cement increases resistivity of the sandstone by occupying pore spaces and decreasing porosity. The upper boundary of the spike (~934 m) coincides (approximately) with the upper boundary of the cemented sandstone in the cores (933.25

Table 4 : Oil-stained sandstone beds in Cores 3B and 4A (from Table 2), listed in descending order of OSI value.

Oil Stain Index (OSI)	Thickness (cm)	Interval (m)	Notes	Tidal flat (T) or channel (C) deposit?
			CORE 3B	
3.0	5	925.69-925.74	very clean	C
2.5	9	926.87-926.96	*Skolithos* traces, ripple foresets, relatively clean	C
2.0	11	925.58-925.69	*Skolithos* traces, ripple foresets, relatively thick	C
1.5	5	927.34-927.39	*Skolithos* traces, very clean, relatively thick	C
1.0	9	926.76-926.85	ripple foresets (?), relatively clean	C
1.0	6	927.28-927.34	flaser bedding	T
1.0	5	921.30-921.35	very clean	C
1.0	4	924.09-924.13	flaser bedding	T
0.5	13	926.01-926.14	interlayered silty and sandy laminae	T
0.5	5	925.49-925.54	flaser bedding	T
0.5	5	927.14-927.19	flaser bedding	T
0.5	3	925.43-925.46	flaser bedding	T
0.5	2	924.51-924.53	flaser bedding	T
			CORE 4A	
3.0	29	927.14-927.43	high silt content throughout	T
3.0	26	929.30-929.56	very clean	C
3.0	23	928.43-928.66	ripple foresets and wave-ripple cross lamination	C
3.0	22	930.09-930.31	*Skolithos* traces, ripple foresets, relatively clean	C
3.0	18	928.23-928.41	ripple foresets, relatively thick	C
3.0	18	928.85-929.03	wave-ripple cross lamination, *Skolithos* traces	C
3.0	17	931.11-931.28	relatively clean	C
3.0	16	931.80-931.96	relatively thick, relatively clean	C
3.0	11	928.05-928.16	very clean	C
3.0	8	932.05-932.13	very clean	C
2.5	36	925.54-925.90	ripple foresets and relatively thick	C
2.5	23	926.07-926.30	clean sandstone and relatively thick	C
2.5	19	925.11-925.30	flaser bedding, high silt content throughout	T
2.5	10	932.20-932.30	*Skolithos* traces, very clean sandstone	C

Table 4 (cont.).

Oil Stain Index (OSI)	Thickness (cm)	Interval (m)	Notes	Tidal flat (T) or channel (C) deposit?
			CORE 4A	
2.5	9	925.33-925.42	flaser bedding, high silt content throughout	T
2.5	6	931.54-931.60	very clean	C
2.5	3	924.28-924.31	very clean	C
2.5	3	926.69-926.72	*Skolithos* traces, very clean	C
2.5	3	926.83-926.86	*Skolithos* traces, relatively clean	C
2.5	3	928.00-928.03	relatively clean	C
2.5	2	926.57-926.59	*Skolithos* traces, very clean	C
2.0	24	927.64-927.88	*Skolithos* traces, very clean	T
2.0	10	931.60-931.70	interlayered silty and sandy laminae	T
2.0	7	926.92-926.99	very clean sandstone, ripple foresets	C
2.0	4	930.70-930.74	relatively clean	C
1.5	6	927.08-927.14	interlayered silty and sandy laminae	T
1.5	2	928.03-928.05	interlayered silty and sandy laminae	T
1.0	35	929.56-929.91	high silt content throughout, flaser bedding	T
1.0	21	924.71-924.92	interlayered silty and sandy laminae	T
1.0	7	932.13-932.20	very clean	C
1.0	4	924.45-924.49	flaser bedding	T
1.0	2	932.30-932.32	relatively clean	C
0.5	12	930.58-930.70	interlayered silty and sandy laminae	T
0.5	11	930.82-930.93	interlayered silty and sandy laminae	T
0.5	5	926.40-926.45	interlayered silty and sandy laminae	T
0.5	4	925.90-925.94	interlayered silty and sandy laminae	T

m in Core 3B, 933.45 m in Core 4A), and so the upper boundary of this resistivity spike, therefore, defines the boundary between the two lithofacies of the Dina formation discussed in section 4.1.3. The discrete width of the spike (~2 m in Core 3B, ~4 m in Core 4A) suggests that the calcium carbonate cement does not pervade the entire Dina formation below the cored intervals, but that it disappears abruptly at ~936 m in Core 3B, and ~938 m in Core 4A. Very similar log responses are observed in the density and neutron porosity logs (DPHI and NPHI), which record a spike of significantly decreased porosity (attributed to the calcium carbonate cement in the sandstone) from ~933-936 m in Core 3B, and ~934-938 m in Core 4A.

Moving upwards along the Dina formation, the gamma ray (GR) and spontaneous potential (SP) logs both gradually climb to the right. These indicate a gradual, upwards increase in shale content (GR log) and a gradual, upwards decrease in permeability (SP log). The gradual increase in shale content is confirmed by the core descriptions (see section 3.1.2), in which silt content (i.e. shale content) gradually increases upwards along the Dina formation. The upwards decrease in permeability, as recorded by the SP log, is also attributed to the upwards increase in silt content.

The oil-stained sandstone beds of the Dina formation are also recorded on the induction (resistivity) logs of Figure 13. The several metres over which oil-stained sandstone beds are concentrated within the cores (~924-928 m in Core 3B, ~923-932 m in Core 4A, see Table 2) show up as relative high values on the induction logs (oil is a poor conductor). Although nearly all of these oil-stained beds are too thin (i.e. less than ~35 cm) to resolve individually on induction logs (including the SFLU), their cumulative thicknesses (>3 m) show up nicely on the induction logs. Using this as rudimentary calibration, it appears that significant accumulations of oil *do not* exist below the cored intervals, because the resistivity values on the well logs progressively decrease with depth.

At the tops of the cored intervals, in the Ostracode zone, the gamma ray (GR) logs for both cores show a well-defined spike to the left (~918-920 m for Core 3B, ~922-923 m for Core 4A), which is typical of carbonates (micritic limestone in this case). Most of the Ostracode zone, however, comprises shale (for example, approximately 70% shale and 30% micritic limestone in Core 3B), and so it is unclear why the shale is not reflected

in the GR logs (as a spike to the right). The thickness of the Ostracode zone in both cores (>1 m) is within resolution of the GR log, but perhaps the shale beds are low in K, U, and Th. There is consistency in the well logs, however, in that the Ostracode zone shows a well-defined spike to the left *in both cores*. The Ostracode zone also displays moderately- to well-defined spikes of high resistivity on the SFLU logs, and very well-defined spikes of low porosity on the DPHI logs, from ~918-920 m in Core 3B, and ~922-923 m in Core 4A. These are typical well log responses of carbonates.

It is interesting to note that the well logs in Figure 13 show the approximate thickness of the Dina formation in the study area. According to Hayes (1994), the Dina formation is less than ~20 m thick in the study area. The boundary defining the bottom of the Dina formation and its contact with the underlying Devonian carbonates is observed on the well logs at ~942 m in Core 3B, and ~944 m in Core 4A, making the Dina formation in the study area approximately 21 m thick. This boundary is defined (moving down the well logs) by 1) abrupt deflection of the spontaneous potential (SP) log to the right (indicating a significant decrease in permeability), 2) deflection of the induction logs (ILM, ILD, and SFLU) to the right (indicating an increase in resistivity, i.e. a decrease in porosity or the presence of hydrocarbons), and 3) deflection of the gamma ray (GR) log to the right (indicating an increase in shale content). These three log responses are reasonable for carbonates. According to Prothero & Schwab (1996), limestones (i.e. carbonates) exhibit low permeability (unless porous or fractured), and also have high resistivities because of relatively high densities. The third log signature (deflection of the GR log to the right), however, indicates that the underlying Devonian carbonate rocks contain significant amounts of shale. One possible explanation for this is that the underlying Devonian carbonate rocks comprise interbedded shales and limestones.

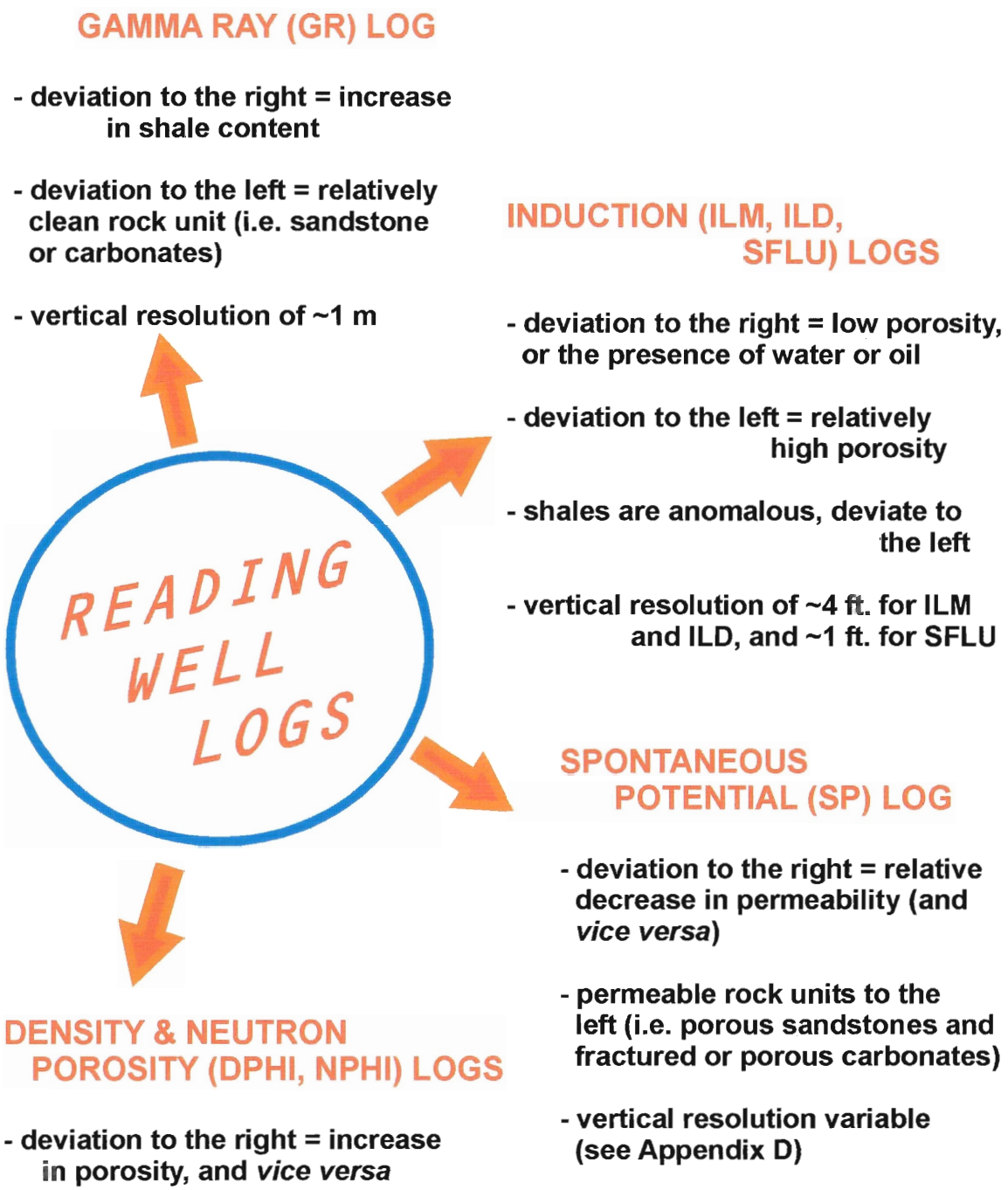

Figure 12 - Summary of well-log interpretation (sources: Dewan, 1983; Prothero & Schwab, 1996).

Figure 13 (*following two pages*) – Well-log correlations for Cores 3B and 4A. Black bars denote the cored intervals. The first page correlates the gamma ray (GR) and porosity (DPHI, NPHI) logs, and the second page correlates the spontaneous potential (SP) and induction (ILM, ILD, and SFLU) logs.

SUNCOR et al. PROVOST

WELL : 3B-23-36-6W4 ← **<500 m** → **WELL : 4A-23-36-6W4**

CORE 3B

Ostracode zn. = 918.33 - 919.91 m

Dina fm. = 919.91 - 933.25 m (and extends below the cored interval)

CORE 4A

Ostracode zn. = 922.61 - 923.40 m

Dina fm. = 923.40 - 937.60 m (and extends below the cored interval)

(Cant & Abrahamson, 1996) MFS

stratigraphic datum = base of Ostracode zn. (Jackson, 1984)

GR (upwards increase in shale content)

lithofacies boundary

GR

$CaCO_3$ cement = low porosity values

regional unconformity (sequence boundary)

bottom of Dina fm.

defined by (moving down the logs) :

- abrupt increase in GR log

- highly variable and lowered DPHI and NPHI logs

= cored interval

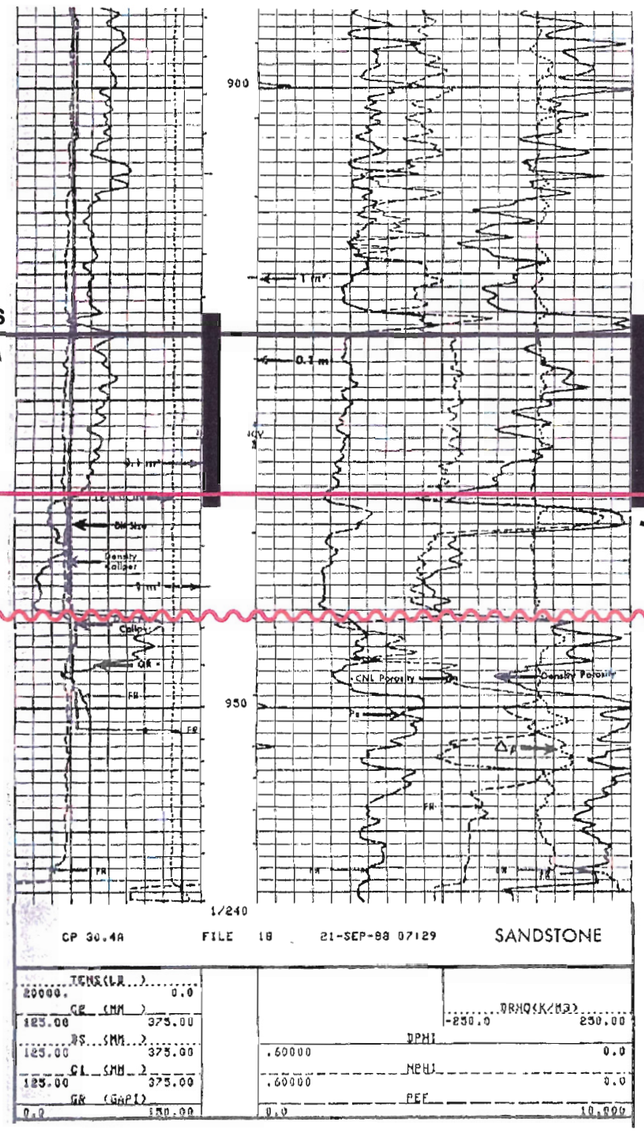

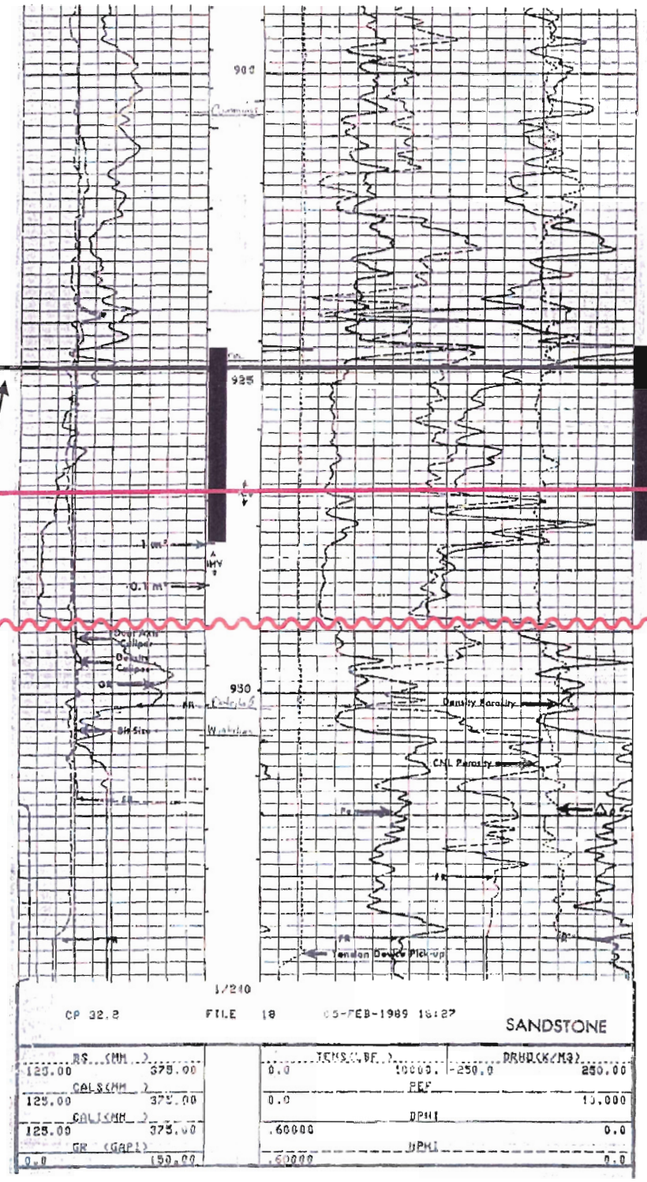

SUNCOR et al. PROVOST

CORE : 3B-23-36-6W4 ← **<500 m** → **CORE : 4A-23-36-6W4**

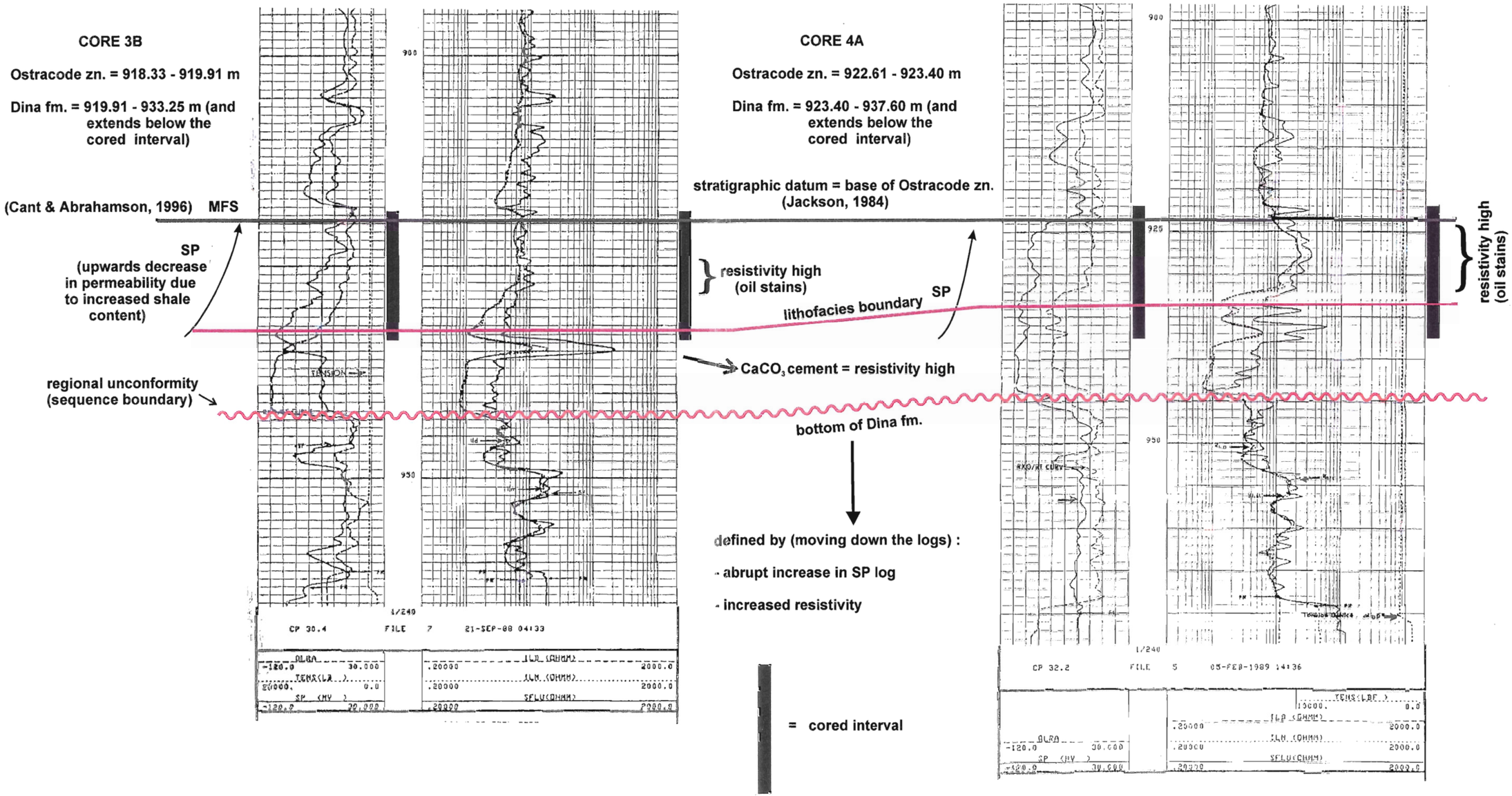

CHAPTER 5 : CONCLUSIONS

5.1 Conclusions

1) The Dina formation of east-central Alberta (Belshill Lake Channel area) was deposited in an estuarine environment (Figure11). The lower lithofacies of the cored intervals comprises marine-influenced channel deposits, and the upper lithofacies comprises brackish-water tidal flat and channel deposits.

2) The Dina formation in the study area records an upwards decrease in energy regime and an upwards increase in marine influence, attributed to Aptian transgression of the Western Canada Sedimentary Basin and the Belshill Lake Channel.

3) Mineralogy of sandstone units in the Dina formation indicates a Canadian Shield provenance, and suggests the Belshill Lake Channel was part of the regional paleo-valley system which drained off of the Canadian Shield and into the eastern margin of the WCSB (as described by Hayes *et al.*, 1994). It remains unclear, however, if the Dina formation of the Belshill Lake Channel includes sediments derived from the Pembina, Wainwright, and Kindersley paleo-highs as suggested by Jackson (1984), although it is possible that some of the quartz in the Dina formation is derived from Jurassic strata of the Pembina and Kindersley paleo-topographic highs.

4) The distribution of oil-stained sandstone beds indicates that oil distribution in the Dina formation is lithofacies dependent. Resistivity values on the well logs support this. Oil stains in the Dina formation are restricted to the upper lithofacies, and concentrated within channel sands. These channel sands are relatively clean (i.e. low silt content), porous, and, therefore, have the greatest reservoir potential.

5) Well logs for the two cores suggest the Dina formation in the study area is ~21 m thick, which is close to the thickness suggested by Hayes *et al.* (1994) of less than ~20 m. The cored intervals of Cores 3B and 4A comprise the top ~14 m of the Dina formation.

The interpretation made in this thesis of the Dina formation as comprising estuarine deposits agrees with interpretations made by M. Sherwin and R. W. MacDonald in the study area (see Riediger *et al.*, 1999), although the specific lithofacies which they describe vary slightly from those observed in Cores 3B and 4A. They describe the Dina

formation (in the study area) as comprising fresh-water meandering channel deposits on the bottom which grade upwards into estuarine channel complexes on top, and which exhibit an overall upwards increase in marine influence (Riediger *et al.*, 1999). These features, except for the fresh-water meandering channel deposits, are seen in Cores 3B and 4A. Marine-influenced channel deposits are observed at the bottom of the cored intervals, and it is possible that fresh-water meandering channel (i.e. fining upwards) deposits exist below the cored intervals, in the ~7 m of the Dina formation not represented in the cored intervals.

Mineralogical observations presented in this thesis differ substantially from those made by M. Sherwin and R. W. MacDonald (see Riediger *et al.*, 1999). This thesis contends that no chert fragments are observed in the three thin sections from the Dina formation in Core 3B, but according to M. Sherwin and R. W. MacDonald, sandstones of the Dina formation contain significant amounts of both light and dark chert (Riediger *et al.*, 1999), which is diagnostic of Cordilleran provenance (Cant, 1989; Jackson, 1984; Hayes *et al.*, 1994). This thesis presents evidence which suggests provenance from the crystalline Canadian Shield instead.

That the Dina formation is derived from the Canadian Shield is supported by other authors, who interpret a similar provenance for other basal rock units of the Mannville Group in central and eastern Alberta (close to the study area of this thesis). Hopkins (1981) concludes Canadian Shield provenance for the Ellerslie formation in central Alberta, and Cant (1989) concludes Canadian Shield provenance for the McMurray formation of (north)eastern Alberta. That the Ellerslie formation of central Alberta exhibits a Canadian Shield influence suggests the Dina formation is derived from the east as well, if one assumes the region *east* of central Alberta (i.e. the Ellerslie formation) represents the region receiving sediments derived from the Canadian Shield.

A complex fluvial drainage system in the Belshill Lake Channel is one possible explanation for the different mineralogical observations made between this thesis and M. Sherwin and R. W. MacDonald (Riediger *et al.*, 1999). The Dina formation was deposited on a regional unconformity, and it is possible that the relief of this paleo-topography created complex drainage systems. Perhaps channels draining different

regions of the WCSB emptied into the Belshill Lake Channel, depositing sediments derived from different sources (i.e. the Cordillera versus the Canadian Shield).

5.2 Further work and recommendations

The presence, or lack of, chert fragments in the Dina formation must be confirmed in order to accurately determine provenance of the Dina formation in the Belshill Lake Channel. According to Nesse (1991), chert fragments in thin section appear as aggregates of micro-crystalline quartz grains. These are not seen in the three thin sections from Core 3B. The reader is reminded, however, that only three thin sections from one core (Core 3B) in the study area are described and interpreted in this thesis, making for a limited data set.

The reader is also reminded that in this thesis, Core 3B refers to Core 2 of Well 3B-23-36-6W4. There is another core, Core 1 of the same well, which comprises over 10 m of the overlying Cummings formation, and which directly overlies Core 2, separated by only 10 cm of missing core. (The bottom of Core 1 is at 918.15 m, and the top of Core 2 is at 918.25 m.) Work should be done to establish the provenance of this 'Cummings' core, its depositional environment(s), and its relationship with the local sequence stratigraphic framework. Abundant lithic fragments in some of the sandstone beds of this Cummings core suggest a Cordilleran provenance (or significant contribution). This Cummings core overlies the Ostracode zone (maximum flooding surface; Cant & Abrahamson, 1996), and is, therefore, part of a different sequence than the underlying Dina formation. The Cummings core comprises grey sandstone (very fine (upper) to very coarse (lower)), with abundant organic material and lithic fragments (angular to rounded, up to ~3 mm wide), very few biogenic sedimentary structures (there are rare to common *Skolithos* traces near the top of the formation), and no oil-stained sandstone beds. This Cummings core is very different from the underlying Dina formation. Together, the two cores from Well 3B (Cores 1 and 2) provide a unique opportunity to study ~30 metres of continuous core, and this thesis has laid the foundation for such work.

The interpretation made in this thesis that brackish-water conditions prevailed during deposition of the upper lithofacies of the Dina formation can be further substantiated using a method outlined by Wightman *et al.* (1987). Wightman *et al.*

(1987) suggest using diagenetic minerals in cores as paleo-salinity indicators, in order to constrain salinity conditions during sediment deposition. According to Wightman *et al.* (1987), diagenetic pyrite and siderite, observed together, imply brackish-water conditions existed during sediment deposition, *if it can be established that the two minerals formed during early diagenesis*. (Wightman *et al.* (1987) report that one diagnostic feature of pyrite or siderite formation during early diagenesis is differential compaction around siderite or pyrite nodules.) Micro-crystalline patches of pyrite are rare to abundant throughout both lithofacies of Cores 3B and 4A, although it is not established if this formed during early diagenesis. The presence of siderite is, as of yet, unconfirmed. Work should be done to assess the presence of early diagenetic pyrite and siderite in Cores 3B and 4A, in order to confirm that brackish-water (i.e. estuarine) conditions prevailed during deposition of the Dina formation as described in this thesis.

The two cores described in this thesis comprise the upper ~14 m of the Dina formation, which is ~21 m thick in the study area. If the lower ~7 m are available, they should be described, interpreted, and integrated with this thesis, and used to confirm observations made by M. Sherwin and R. W. MacDonald (see Riediger *et al.*, 1999), that fresh-water meandering channel deposits exist in the basal portion of the Dina formation.

Finally, the correlation of lithofacies and well logs described in this thesis from Cores 3B and 4A should be correlated with more wells from the region, in order to increase the size of the data set, and to confirm and constrain observations made in this thesis. For example, is the calcareous cement observed in the lower lithofacies regional in distribution? The two wells correlated in this thesis are less than 0.5 km apart, and offer a relatively limited transect of the Belshill Lake Channel, but the detailed core descriptions and well log correlations presented in this thesis lay the groundwork for future correlation with other wells from the region.

REFERENCES

- Alspatch, S. 2002. Introduction to log analysis and mapping. Short course notes from the Student Industry Field Trip, 2002, Calgary, Alberta, p. 1-15.

- Cant, D. J. 1989. Chapter 11, Zuni Sequence : the Foreland Basin, Lower Zuni Sequence : Middle Jurassic to Middle Cretaceous. *In* : Western Canada Sedimentary Basin, A Case History. B. D. Ricketts (ed.). Canadian Society of Petroleum Geologists, p. 251-284.

- Cant, D. J. and Abrahamson, B. 1996. Regional distribution and internal stratigraphy of the Lower Mannville. Bulletin of Canadian Petroleum Geology, vol. 44, no. 3, p. 508-529.

- Collinson, J. D. 1986. Alluvial Sediments. *In* : Sedimentary Environments and Facies, Second Edition. H. G. Reading (ed.). Blackwell Scientific Publications, p. 20-62.

- Dewan, J. T. 1983. Essentials of Modern Open-Hole Log Interpretation. PennWell Publishing Company, USA, pp. 361.

- Elliott, T. 1986. Siliciclastic Shorelines. *In* : Sedimentary Environments and Facies, Second Edition. H. G. Reading (ed.). Blackwell Scientific Publications, p. 155-188.

- Frey, R. W. & Pemberton, S. G. 1984. Trace Fossil Facies Models. Facies Models, Second Edition. Geoscience Canada, Reprint Series 1, p. 189-207.

- Hayes, B. J. R., Christopher, J. E., Rosenthal, L., Los, G., McKercher, B., Minken, D., Tremblay, Y. M., Fennell, J., and Smith, D. G. 1994. Cretaceous Mannville Group of the Western Canada Sedimentary Basin. *In* : Geological Atlas of the Western Canada Sedimentary Basin, G. D. Mossop and I. Shetsen (comps.). Canadian Society of Petroleum Geologists and Alberta Research Council, p. 317-334.

- Hopkins, J. C. 1981. Sedimentology of quartzose sandstones of Lower Mannville and associated units, Medicine River area, central Alberta. Bulletin of Canadian Petroleum Geology, vol. 29, no. 1, p. 12-41.

- Jackson, P. C. 1984. Paleogeography of the Lower Cretaceous Mannville Group of Western Canada. *In* : Elmworth : Case Study of a Depp Basin Gas Field. A. J. Masters (ed.). American Association of Petroleum Geologists, p. 49-77.

- Johnson, H. D. & Baldwin, C. T. 1986. Shallow Siliciclastic Seas. *In* : Sedimentary Environments and Facies, Second Edition. H. G. Reading (ed.). Blackwell Scientific Publications, p. 229-282.

- Leckie, D. A. and Reinson, G. E. 1993. Effects of Middle to Late Albian sea-level fluctuations in the Cretaceous Interior Seaway, western Canada. *In* : Evolution of the Western Interior Basin, W. G. E. Caldwell and E. G. Kauffman (eds.). Geological Association of Canada, Special Paper 39, p. 151-175.

- Mossop, G. and Shetsen, I. 1994. Introduction to the Geological Atlas of the Western Canada Sedimentary Basin. *In* : Geological Atlas of the Western Canada Sedimentary Basin, G. D. Mossop and I. Shetsen (comps.). Canadian Society of Petroleum Geologists and Alberta Research Council, p. 1-11.

- Nesse, W. D. 1991. Introduction to Optical Mineralogy, Second Edition. Oxford University Press, Inc., pp. 335.

- Pemberton, S. G. 1989. Ichnology : the study of animal-sediment interactions. Short course notes, pp. 159.

- Pemberton, S. G., MacEachern, J. A. & Frey, R. W. 1992. Trace Fossil Facies Models : Environmental and Allostratigraphic Significance. *In* : Facies Models : Response to Sea Level Change, R. G. Walker & N. P. James (eds.). Geological Association of Canada, p. 47-73.

- Pemberton, S. G. & Wach, G. D. 1998. Core Atlas of Trace Fossil Descriptions. Private publication by Texaco Exploration and Production Technology Team, pp. 80.

- Podruski, J. A., Barclay, J. E., Hamblin, A. P., Lee, P. J., Osadetz, K. G., Procter, R. M. & Taylor, G. C. 1987. Part I : Resource Endowment. *In* : Conventional Oil Resources of Western Canada, Light and Medium. Geological Survey of Canada, paper 87-26, p. 7-125.

- Price, R. A. 1994. Cordilleran tectonics and the evolution of the Western Sedimentary Basin. *In* : Geological Atlas of the Western Canada Sedimentary Basin, G. D. Mossop and I. Shetsen (comps.). Canadian Society of Petroleum Geologists and Alberta Research Council, p. 13-25.

- Prothero, D. R. & Schwab, F. 1996. Sedimentary Geology : An Introduction to Sedimentary Rocks and Stratigraphy. W. H. Freeman and Company, pp. 575.

- Reineck, H.-E. & Singh, I. B. 1986. Depositional Sedimentary Environments with Reference to Terrigenous Clastics : Second, Revised and Updated Version, Corrected Second Printing. Springer-Verlag, pp. 551.

- Rennie, J. A. 1987. Sedimentology of the McMurray formation on the Sandalta project study area, northern Alberta, and implications for oil sands development. *In* : Reservoir Sedimentology, R. W. Tillman & K. J. Weber (eds.). Society of Economic Paleontologists and Mineralogists, Special Publication no. 40, p. 169-188.

• Riediger, C. L., MacDonald, R., Fowler, M. G., Snowdon, L. R., and Sherwin, M. D. 1999. Origin and alteration of Lower Cretaceous Mannville Group oils from the Provost oil field, east central Alberta, Canada. Bulletin of Canadian Petroleum Geology, vol. 47, no. 1, p. 43-62.

• Smith, D. G. 1994. Paleogeographic Evolution of the Western Canada Foreland Basin. *In* : Geological Atlas of the Western Canada Sedimentary Basin, G. D. Mossop and I. Shetsen (comps.). Canadian Society of Petroleum Geologists and Alberta Research Council, p. 277-296.

• Stott, D. F. 1984. Cretaceous sequences of the foothills of the Canadian Rocky Mountains. *In* : The Mesozoic of Middle North America, D. F. Stott and D. J. Glass (eds.). Canadian Society of Petroleum Geologists, Memoir 9, p. 85-107.

• Vail, P. R., Mitchum, Jr., R. M. & Thompson, S. 1977. Part Four : Global cycles of relative changes of sea level. *In* : Seismic Stratigraphy – applications to hydrocarbon exploration, C. E. Payton (ed.). American Association of Petroleum Geologists, Memoir 26, p. 83-98.

• Wendte, J., Stoakes, F. A. & Campbell, C. V. 1992. Devonian-Early Mississippian carbonates of the Western Canada Sedimentary Basin : A sequence stratigraphic framework. Wendte, J., Stoakes, F. A. & Campbell, C. V. (eds.). SEPM short course notes, no. 28, p. 1-24.

• Wightman, D. M., Pemberton, S. G. & Singh C. 1987. Depositional modelling of the Upper Mannville (lower Cretaceous), east central Alberta : Implications for the recognition of brackish water deposits. *In* : Reservoir Sedimentology, R. W. Tillman & K. J. Weber (eds.). Society of Economic Paleontologists and Mineralogists, Special Publication no. 40, p. 189-220.

• Williams, G. D. 1963. The Mannville Group (Lower Cretaceous) of Central Alberta. Bulletin of Canadian Petroleum Geology, vol. 11, no. 4, p. 350-368.

• Wright, G. N., McMechan, M. E. & Potter, D. E. G. 1994. Structure and Architecture of the Western Canada Sedimentary Basin. *In* : Geological Atlas of the Western Canada Sedimentary Basin, G. D. Mossop and I. Shetsen (comps.). Canadian Society of Petroleum Geologists and Alberta Research Council, p. 25-40.

APPENDIX A: Pictures of core boxes

Well 3B-23-36-6W4, Core 2

Box 1…918.25-920.59 m
Box 2…920.59-922.83 m
Box 3…922.83-925.18 m
Box 4…925.18-927.42 m
Box 5…927.42-929.67 m
Box 6…929.67-931.79 m
Box 7…931.79-933.25 m

- **top of each core box** = upper right corner
- **bottom of each core box** = lower left corner

931.79 m

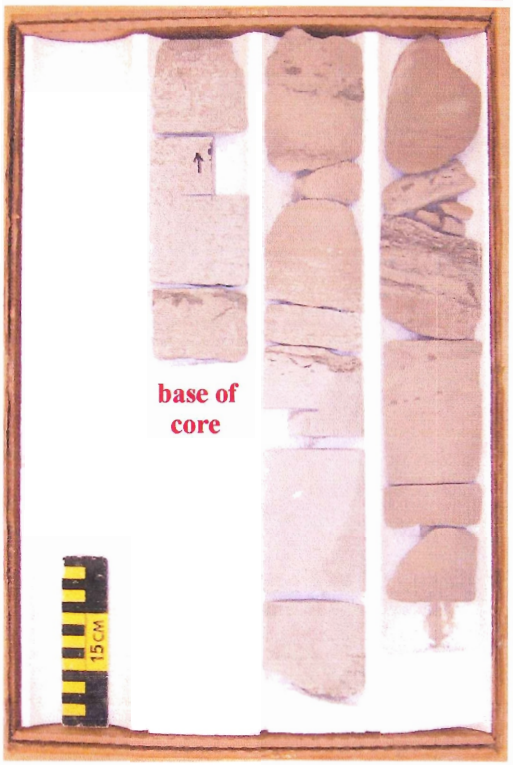

933.25 m Box 7 of 7

929.67 m

931.79 m Box 6 of 7

927.42 m

929.67 m Box 5 of 7

925.18 m

927.42 m Box 4 of 7

922.83 m

925.18 m Box 3 of 7

920.59 m

922.83 m Box 2 of 7

918.25 m

920.59 m Box 1 of 7

Well 4A-23-36-6W4, Core 1

Box 1…922.00-924.45 m
Box 2…924.45-926.90 m
Box 3…926.90-929.35 m
Box 4…929.35-931.80 m
Box 5…931.80-934.25 m
Box 6…934.25-936.70 m
Box 7…936.70-937.60 m

- **top of each core box** = upper right corner
- **bottom of each core box** = lower left corner

936.70 m

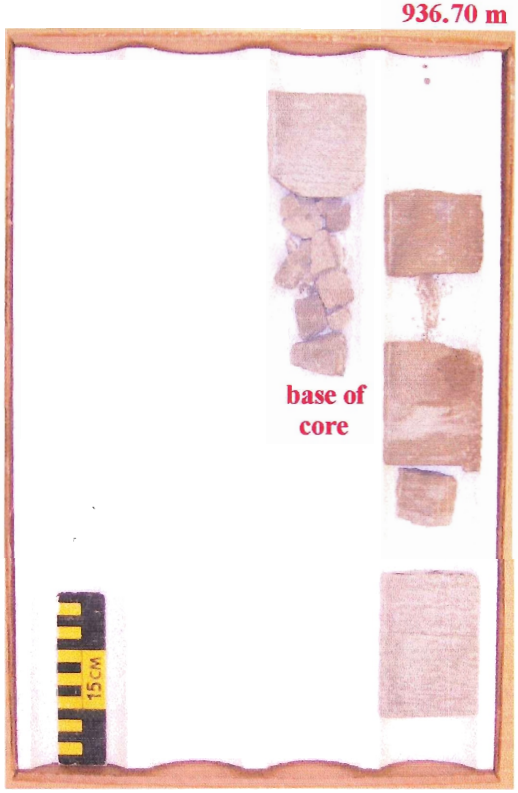

937.60 m Box 7 of 7

934.25 m

936.70 m Box 6 of 7

931.80 m

934.25 m Box 5 of 7

929.35 m

931.80 m Box 4 of 7

926.90 m

929.35 m Box 3 of 7

924.45 m

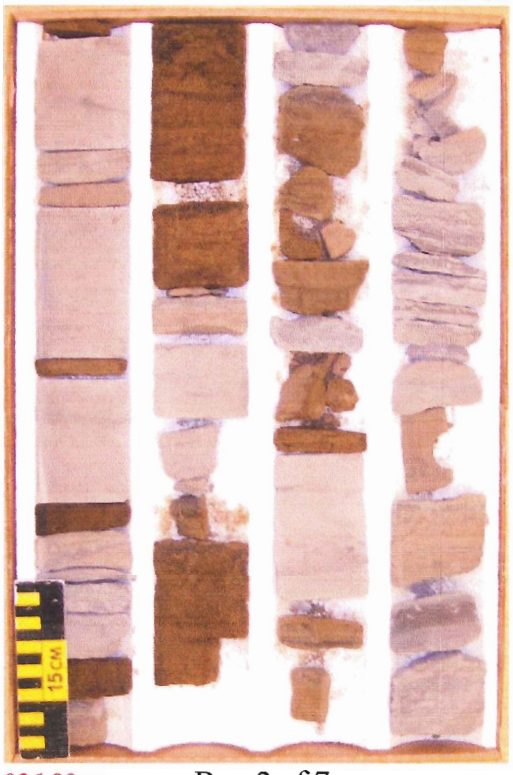

926.90 m Box 2 of 7

922.00 m

924.45 m Box 1 of 7

APPENDIX B : Ichnofacies and trace fossil terminology

biogenic sedimentary structures – sedimentary structures formed by organisms upon or within unconsolidated substrate (Pemberton, 1989).

bioturbation - disruption of stratified sediments by organisms (Pemberton, 1989).

ichnofacies - particular assemblages of trace fossils, recurrent in space and time, which are indicative of particular environmental conditions (i.e. substrate stability, current, rate of deposition, *etc.*) (Pemberton, 1989).

***Cruziana* ichnofacies** – is indicative of moderate- to relatively low-energy conditions and poorly sorted, unconsolidated substrates, in which most burrows are horizontally-aligned, although a few may be vertical or steeply-inclined (Frey & Pemberton, 1984). The *Cruziana* ichnofacies is associated with a considerable range of environments, such as shallow water (below fair-weather wave base but above storm wave base), intertidal and subtidal zones, and deeper, quieter waters offshore (Frey & Pemberton, 1984).

***Skolithos* ichnofacies** – is indicative of relatively high-energy regimes (wave or current action) and loose, shifting, particulate substrates in which burrows are generally vertical and reinforced (lined) (Frey & Pemberton, 1984). The *Skolithos* ichnofacies is associated with foreshore and shoreface environments (i.e. sandy beaches, bars, and spits), and also with high-energy tidal flats, tidal deltas, and estuarine point bars (Frey & Pemberton, 1984). The *Skolithos* ichnofacies grades seaward into the lower-energy *Cruziana* ichnofacies (Frey & Pemberton, 1984).

physical sedimentary structures - sedimentary structures formed by physical processes without the influence of organisms (Prothero & Schwab, 1996).

trace fossils – biogenic sedimentary structures, including fossilised tracks, trails, burrows, borings, and other similar features created by once-living organisms (Pemberton, 1989).

Chondrites are defined (in cross-section) by a series of small, vertically- to horizontally-aligned, elliptical dots of uniform size which do not cut across one another (Pemberton, 1989; Pemberton & Wach, 1998). *Chondrites* represents a root-like burrow system of a deposit-feeder, and although observed in several ichnofacies, is most indicative of the *Cruziana* ichnofacies (Pemberton & Wach, 1998).

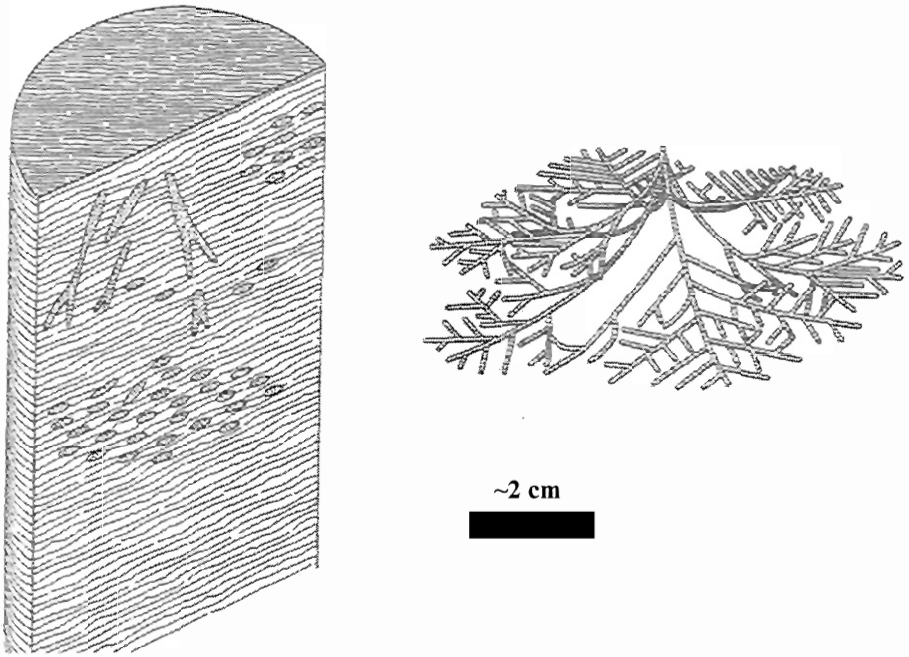

Figure 14 : Schematic diagrams of *Chondrites* (from Pemberton & Wach, 1998).

Cylindrichnus traces are straight to gently curved burrows with multiple, concentrically-layered walls (Pemberton, 1989), and their orientation ranges from horizontal to vertical (Pemberton & Wach, 1998). *Cylindrichnus* represents the dwelling burrow of a suspension-feeder, and is common in the *Skolithos* ichnofacies, associated with sandy tidal flats and lateral accretion bars of estuarine channels (Pemberton & Wach, 1998).

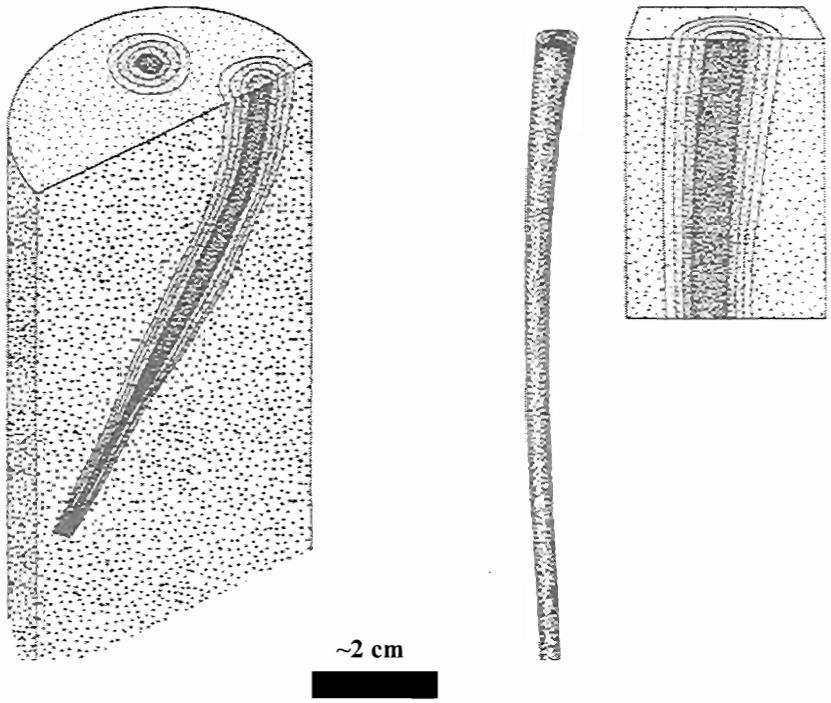

Figure 15 : Schematic diagrams of *Cylindrichnus* (from Pemberton & Wach, 1998).

Palaeophycus is defined by distinctly lined, horizontal to inclined burrows filled with sediment of the same composition and texture as the host rock (Pemberton, 1989). *Palaeophycus* represents the dwelling burrow of a predatory polychaete associated with the *Skolithos* ichnofacies, and associated with shoreface environments, episodic storm sands, and brackish-water environments (Pemberton & Wach, 1998).

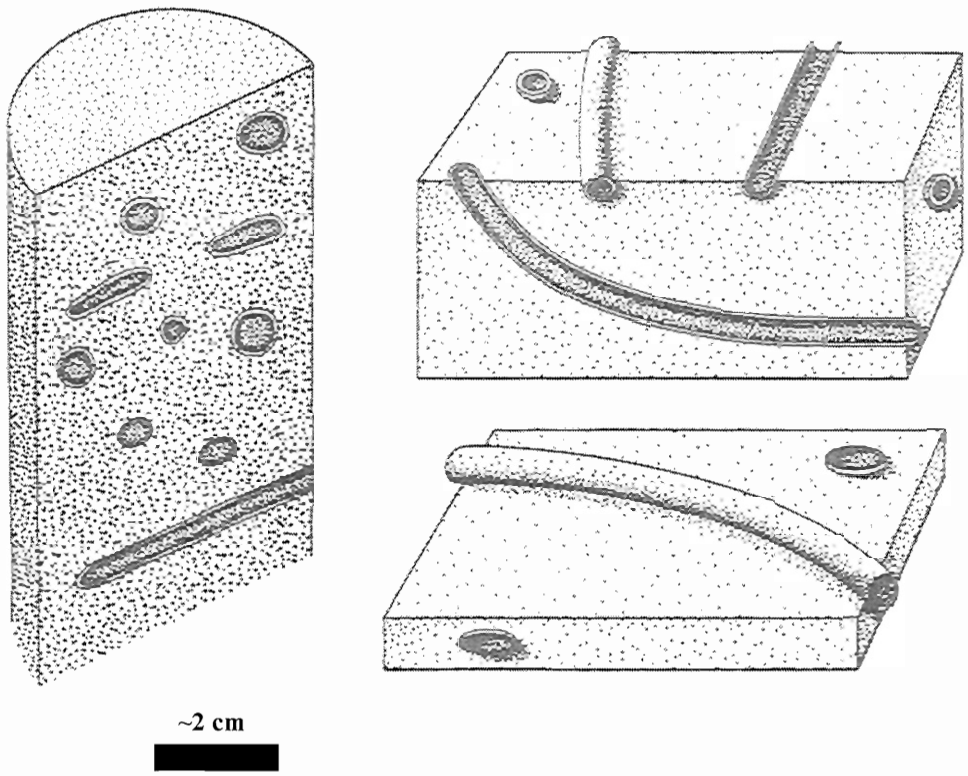

Figure 16 : Schematic diagrams of *Palaeophycus* (from Pemberton & Wach, 1998).

Planolites are defined by straight to tortuous, circular to elliptical (in cross-section), and smooth, horizontally-aligned burrows of variable dimensions and configurations, which are filled with material differing in lithology from the host rock (Pemberton, 1989; Pemberton & Wach, 1998). *Planolites* represent feeding burrows of a deposit-feeder, but *Planolites* are not associated with any particular ichnofacies, because they are preserved in virtually all environments, from fresh water to deep marine (Pemberton & Wach, 1998).

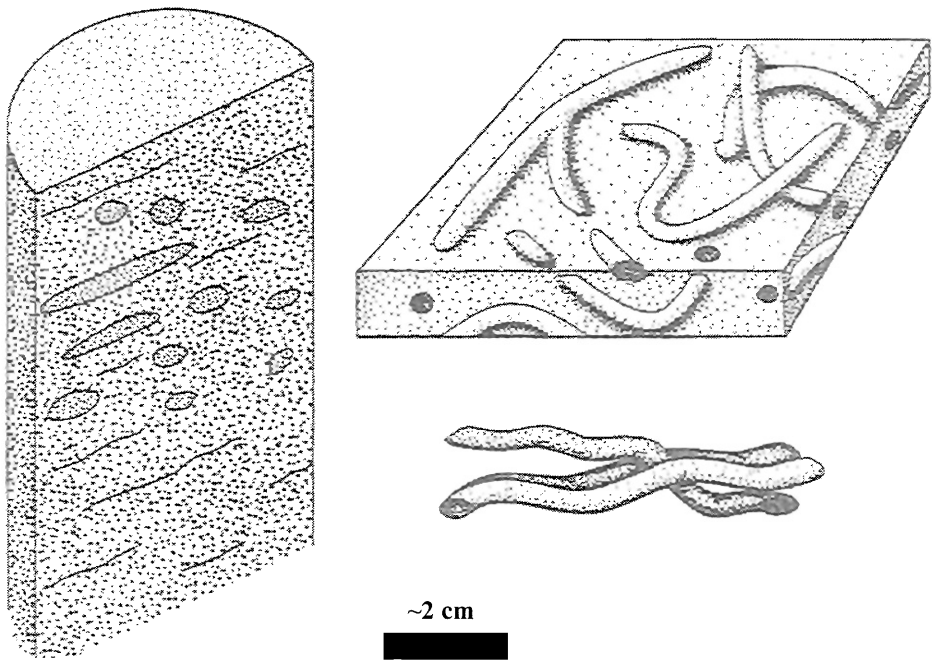

Figure 17 : Schematic diagrams of *Planolites* (from Pemberton & Wach, 1998).

Skolithos are defined by straight to curved, vertical to subvertical, and distinctly-lined burrows which are usually filled with structureless material, and which do not cross one another (Pemberton, 1989). *Skolithos* represents the dwelling burrow of a suspension-feeding organism, and although it is preserved in virtually every type of environment from marine to non-marine, it is most indicative of the *Skolithos* ichnofacies (Pemberton & Wach, 1998). According to Wightman *et al.* (1987), only *Skolithos* burrows formed in marine-influenced waters are lined, and fresh-water *Skolithos* burrows are unlined.

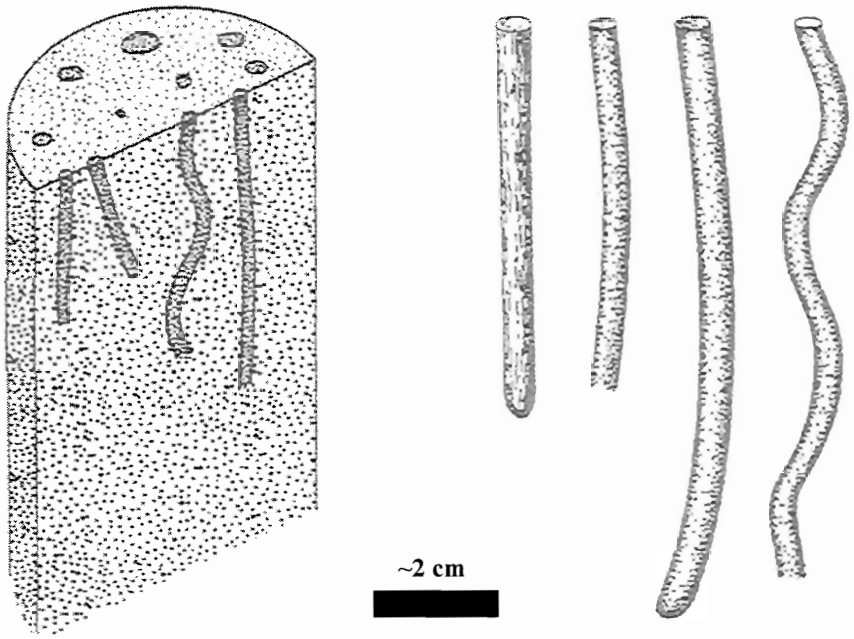

Figure 18 : Schematic diagrams of *Skolithos* (from Pemberton & Wach, 1998).

Townships and Ranges

The Township assigned to a well represents its north-south location, while the Range gives its east-west location. Townships are numbered northwards, beginning with Township 1 at the Canada-USA border, and Ranges are numbered westwards, beginning with Range 1 at *each* meridian. A well is located on the DLS 'grid' by using the Township and Range numbers in the UWI. A Township is usually 6 mi. x 6 mi., and comprises 36 equally-sized Sections, numbered as shown in Figure 21. In this thesis, the two wells discussed are both from Township 36-6W4, which is the 36th Township (north of the Canada-USA border) in the 6th Range west of the 4th meridian.

Sections

There are 36 Sections in a Township. A Section is usually 1 mi. x 1 mi., and comprises 16 equally-sized Legal Subdivisions (LSD), numbered as shown in Figure 21. In this thesis, the two wells discussed are both from Section 23.

Legal subdivisions (LSD) and the Special Exception Position

There are 16 Legal Subdivisions (LSD) in a Section. Each LSD measures ¼ mi. x ¼ mi., or ~200 m x ~200 m. According to B. Fraser (personal communication, 2003), some Legal Subdivisions are further divided into four quadrants (the Special Exception Positions), which are labelled A, B, C, and D for the SE, SW, NW, and NE quadrants respectively (Figure 21) . The two wells discussed in this thesis are from adjacent quadrants of adjacent Legal Subdivisions (Legal Subdivisions 3B and 4A).

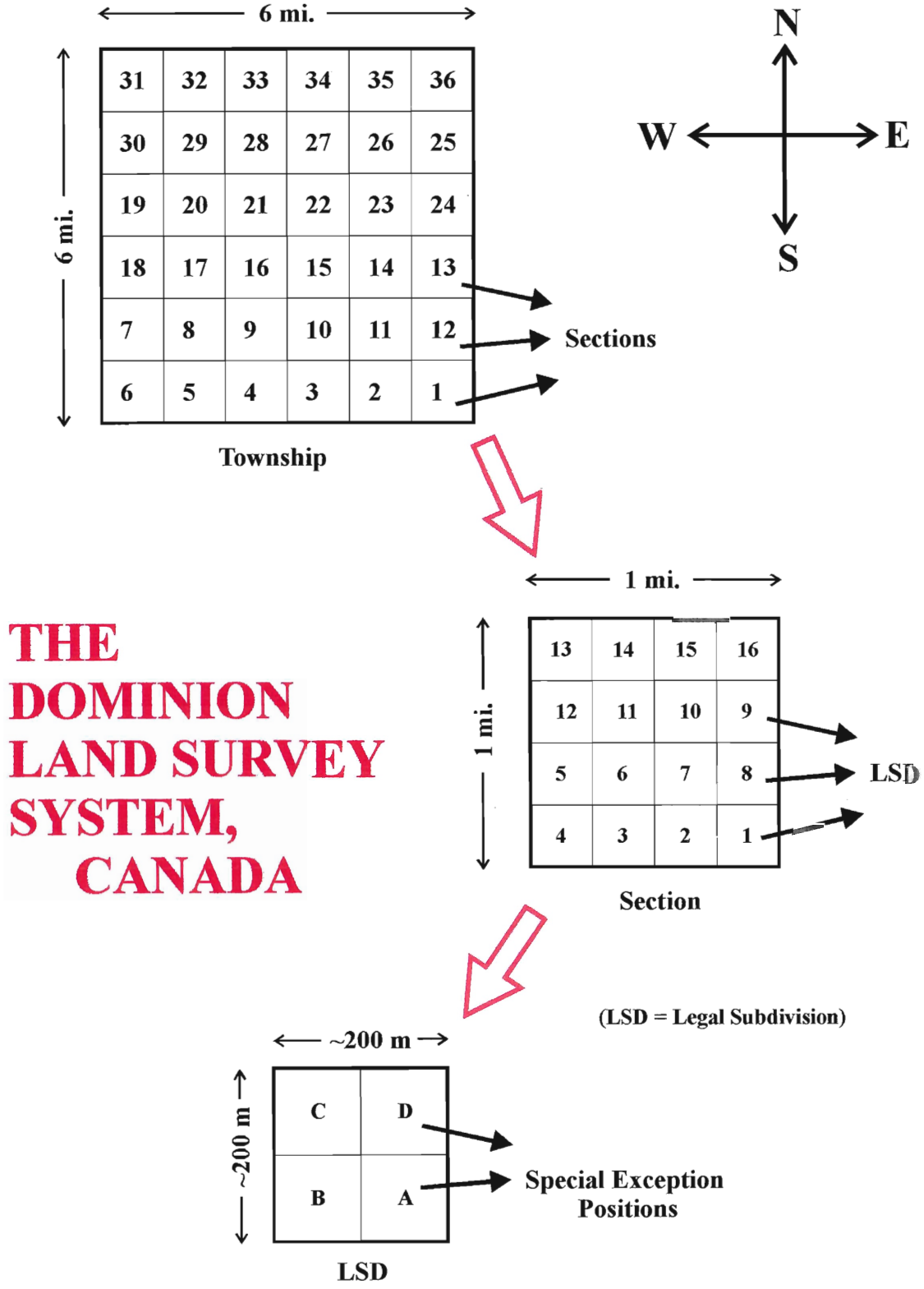

Figure 21 - Components of the Dominion Land Survey System.

APPENDIX D: Background on well logs

gamma ray (GR)

The gamma ray (GR) log has a vertical resolution of approximately 1 m (or 3 ft), and measures gamma ray intensity (along the borehole) caused by the natural decay of radioactive potassium (K), uranium (U), and thorium (Th) atoms within the strata (Dewan, 1983). According to Dewan (1983), these three radioactive elements are concentrated within shales, and shales show up on the gamma ray log as relative highs (deviations to the right). Rock units with relatively little or no shale (such as clean sandstones and carbonates) show up on the gamma-ray log as relative lows, or deviations to the left (Prothero & Schwab, 1996). An increase to the right on the gamma ray log, therefore, indicates an increase in shale content of the rock. Arkosic, lithic, and muddy sandstones also exhibit relatively high gamma ray readings because of their high radioactive potassium content (Prothero & Schwab, 1996). According to Dewan (1983), gamma ray logs are measured in API units (American Petroleum Institute units). Each API unit represents $1/200^{th}$ of a calibrated response from an artificial rock formation maintained in Houston, Texas, by the American Petroleum Institute (Dewan, 1983).

spontaneous potential (SP)

The spontaneous potential (SP) log is an indirect measure of permeability (Alspatch, 2002), but is really a measurement of the voltage drop (electrical potential) across two electrodes: one grounded on the surface of the Earth and a second which ascends the borehole (Prothero & Schwab, 1996). As the electrode moving upwards along the borehole encounters relatively permeable rock (i.e. porous sandstone), it records a drop in voltage induced (for the most part) by the movement of ions from within the rock into the borehole (Prothero & Schwab, 1996). The spontaneous potential logs are measured in millivolts (mV) and decrease to the left, so that permeable rock units (voltage drops) deviate to the left, and vice versa (Dewan, 1983). Limestones are impermeable unless porous or fractured (Prothero & Schwab, 1996). The vertical resolution of spontaneous potential logs is difficult to express in units of distance,

because it is affected by changes in permeability, not lithology (although one is generally a good indication of the other, i.e. shales are impermeable, sandstones are generally permeable). According to Dewan (1983), spontaneous potential logs are capable of resolving permeability changes as low as a fraction of a millidarcy.

induction (ILM and ILD)

Induction logs (ILM and ILD) have a vertical resolution of approximately 1.3 m (4 ft), and measure the electrical resistivity of rock along the borehole by inducing current flow through the rock (Dewan, 1983). According to Prothero & Schwab (1996), the resistivity of rock is an expression of its porosity and pore fluids. Natural pore fluids have low resistivity, so porous rock units show up as relative lows on the logs, or deviations to the left (Prothero & Schwab, 1996). Dense rock units with low porosity, or porous rock units filled with resistive fluids (such as fresh water or oil), have high resistivities and are represented by relative highs on the logs, or deviations to the right (Prothero & Schwab, 1996). According to Prothero & Schwab (1996), shales are anomalous in that they have low porosity but also low resistivity, and show up as relative lows on the logs (deviations to the left). According to Dewan (1983), the ILM and ILD logs differ by the lateral distance from the bore hole at which they record the resistivity of the rock (ILM – medium, ILD – deep). The induction logs (ILM and ILD) included in Appendix G are scaled in ohm metres (Ω·m) on a logarithmic scale which increases to the right from 0.2 to 2000 Ω·m.

spherically focused log (SFLU)

The spherically focused log (SFLU) is similar to the induction (ILM and ILD) logs, but has better vertical resolution. As with the ILM and ILD logs, it measures the resistivity of rock along the borehole by inducing current flow through the rock, and it is plotted together with the induction logs on the same scale: 0.2 to 2000 ohm metres (Ω·m), increasing to the right (Dewan, 1983). According to Dewan (1983), however, the SFLU is special in that it has better vertical resolution (less than 0.5 m, approximately 1 ft) than the ILM and ILD logs.

density porosity (DPHI)

The density porosity (DPHI) log has a vertical resolution of approximately 1 m (3 ft), and is a measure of porosity along the borehole (Dewan, 1983). According to Alspatch (2002), however, it does not distinguish between ineffective and effective porosity. The density porosity log is calculated by solving Equation 1 (below) continuously along the borehole (this is done by a computer) (Dewan, 1983).

(Equation 1) $\varphi = (\rho_{ma} - \rho_b) / (\rho_{ma} - \rho_f)$ where :

φ = porosity of rock, with matrix density ρ_{ma}, bulk density ρ_b, and fluid density ρ_f.

According to Dewan (1983), the matrix density (ρ_{ma}) and fluid density (ρ_f) are chosen by the on-site well operators, who must select values representative of the area (typical values include 2.65 or 2.68 for sandstone, 1.0 or 1.1 for fluid density). The bulk density (ρ_b) values are recorded by a device which measures the attenuation of gamma rays (emitted by a small source) along the borehole (Dewan, 1983). It is this device which determines the vertical resolution of the density porosity log. An increase in gamma ray attenuation indicates an increase in bulk density, which represents a decrease in density porosity (see Equation 1) (Dewan, 1983). On the well logs, density porosity is recorded as a fraction (i.e. percentage porosity divided by 100%), and increases to the left (from 0.0 to 0.6), so that porous rock units (relatively low bulk densities) are represented by deviations to the left (and vice versa).

neutron porosity (NPHI) –

The neutron porosity (NPHI) log has a vertical resolution of approximately 1 m (3 ft), and is a measure of porosity along the borehole (Dewan, 1983). The porosity is measured by a device which moves through the borehole and records the relative abundance of hydrogen atoms in the rock (Dewan, 1983), which is controlled by the pore fluids (Alspatch, 2002). Natural pore fluids contain water, which is relatively rich

in hydrogen atoms, and so porous rock units show up as highs on the neutron porosity log, or deviations to the left (Alspatch, 2002). Rock units with low porosity show the opposite effect. According to Alspatch (2002), however, gas-filled reservoirs are anomalous in that they display low neutron porosity values (because gas has relatively few hydrogen atoms) but high density porosity values (because reservoir rock has low bulk density), resulting in the 'gas cross-over' effect, where the density and neutron porosity logs cross one another. (This cross-over effect is not observed over the cored intervals in the well logs in Appendix G.) As with the density porosity log, neutron porosity is recorded as a fraction (i.e. percentage porosity divided by 100%), and increases to the left, from 0.0 to 0.6.

APPENDIX E: Core Description Sheets

(16 sheets in total)

LEGEND

SURFACE DESCRIPTION
PL - PLANAR
CR - CURVED
W - WAVY
CB - CORE BREAK
S - SHARP

SURFACE INTERPRETATION
LSS - LAMINAE SET SURFACE
BS - BED SURFACE
BSS - BEDSET SURFACE

LAMINAE GEOMETRY
PLANAR PARALLEL
PLANAR NONPARALLEL
CURVED PARALLEL
CURVED NONPARALLEL
WAVY PARALLEL
WAVY NONPARALLEL

BED TYPE INTERPRETATION
TROUGH CROSS BEDS
PLANAR CROSS BEDS
HUMMOCKY CROSS BEDS
SIGMOIDAL CROSS BEDS
TIDAL BUNDLES
CURRENT RIPPLES
CLIMBING RIPPLES
IN-PHASE CLIMBING RIPPLES
WAVE RIPPLES
COMBINED FLOW RIPPLES
PLANAR BED
FL/W/L FLASER/WAVY/ LENTICULAR BEDDING
H HOMOGENOUS BED

SEDIMENTARY STRUCTURES
ROOTS
CHURNED
BURROWED
SWIRLED
CONTORTED
DISH + PILLAR STRUCTURE
MICROFAULT
FRACTURE
FLAME CAST
LOAD CAST
GROOVE CAST
FLUTE CAST
STYLOLITE
MUDCRACK
SCOUR
SYMMETRICAL RIPPLE MARK
ASYMETRICAL RIPPLE MARK
FOSSIL
FORAM
G GLAUCONITE
CONCRETION
ORGANIC MATERIAL
MUDROCK CLAST
PYRITE
? QUESTIONABLE
GR GRADATIONAL

CHRONOSTRATIGRAPHY
PSSB -PARASEQUENCE SET BOUNDARY
SB - SEQUENCE BOUNDARY
FSSB - FLOODING SURFACE SEQUENCE BOUNDARY
CS - CONDENSED SECTION
LST - LOWSTAND SYSTEMS TRACT
TST - TRANSGRESSIVE SYSTEM TRACT
HST - HIGHSTAND SYSTEMS TRACT
FS - FLOODING SURFACE

LITHOLOGY
CONG - CONGLOMERATE
CONG SD - CONGLOMERATE SANDSTONE
SAND ST - SANDSTONE
MUD ST - MUDDY MUDSTONE
SD MUD - SANDY MUDSTONE
MUDST - MUDSTONE
SHALE
COAL

GRAIN SIZE
256mm
CBL - COBBLE
64mm
PBL - PEBBLE
4mm
GRAIN - GRANULE
2mm
VC - VERY COARSE SAND
C - COARSE SAND
M - MEDIUM SAND
F - FINE SAND
VF - VERY FINE SAND
.062mm
SLT - SILT
CL - CLAY

TRACE FOSSILS
Ar - Arenicolites
An - Anconichnus
As - Asterosoma
B - Bergaueria
Ch - Chondrites
Co - Conichnus
Cy - Cylindrichnus
D - Diplocraterion
H - Helminthopsis
L - Lockeia
Ma - Macaronichnus
Mo - Monocraterion
O - Ophiomopha
Pa - Palaeophycus
Pl - Planolites
Rh - Rhizocorallium
Ro - Rosselia
Sk - Skolithos
Su - Subphyllochorda
Ta - Taenidium
Te - Teichichnus
Tr - Terebellina
Tri - Trichichnus
T - Thalassinoides
Z - Zoophycos

CLAST
F FINING-UP
C COARSENING-UP
S SULPHUR
SID SIDERITE
Fe IRON STAINING
HCl HCl (10%) REACTION

BIOTURBATION INDEX

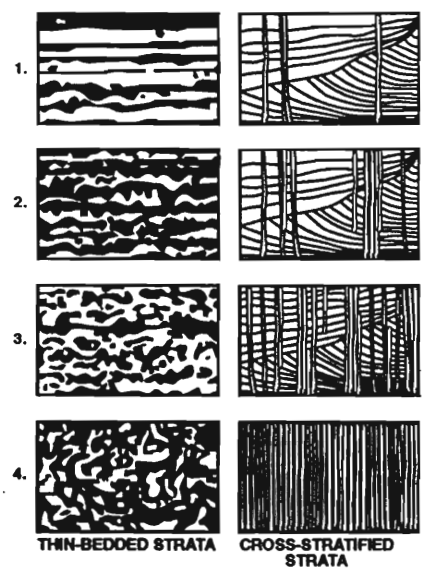

THIN-BEDDED STRATA
CROSS-STRATIFIED STRATA

OIL STAIN INDEX (OSI)

OSI = 1
OSI = 2
OSI = 3

WELL : SUNCOR et al. PROVOST LOCATION : 3B-23-36-6W4 GEOLOGIST : Joe Kidston DATE : Oct./02 SHEET 1 OF 8

DEPTH (m)	SAMPLES OR PICS	SEDIMENTARY STRUCTURES	GRAIN SIZE (CBL PBL GRAN VC C M F VF SILT CLAY)	SURFACE DESC	SURFACE INT	LAMINAE GEOMETRY	BIO-TURBATION INDEX	TRACE FOSSILS	ICHNO-FACIES	OIL-STAINED INDEX	NOTES	LITHO-FACIES	DEP. ENVIRON-MENT	NAME OF ROCK UNIT
918.00														
.10											Cummings Fm. (part)	fining-upwards, poorly sorted pebble conglomerate	fluvial channel (basal lag)	Cummings Fm. (part)
.20	core begins at 918.25 m Box 1										'drapes' the underlying conglomerate			
.30				PL							minorganic material, rounded silt rip-up clasts up to ~2.2 cm wide			
.40		HCl		CB							rubble chips			
.50		HCl		CB										
.60		HCl				10°		An common						
.70		HCl				6°					microcrystalline pyrite throughout			
.80											fossils at bottom defined by *Pelecypod* (undifferentiated) shell fragments ≤1 cm wide			
.90		HCl						Sk?						
919.00				GR								lightly burrowed, interbedded calcareous shale and micritic limestone, clay to silt	shallow, restricted, brackish-water marine embayment (Riediger *et al.*, 1999)	Ostracode zone
.10		HCl							mixed *Skolithos/Cruziana*?					
.20														
.30														
.40											*Planolites* burrows generally <1 cm wide, green in colour			
.50		HCl						Pl common						
.60														
.70		HCl									*Pelecypod* (undifferentiated) shell fragments concentrated in shale from 919.64-919.69 m, ≤1 cm wide			
.80														
.90		HCl		GR										
920.00									(next page)		burrowed and churned	(next page)	(next page)	Dina Fm.

DEPTH (m)	SAMPLES OR PICS	SEDIMENTARY STRUCTURES	GRAIN SIZE	SURFACE	LAMINAE GEOMETRY	BIO-TURBATION INDEX	TRACE FOSSILS	ICHNO-FACIES	OIL-STAINED INDEX	NOTES	LITHO-FACIES	DEP. ENVIRON-MENT	NAME OF ROCK UNIT
920.00			CBL PBL GRAN VC U L C U L M U L F U L VF U L SILT CLAY	DESC INT		1 2 3 4			1 2 3				
.10							Pl, Sk, Ch all rare			rubble pieces			
.20				CB									
.30							Pl abund., Ch common, Sk? rare						
.40													
.50				CB	12°								
	Box 2	(missing core)								(missing core)			
.60							Pl abund., Ch common	mixed *Skolithos/Cruziana*		sandy siltstone	interbedded sandstone and siltstone, lightly to heavily burrowed, silt to fine (l), some sandstone beds oil-stained	Tidal flat with channel deposits (estuarine environment)	Dina Fm.
.70													
.80													
.90													
921.00										silty sandstone			
.10										sandy siltstone			
.20													
.30				PL									
				CB			Pl, Sk, O all rare						
.40													
.50							Pl, Ch both abund.						
.60													
.70				CB									
		(missing core)								(missing core)			
.80													
.90							Pl, Ch both abund.						
922.00													

WELL : SUNCOR et al. PROVOST LOCATION : 3B-23-36-6W4 GEOLOGIST : Joe Kidston DATE : Oct./02 SHEET 3 OF 8

DEPTH (m)	SAMPLES OR PICS	SEDIMENTARY STRUCTURES	GRAIN SIZE	SURFACE DESC	SURFACE INT	LAMINAE GEOMETRY	BIO-TURBATION INDEX	TRACE FOSSILS	ICHNO-FACIES	OIL-STAINED INDEX	NOTES	LITHO-FACIES	DEP. ENVIRON-MENT	NAME OF ROCK UNIT
922.00			CBL PBL GRAN VC C M F VF SILT CLAY				1 2 3 4			1 2 3				
.10				CB										
.20														
.30								Pl, Ch both abund., Z? common			questionable *Zoophycos* traces, see Plate 9			
.40														
.50		Z? Z? Z?												
.60														
.70		Z?		CB					mixed *Skolithos/Cruziana*			interbedded sandstone and siltstone, lightly to heavily burrowed, silt to fine (l), some sandstone beds oil-stained	tidal flat with channel deposits (estuarine environment)	Dina Fm.
.80	Box 3	(missing core)									(missing core)			
.90								Pl, Ch both abund., Z? rare						
923.00														
.10														
.20														
.30		Z?		CB										
.40		(missing core)									(missing core)			
.50				CB				Pl, Ch both abund.						
.60		(missing core)									(missing core)			
.70		Cy						Pl, Ch both abund., Cy rare			relatively large *Cylindrichnus* trace (~7 cm long, ~3 mm wide) observed at 923.68 m (see Plate 8)			
.80														
.90	XRD #1392													
924.00														

WELL : SUNCOR et al. PROVOST LOCATION : 3B-23-36-6W4 GEOLOGIST : Joe Kidston DATE : Oct./02 SHEET 4 OF 8

DEPTH (m)	SAMPLES OR PICS	SEDIMENTARY STRUCTURES	GRAIN SIZE	SURFACE DESC	SURFACE INT	LAMINAE GEOMETRY	BIO-TURBATION INDEX	TRACE FOSSILS	ICHNO-FACIES	OIL-STAINED INDEX	NOTES	LITHO-FACIES	DEP. ENVIRON-MENT	NAME OF ROCK UNIT
924.00			CBL PBL GRAN VC U L C U L M U L F U L VF U L SILT CLAY				1 2 3 4			1 2 3				
				GR										
.10				CB				Pl common, Sk rare						
.20				CB				Pl common			rubble pieces			
				GR										
	TS#3, XRD # 1379			CB							no bioturbation			
.30														
.40								Pl abund., Ch common, Sk rare						
.50				CB										
				CB				Pl rare						
				CB										
.60		(missing core)									(missing core)			
.70				CB										
		(missing core)									(missing core)			
.80				CB				Pl, Ch both abund., Sk rare						
.90														
		(missing core)							mixed *Skolithos/Cruziana*		(missing core)	interbedded sandstone and siltstone, lightly to heavily burrowed, silt to fine (l), some sandstone beds oil-stained	tidal flat with channel deposits (estuarine environment)	Dina Fm.
925.00														
.10														
	Box 4													
.20														
.30														
.40				GR										
				GR				Pl common, Sk rare						
				GR				Pl, Ch abund., Sk rare						
.50				CB				Pl common, Sk rare						
				GR				Pl, Sk both abund.						
.60											relatively large *Skolithos* trace ~3.5 cm long, ~2 mm wide,ripple foresets (925.65-925.68) defined by laminae (max ~3 mm wide) dipping by ~25°			
				CB				Pl, Sk both common						
.70				CB				Pl common			rubble pieces			
				CB				Pl common			rubble pieces			
.80		(missing core)									(missing core)			
.90								Pl abund., Ch common						
926.00														

WELL : SUNCOR et al. PROVOST LOCATION : 3B-23-36-6W4 GEOLOGIST : Joe Kidston DATE : Oct./02 SHEET 5 OF 8

DEPTH (m)	SAMPLES OR PICS	SEDIMENTARY STRUCTURES	GRAIN SIZE (CBL, PBL, GRAN, VC, C, M, F, VF, SILT, CLAY)	SURFACE DESC	SURFACE INT	LAMINAE GEOMETRY	BIO-TURBATION INDEX	TRACE FOSSILS	ICHNO-FACIES	OIL-STAINED INDEX	NOTES	LITHO-FACIES	DEP. ENVIRON-MENT	NAME OF ROCK UNIT
926.00														
.10				GR				Pl, Ch both abund.						
				CB										
.20								Pl, Ch both abund. Sk rare, Cy rare			relatively large *Cylindrichnus* trace ~3 cm long, ~7 mm wide			
.30		Cy												
				CB										
.40				CB				Pl abund., Ch common						
.50								Pl, Ch both abund.						
.60				CB										
.70	TS#2, XRD #999			CB				Pl, Ch both common	mixed *Skolithos/Cruziana*			interbedded sandstone and siltstone, lightly to heavily burrowed, silt to fine (l), some sandstone beds oil-stained	tidal flat with channel deposits (estuarine environment)	Dina Fm.
.80				CB				Pl, Sk both common						
				CB										
.90				CB				Pl, Sk both rare						
		Z?		PL										
927.00						20°		Sk rare			relatively clean			
.10				GR		0-10°		Pl, Ch both abund.						
				GR				Pl common, Sk rare						
.20				GR				Pl, Ch both abund.						
.30				CB				Pl abund., Ch common, Sk rare						
.40	Box 5			CB										
.50														
.60								Pl, Ch both abund.						
.70														
.80														
.90														
928.00				GR										

WELL : SUNCOR et al. PROVOST LOCATION : 3B-23-36-6W4 GEOLOGIST : Joe Kidston DATE : Oct./02 SHEET 6 OF 8

DEPTH (m)	SAMPLES OR PICS	SEDIMENTARY STRUCTURES	SURFACE DESC	SURFACE INT	LAMINAE GEOMETRY	BIO-TURBATION INDEX	TRACE FOSSILS	ICHNO-FACIES	OIL-STAINED INDEX	NOTES	LITHO-FACIES	DEP. ENVIRON-MENT	NAME OF ROCK UNIT
928.00													
.10			GR				Pl rare			virtually no bioturbation			
			S							scoured bottom surface			
.20													
.30							Pl, Ch both abund.						
.40													
.50			CB										
.60													
.70										rubble pieces			
.80			CB										
.90			CB										
			CB				Pl, Ch both abund.						
929.00			CB					mixed *Skolithos/Cruziana*			interbedded sandstone and siltstone, lightly to heavily burrowed, silt to fine (l), some sandstone beds oil-stained	tidal flat with channel deposits (estuarine environment)	Dina Fm.
.10		(missing core)								(missing core)			
.20			CB				Pl, Ch both abund.						
.30		#syn	CB				Pl, Ch both abund.			syneresis crack at 929.30 m, ~3 cm long, ~3 mm wide, filled with sandy sediments (see Plate 4)			
.40			CB				Pl rare			rubble pieces			
			CB				Pl, Sk both rare			relatively clean			
.50													
.60	Box 6		CB				Pl, Ch both abund.						
.70													
.80							Pl, Ch both abund., Sk rare						
.90			CB										
930.00			CB				Pl, Sk both rare						

WELL : SUNCOR et al. PROVOST LOCATION : 3B-23-36-6W4 GEOLOGIST : Joe Kidston DATE : Oct./02 SHEET 7 OF 8

DEPTH (m)	SAMPLES OR PICS	SEDIMENTARY STRUCTURES	SURFACE DESC	SURFACE INT	LAMINAE GEOMETRY	BIO-TURBATION INDEX	TRACE FOSSILS	ICHNO-FACIES	OIL-STAINED INDEX	NOTES	LITHO-FACIES	DEP. ENVIRON-MENT	NAME OF ROCK UNIT
930.00			CB			1 2 3 4	Pl, Ch both abund.	mixed *Skolithos/Cruziana*	1 2 3		interbedded sandstone and siltstone, lightly to heavily burrowed, silt to fine (J), some sandstone beds oil-stained	tidal flat with channel deposits (estuarine environment)	Dina Fm.
.10			GR				Pl, Sk both rare			rubble pieces (from 930.08-930.16 m)			
.20			CB		15°		Pl, Ch both abund.						
.30													
			CB				Pl rare						
.40		(missing core)								(missing core)			
.50			GR		10°		Pl, Ch both abund.						
.60			GR		5°		Pl abund., Ch common						
.70			CB		12°		Pl, Ch both abund.						
.80			CB				Pl, Ch both rare						
		(missing core)								(missing core)			
.90			CB				Pl rare			rubble pieces			
931.00					10°								
.10													
.20							Pl abund., Ch common						
.30													
.40													
.50			CB										
.60			CB				Pl rare						
			GR										
.70	Box 7		CB				Pl, Ch both abund.			rubble pieces (from 931.75-931.79 m)			
.80			CB							no bioturbation			
.90													
932.00					15°		Pl abund., Ch common, Sk rare						

WELL : SUNCOR et al. PROVOST LOCATION : 4A-23-36-6W4 GEOLOGIST : Joe Kidston DATE : Jan./03 SHEET 1 OF 8

DEPTH (m)	SAMPLES OR PICS	SEDIMENTARY STRUCTURES	GRAIN SIZE (CBL PBL GRAN VC C M F VF SILT CLAY; U L)	SURFACE DESC INT	LAMINAE GEOMETRY	BIO-TURBATION INDEX (1 2 3 4)	TRACE FOSSILS	ICHNO-FACIES	OIL-STAINED INDEX (1 2 3)	NOTES	LITHO-FACIES	DEP. ENVIRON-MENT	NAME OF ROCK UNIT
922.00	Box 1 core begins at 922.00 m												
.10										organic material defined by fragments ≤1 cm long (black)	sandy siltstone/silty sandstone, silt to medium (l), contorted and wavy non-parallel bedding	shallow marine embayment?	Cummings fm. (part)
.20				GR									
.30				CB						pyrite nodules up to ~1 mm wide, round in shape			
.40		(missing core)								(missing core)			
.50				CB						pyrite nodules up to ~1 mm wide, round in shape			
.60		(missing core)								(missing core)			
.70		HCl		CB						patches of microcrystalline pyrite ≤0.5 cm wide			
				CB	15°								
.80		HCl		CB						fossils defined by shell fragments of *Pelecypod* (undifferentiated) ≤0.6 cm wide			
				CB									
.90		(missing core)		CB				*Skolithos? Cruziana?*		(missing core)	lightly burrowed, interbedded calcareous shale and micritic limestone, clay to silt, also two beds of the overlying lithofacies (with organic material) from 922.72-.77, 922.82-.85 m)	shallow, restricted, brackish-water marine embayment (Riediger et al., 1999)	Ostracode zone
923.00													
.10													
.20													
.30		HCl		CB						*Pelecypod* shell fragments ≤1 cm wide			
.40													
.50		(missing core)						mixed *Skolithos/Cruziana*		(missing core)	interbedded sandstone and siltstone, lightly to heavily burrowed, silt to fine (l), some sandstone beds oil-stained	Tidal flat with channel deposits (estuarine environment)	Dina fm.
.60				CB			Pl, Ch both abund., Sk rare, Co rare			*Skolithos* (?) trace ~3.5 cm long, ~0.5 cm wide			
.70		(missing core)								(missing core)			
.80				CB						flame casts ~1 cm wide each			
.90		HCl		CB			Pl, Ch both common, Sk rare			*Pelecypod* shell fragments ≤0.4 cm wide			
924.00													

WELL : SUNCOR et al. PROVOST LOCATION : 4A-23-36-6W4 GEOLOGIST : Joe Kidston DATE : Jan./03 SHEET 2 OF 8

DEPTH (m)	SAMPLES OR PICS	SEDIMENTARY STRUCTURES	SURFACE DESC	SURFACE INT	LAMINAE GEOMETRY	BIO-TURBATION INDEX	TRACE FOSSILS	ICHNO-FACIES	OIL-STAINED INDEX	NOTES	LITHO-FACIES	DEP. ENVIRON-MENT	NAME OF ROCK UNIT
924.00													
.10			CB				Pl abund.						
.20			CB				Pl common.			rubble pieces			
.30			CB				Pl rare						
			CB		10°		Pl abund., Ch common						
.40	Box 2	(missing core)								(missing core)			
			CB				Pl rare						
.50													
.60			CB		5°		Pl, Ch both abund.			rubble pieces			
.70													
.80			CB				Pl abund., Ch rare, Sk rare	mixed *Skolithos/Cruziana*			interbedded sandstone and siltstone, lightly to heavily burrowed, silt to fine (l), some sandstone beds oil-stained	tidal flat with channel deposits (estuarine environment)	Dina fm.
.90			GR										
925.00			GR				Pl, Ch both abund., Sk rare						
.10			CB				Pl common						
.20			CB				Pl common						
.30			CB				Pl abund., Ch common						
.40			CB				Pl, Ch, Sk all rare						
.50			CB				Sk common						
.60		?											
.70			CB				Pl common, Ch rare, Sk common			silt rip-up clasts (one rounded, the other angular) each ~1 cm x ~0.5 cm, ripple foresets (925.80 m) defined by laminae (max ~1 mm wide) dipping by ~20°			
.80													
.90			CB				Pl common						
926.00			CB				Sk abund., Pl, Ch both rare			ripple foresets (926.00 m) defined by laminae (max ~3 mm wide) dipping ~33°			

WELL : SUNCOR et al. PROVOST LOCATION : 4A-23-36-6W4 GEOLOGIST : Joe Kidston DATE : Jan./03 SHEET 3 OF 8

DEPTH (m)	SAMPLES OR PICS	SEDIMENTARY STRUCTURES	SURFACE DESC	SURFACE INT	LAMINAE GEOMETRY	BIO-TURBATION INDEX	TRACE FOSSILS	ICHNO-FACIES	OIL-STAINED INDEX	NOTES	LITHO-FACIES	DEP. ENVIRON-MENT	NAME OF ROCK UNIT
926.00			CB				Pl abund., Ch common	mixed *Skolithos/Cruziana*			interbedded sandstone and siltstone, lightly to heavily burrowed, silt to fine (J), some sandstone beds oil-stained	tidal flat with channel deposits (estuarine environment)	Dina fm.
.10							Pl, Ch both common, Sk rare						
.20													
.30			CB										
.40			CB				Pl, Ch both common						
.50			CB				Pl, Ch both abund.						
.60			CB				Pl rare, Sk common			ripple foresets (~926.55 m) defined by laminae (max ~2 mm wide) dipping by ~19°			
.70			CB				Sk common						
.80			CB				Pl, Sk both common						
.90	Box 3		CB				Pl, Ch both abund.						
927.00			CB				Sk common						
.10			GR				Pl common						
.20							Pl, Sk both rare			ripple foresets (~926.96 m) defined by laminae (max ~2 mm wide) dipping ~26°			
.30							Pl, Sk both common						
.40			CB				Pl, Ch both abund.			questionable *Cylindrichnus* traces (two at ~927.80 m) ≤3 cm long			
.50		(missing core)								(missing core)			
.60			CB				Pl, Ch both common						
.70		Cy? Cy?	CB				Pl, Sk both common, Ch rare, Cy? rare						
.80													
.90			CB				Pl, Sk both rare						
928.00													

WELL : SUNCOR et al. PROVOST LOCATION : 4A-23-36-6W4 GEOLOGIST : Joe Kidston DATE : Jan./03 SHEET 4 OF 8

DEPTH (m)	SAMPLES OR PICS	SEDIMENTARY STRUCTURES	GRAIN SIZE	SURFACE DESC	SURFACE INT	LAMINAE GEOMETRY	BIO-TURBATION INDEX	TRACE FOSSILS	ICHNO-FACIES	OIL-STAINED INDEX	NOTES	LITHO-FACIES	DEP. ENVIRON-MENT	NAME OF ROCK UNIT
928.00		∪		CB		≡		Pl rare						
.10				CB				Pl rare						
.20		∪		CB		≡		Pl rare, Sk common			questionable (vague) ripple foresets at ~928.20 m			
.30		∪ ♦ ∪		CB		≡		Pl, Sk both rare			ripple foresets at ~928.26 m defined by laminae (max ~2 mm wide) dipping by ~21°			
.40		∪		CB		≡		Pl rare						
		∪		CB		≡		Pl, Sk both rare						
.50		∪		CB		≡								
.60		∿ (or≈?) F F F		CB		≡		Pl common			questionable wave ripple lamination (~928.55 m) defined by stacked ripple laminae (max ~6 mm wide) ripple foresets at 928.62-.66 m defined by laminae (max ~2 mm wide) dipping by ~20-30°			
.70		∪		CB		≡								
		(missing core)									(missing core)			
.80		∪		CB		≡		Pl, Sk both rare						
.90		F ∿ (or≈?) F		CB		≡		Pl, Sk both rare	mixed *Skolithos/Cruziana*		questionable wave ripple lamination (~928.95 m) defined by stacked ripple laminae (max ~3 mm wide) ripple foresets at ~928.86 m defined by laminae (max ~3 mm wide) dipping by ~19°, and at ~929.00 m by laminae (max ~1 mm wide) dipping by ~13°	interbedded sandstone and siltstone, lightly to heavily burrowed, silt to fine (l), some sandstone beds oil-stained	tidal flat with channel deposits (estuarine environment)	Dina fm.
929.00				CB		≡		Pl, Ch both abund., Sk rare						
.10		∪		CB		≡		Pl, Ch both abund., Sk rare						
.20		∪		CB		≡		Pl common, Sk rare						
.30		∪		CB										
.40	Box 4			CB				Pl common, Sk rare			rubble pieces			
.50		∪		CB		≡		Pl abund., Ch common			rubble pieces			
.60		∪												
.70														
.80		∪		CB		≡		Pl abund., Sk rare			rubble pieces			
.90														
930.00														

WELL : SUNCOR et al. PROVOST LOCATION : 4A-23-36-6W4 GEOLOGIST : Joe Kidston DATE : Jan./03 SHEET 5 OF 8

DEPTH (m)	SAMPLES OR PICS	SEDIMENTARY STRUCTURES	SURFACE DESC	SURFACE INT	LAMINAE GEOMETRY	TRACE FOSSILS	ICHNO-FACIES	NOTES	LITHO-FACIES	DEP. ENVIRON-MENT	NAME OF ROCK UNIT
930.00		∪ ♦	CB		≡	Pl abund., Sk rare	mixed *Skolithos/Cruziana*	'patch' of microcrystalline pyrite ~2 cm x ~2 cm wide	interbedded sandstone and siltstone, lightly to heavily burrowed, silt to fine (J), some sandstone beds oil-stained	tidal flat with channel deposits (estuarine environment)	Dina Fm.
.10		∪			≡	Pl rare, Sk common					
.20											
.30			CB								
		∪	CB		≡	Pl common					
		∪	CB			Sk rare					
.40		∪			≡	Pl common					
			CB								
.50		∪			≡	Pl, Sk both common					
			CB								
.60		∪			≡	Pl common, Sk rare					
.70		∪	CB			Sk rare					
			CB								
.80		∪			≡	Pl common					
			CB								
.90		∪			≡	Pl common					
			CB								
931.00		∪			≡	Pl, Ch both common					
.10			GR								
.20		∪			≡	Pl common, Sk rare					
			CB								
.30		♦	CB		≡			'patch' of microcrystalline pyrite ~3 cm x ~2 cm wide			
.40		∪			≡	Pl, Ch both common, Sk rare					
.50		∪	CB								
.60		∪	CB			Pl rare					
		∪			≡	Pl abund., Sk rare					
.70			CB								
		∪	CB		≡	Sk common		relatively large *Skolithos* traces ≤1.5 cm long			
.80	Box 5	∪	CB		≡	Pl common					
		∪				Pl rare		rubble pieces			
.90			CB								
932.00		∪			≡						

DEPTH (m)	SAMPLES OR PICS	SEDIMENTARY STRUCTURES	GRAIN SIZE	SURFACE DESC	SURFACE INT	LAMINAE GEOMETRY	BIO-TURBATION INDEX	TRACE FOSSILS	ICHNO-FACIES	OIL-STAINED INDEX	NOTES	LITHO-FACIES	DEP. ENVIRON-MENT	NAME OF ROCK UNIT
932.00			CBL PBL GRAN VC C M F VF SILT CLAY				1 2 3 4			1 2 3				
				CB										
.10				CB				Pl rare						
				CB				Pl, Sk both rare						
.20														
				CB				Pl, Sk both rare						
.30				CB										
.40				CB				Pl, Sk both common						
.50														
.60				CB		20°		Pl common, Sk rare						
.70				CB				Pl, Sk both rare	mixed *Skolithos/Cruziana*			interbedded sandstone and siltstone, lightly to heavily burrowed, silt to fine (l), some sandstone beds oil-stained	tidal flat with channel deposits (estuarine environment)	Dina fm.
.80														
.90				CB				Pl common, Sk rare						
933.00				CB				Sk rare						
				GR				Pl, Sk both rare						
.10														
.20								Pl, Sk both rare						
.30														
.40				CB										
.50		HCl		CB				Pl, Sk both rare	*Skolithos*		calcium carbonate cement	$CaCO_3$-cemented, lightly burrowed, sandstone (with rare silty laminae and rip-up clasts), very fine (u) to fine (u)	marine-influenced channel deposits in an estuarine environment	
.60		HCl		CB							calcium carbonate cement			
.70		HCl		CB				Pl, Sk both rare, Pa? rare			silt rip-up clasts at 933.77 m (sub-rounded, ~1 cm x ~1 cm) and 933.49 m (subangular, ~2.5 cm x ~0.5 cm)			
.80											questionable *Palaeophycus* traces may actually be *Skolithos*			
.90		HCl												
934.00														

WELL : SUNCOR et al. PROVOST LOCATION : 4A-23-36-6W4 GEOLOGIST : Joe Kidston DATE : Jan./03 SHEET 7 OF 8

DEPTH (m)	SAMPLES OR PICS	SEDIMENTARY STRUCTURES	SURFACE DESC	SURFACE INT	LAMINAE GEOMETRY	BIO-TURBATION INDEX	TRACE FOSSILS	ICHNO-FACIES	OIL-STAINED INDEX	NOTES	LITHO-FACIES	DEP. ENVIRON-MENT	NAME OF ROCK UNIT
934.00		HCl	CB				Pl, Sk both rare, Pa? rare						
.10													
.20	Box 6	HCl?	CB							reaction to HCl questionable			
.30		HCl	CB				Sk rare, Pa? rare			calcium carbonate cement ripple foresets at ~934.46 m defined by laminae (max ~3 mm wide) dipping by ~22°			
.40													
.50			CB				Pl rare						
.60										relatively clean sandstone			
.70							Pl, Sk both rare, Pa? rare						
.80													
.90			CB										
935.00								*Skolithos*					
.10			CB				Pl rare			'patch' of microcrystalline pyrite ~6 cm long and ~2.5 cm wide			
.20										ripple foresets at 935.16 m defined by laminae (max ~4 mm wide) dipping by ~21° ripple foresets at 935.20 m defined by laminae (max ~3 mm wide) dipping by ~22° (these two sets dip in opposite directions and are separated by ~2 cm of clean sandstone			
.30			GR										
.40			S							scoured bottom surface			
		(missing core)								(missing core)			
.50		HCl	GR							climbing ripple lamination at ~935.50 m (Plate 3) defined by stacked laminae sets (max ~1 cm thick, dipping by ~14°) of ripple laminae (max ~7 mm wide)			
.60													
.70		HCl	GR							calcium carbonate cement			
.80		HCl					Pl, Sk both common, Pa rare			calcium carbonate cement			
.90													
936.00													

GRAIN SIZE: CBL PBL GRAN | VC U L | C U L | M U L | F U L | VF U L | SILT | CLAY

BIO-TURBATION INDEX: 1 2 3 4

OIL-STAINED INDEX: 1 2 3

LITHO-FACIES: $CaCO_3$-cemented, lightly burrowed, sandstone (with rare silty laminae and rip-up clasts), very fine (u) to fine (u)

DEP. ENVIRON-MENT: marine-influenced channel deposits in an estuarine environment

NAME OF ROCK UNIT: Dina fm.

DEPTH (m)	SAMPLES OR PICS	SEDIMENTARY STRUCTURES	GRAIN SIZE (CBL PBL GRAN VC C M F VF SILT CLAY; U L)	SURFACE DESC	SURFACE INT	LAMINAE GEOMETRY	BIO-TURBATION INDEX (1 2 3 4)	TRACE FOSSILS	ICHNO-FACIES	OIL-STAINED INDEX (1 2 3)	NOTES	LITHO-FACIES	DEP. ENVIRON-MENT	NAME OF ROCK UNIT
932.00		∪		CB		15°		Pl abund., Ch common, Sk rare	mixed *Skolithos/Cruziana*			interbedded sandstone and siltstone, lightly to heavily burrowed, silt to fine (l), some sandstone beds oil-stained	tidal flat with channel deposits (estuarine environment)	Dina Fm.
.10		∪				≡		Pl rare						
.20				CB										
.30		(missing core)									(missing core)			
.40		∪				≡		Pl rare						
.50				GR										
.60		HCl									calcium carbonate cement	lightly burrowed, sandstone (with and rip-up clasts), very fine (u) to fine (u)	CaCO$_3$-cemented channel deposits	
.70		HCl				5°		Sk? rare			silty lamina (<1 cm thick) at 932.70 m			
.80														
.90				CB										
		(missing core)									(missing core)			
933.00		HCl				≡			*Skolithos*		calcium carbonate cement	CaCO$_3$-cemented, lightly burrowed, sandstone (with rare silty laminae and rip-up clasts), very fine (u) to fine (u)	marine-influenced channel deposits in an estuarine environment	
.10	TS#3, XRD # 1391										silty lamina (<1 cm thick) at 933.19 m			
.20	end of core at 933.25 m	HCl				4°		Sk? rare						
.30														
.40														
.50														
.60														
.70														
.80														
.90														
934.00														

DEPTH (m)	SAMPLES OR PICS	SEDIMENTARY STRUCTURES	SURFACE DESC	SURFACE INT	LAMINAE GEOMETRY	BIO-TURBATION INDEX	TRACE FOSSILS	ICHNO-FACIES	OIL-STAINED INDEX	NOTES	LITHO-FACIES	DEP. ENVIRON-MENT	NAME OF ROCK UNIT
936.00		HCl	CB										
.10		HCl			20°					calcium carbonate cement ripple foresets at 936.32 m defined by laminae (max ~2 mm wide) dipping by ~19°	$CaCO_3$-cemented, lightly burrowed, sandstone (with rare silty laminae and rip-up clasts), very fine (u) to fine (u)	marine-influenced channel deposits in an estuarine environment	Dina fm.
.20													
.30													
.40		HCl											
.50			CB										
.60			CB		15°								
.70	Box 7	(missing core)								(missing core)			
.80													
.90		HCl						*Skolithos*		calcium carbonate cement			
937.00													
.10			CB										
.20		HCl								calcium carbonate cement			
.30													
.40			CB										
.50		HCl								calcium carbonate cement			
.60	end of core at 937.60 m		CB										
.70													
.80													
.90													
938.00													

APPENDIX F : XRD analyses raw data

Philips Analytical X-Ray B.V. PC-APD, Diffracti

Sample identification: 1391
Data measured at: Jan-28-2003 9:30:00

Diffractometer type: PW1710 BASED
Tube anode: Cu
Generator tension [kV]: 40
Generator current [mA]: 30
Wavelength Alpha1 []: 1.54056
Wavelength Alpha2 []: 1.54439
Intensity ratio (alpha2/alpha1): 0.500
Divergence slit: AUTOMATIC
Irradiated length [mm]: 12
Receiving slit: 0.2
Monochromator used: YES

Start angle [x2i]: 2.000
End angle [x2i]: 72.000
Step size [x2i]: 0.025
Maximum intensity: 6609.690
Time per step [s]: 1.000
Type of scan: CONTINUOUS
Intensities converted to: FIXED

Peak positions defined by: Minimum of 2nd derivative of peak
Minimum peak tip width: 0.00
Maximum peak tip width: 1.00
Peak base width: 2.00
Minimum significance: 0.75
Number of peaks: 45

Angle [x2i]	d-value α_1 []	d-value α_2 []	Peak width [x2i]	Peak int [counts]	Back. int [counts]	Rel. int [%]	Signif.
2.120	41.6381	41.7415	0.300	1076	870	16.3	1.33
20.785	4.2701	4.2807	0.150	1122	49	17.0	10.52
22.980	3.8669	3.8765	0.100	137	42	2.1	1.11
26.560	3.3533	3.3616	0.150	6610	37	100.0	30.81
27.400	3.2524	3.2604	0.100	41	36	0.6	0.96
29.325	3.0431	3.0506	0.200	1197	31	18.1	21.12
31.390	2.8474	2.8545	0.075	32	28	0.5	1.02
32.955	2.7157	2.7225	0.150	41	26	0.6	2.83
35.970	2.4947	2.5009	0.100	272	25	4.1	2.19
36.455	2.4626	2.4687	0.200	471	23	7.1	15.19
38.200	2.3540	2.3599	0.150	17	22	0.3	0.84
39.370	2.2867	2.2924	0.175	666	22	10.1	13.06
40.205	2.2411	2.2467	0.125	190	21	2.9	2.48
42.355	2.1322	2.1375	0.125	467	21	7.1	5.54
42.485	2.1260	2.1313	0.050	228	21	3.4	1.65
43.090	2.0975	2.1027	0.100	207	21	3.1	1.52
44.470	2.0356	2.0407	0.150	10	21	0.2	0.84
45.705	1.9834	1.9883	0.125	400	20	6.1	5.74
45.840	1.9779	1.9828	0.050	174	20	2.6	0.96
47.045	1.9300	1.9348	0.150	69	19	1.0	1.70

File: 1391.DI Jan-28-2003 10:17

Philips Analytical X-Ray B.V. PC-APD, Diffraction software

Angle [x2i]	d-value '1 []	d-value '2 []	Peak width [x2i]	Peak int [counts]	Back. int [counts]	Rel. int [%]	Signif.
47.445	1.9147	1.9194	0.150	286	19	4.3	5.09
48.405	1.8789	1.8836	0.100	219	20	3.3	1.33
48.540	1.8740	1.8787	0.125	190	20	2.9	1.65
50.055	1.8208	1.8253	0.175	610	19	9.2	11.19
54.780	1.6744	1.6785	0.075	350	18	5.3	2.09
54.940	1.6699	1.6740	0.050	166	18	2.5	4.44
55.265	1.6608	1.6649	0.075	88	18	1.3	2.50
56.515	1.6270	1.6310	0.250	25	18	0.4	1.70
57.355	1.6052	1.6091	0.100	112	17	1.7	1.19
59.845	1.5442	1.5480	0.150	471	16	7.1	8.77
60.055	1.5393	1.5431	0.075	243	16	3.7	0.79
60.590	1.5270	1.5308	0.075	71	16	1.1	2.94
60.985	1.5180	1.5218	0.400	29	16	0.4	0.95
61.390	1.5090	1.5127	0.150	28	16	0.4	1.18
62.995	1.4743	1.4780	0.250	20	16	0.3	1.10
63.920	1.4552	1.4588	0.125	100	15	1.5	2.84
64.155	1.4504	1.4540	0.075	76	15	1.1	0.87
64.610	1.4413	1.4449	0.075	53	15	0.8	1.11
65.655	1.4209	1.4244	0.350	40	16	0.6	4.89
67.635	1.3840	1.3875	0.125	286	15	4.3	5.05
68.055	1.3765	1.3799	0.075	303	15	4.6	4.04
68.230	1.3734	1.3768	0.075	388	15	5.9	1.47
68.425	1.3700	1.3734	0.075	125	15	1.9	1.21
69.185	1.3568	1.3601	0.400	15	15	0.2	1.37
70.200	1.3396	1.3429	0.200	18	14	0.3	1.05

Philips Analytical X-Ray B.V. PC-APD, Diffraction software

Sample identification: **999**
Data measured at: Jan-28-2003 10:18:00

Diffractometer type: PW1710 BASED
Tube anode: Cu
Generator tension [kV]: 40
Generator current [mA]: 30
Wavelength Alpha1 []: 1.54056
Wavelength Alpha2 []: 1.54439
Intensity ratio (alpha2/alpha1): 0.500
Divergence slit: AUTOMATIC
Irradiated length [mm]: 12
Receiving slit: 0.2
Monochromator used: YES

Start angle [x2i]: 2.000
End angle [x2i]: 72.000
Step size [x2i]: 0.025
Maximum intensity: 8873.640
Time per step [s]: 1.000
Type of scan: CONTINUOUS
Intensities converted to: FIXED

Peak positions defined by: Minimum of 2nd derivative of peak
Minimum peak tip width: 0.00
Maximum peak tip width: 1.00
Peak base width: 2.00
Minimum significance: 0.75
Number of peaks: 33

Angle [x2i]	d-value '1 []	d-value '2 []	Peak width [x2i]	Peak int [counts]	Back. int [counts]	Rel. int [%]	Signif.
8.750	10.0975	10.1226	0.500	20	104	0.2	0.82
12.270	7.2075	7.2255	0.200	59	83	0.7	0.85
13.410	6.5973	6.6137	0.500	31	76	0.4	0.79
19.865	4.4657	4.4768	0.150	72	58	0.8	1.03
20.830	4.2610	4.2715	0.150	1560	59	17.6	11.00
24.830	3.5829	3.5918	0.200	59	50	0.7	1.20
26.605	3.3477	3.3560	0.175	8874	48	100.0	46.72
28.510	3.1282	3.1360	0.200	9	44	0.1	0.95
29.390	3.0365	3.0441	0.150	44	42	0.5	2.42
32.975	2.7141	2.7209	0.200	32	31	0.4	1.29
34.885	2.5698	2.5761	0.200	46	30	0.5	0.94
36.505	2.4593	2.4655	0.175	1050	29	11.8	16.85
38.340	2.3458	2.3516	0.300	32	28	0.4	0.83
39.425	2.2837	2.2893	0.125	640	28	7.2	5.67
40.215	2.2406	2.2462	0.150	282	27	3.2	5.74
42.405	2.1298	2.1351	0.075	666	26	7.5	1.85
45.745	1.9818	1.9867	0.150	320	26	3.6	6.28
47.405	1.9162	1.9209	0.300	16	24	0.2	1.25
48.420	1.8784	1.8830	0.250	12	23	0.1	0.95
50.080	1.8199	1.8244	0.200	847	21	9.5	17.77

File: 999.DI Jan-28-2003 11:05

Philips Analytical X-Ray B.V. PC-APD, Diffraction software

Angle [x2i]	d-value '1 []	d-value '2 []	Peak width [x2i]	Peak int [counts]	Back. int [counts]	Rel. int [%]	Signif.
54.805	1.6737	1.6778	0.125	289	22	3.3	3.66
55.250	1.6612	1.6654	0.100	123	21	1.4	1.36
56.160	1.6364	1.6405	0.250	34	22	0.4	1.96
57.200	1.6091	1.6131	0.150	26	21	0.3	1.73
59.860	1.5438	1.5477	0.100	1089	22	12.3	6.77
60.040	1.5396	1.5435	0.100	600	22	6.8	2.34
62.295	1.4892	1.4929	0.250	16	22	0.2	0.90
63.935	1.4549	1.4585	0.150	119	22	1.3	3.39
64.160	1.4503	1.4539	0.075	81	22	0.9	1.22
65.735	1.4194	1.4229	0.100	46	21	0.5	1.28
67.680	1.3832	1.3867	0.125	400	23	4.5	4.68
68.085	1.3760	1.3794	0.125	600	23	6.8	2.84
68.275	1.3726	1.3760	0.125	595	24	6.7	3.75

: 1379.DI Jan-28-2003 11:53

Philips Analytical X-Ray B.V. PC-APD, Diffraction software

Sample identification: 1379
Data measured at: Jan-28-2003 11:06:00

Diffractometer type: PW1710 BASED
Tube anode: Cu
Generator tension [kV]: 40
Generator current [mA]: 30
Wavelength Alpha1 []: 1.54056
Wavelength Alpha2 []: 1.54439
Intensity ratio (alpha2/alpha1): 0.500
Divergence slit: AUTOMATIC
Irradiated length [mm]: 12
Receiving slit: 0.2
Monochromator used: YES

Start angle [x2i]: 2.000
End angle [x2i]: 72.000
Step size [x2i]: 0.025
Maximum intensity: 7903.210
Time per step [s]: 1.000
Type of scan: CONTINUOUS
Intensities converted to: FIXED

Peak positions defined by: Minimum of 2nd derivative of peak
Minimum peak tip width: 0.00
Maximum peak tip width: 1.00
Peak base width: 2.00
Minimum significance: 0.75
Number of peaks: 38

Angle [x2i]	d-value '1 []	d-value '2 []	Peak width [x2i]	Peak int [counts]	Back. int [counts]	Rel. int [%]	Signif.
8.370	10.5551	10.5813	0.075	76	104	1.0	0.75
8.810	10.0289	10.0538	0.300	40	102	0.5	0.90
12.380	7.1438	7.1615	0.250	135	90	1.7	2.45
17.860	4.9623	4.9746	0.350	21	62	0.3	0.94
19.835	4.4724	4.4835	0.300	137	62	1.7	2.89
20.890	4.2489	4.2594	0.150	1529	61	19.3	10.00
23.470	3.7873	3.7967	0.150	56	61	0.7	1.14
24.875	3.5765	3.5854	0.100	151	61	1.9	0.85
26.685	3.3379	3.3461	0.225	7903	59	100.0	56.38
29.965	2.9854	2.9928	0.250	18	49	0.2	0.82
33.015	2.7109	2.7176	0.075	48	37	0.6	0.77
34.990	2.5623	2.5687	0.250	125	34	1.6	2.96
36.560	2.4558	2.4619	0.200	408	32	5.2	11.39
37.635	2.3881	2.3940	0.300	44	32	0.6	1.65
38.415	2.3413	2.3472	0.300	76	32	1.0	2.68
39.465	2.2814	2.2871	0.225	445	32	5.6	16.07
40.260	2.2382	2.2438	0.175	246	31	3.1	6.11
40.760	2.2119	2.2174	0.075	32	31	0.4	0.86
42.495	2.1255	2.1308	0.250	350	31	4.4	18.17
45.790	1.9799	1.9849	0.125	228	37	2.9	2.89

File: 1379.DI Jan-28-2003 11:53

Philips Analytical X-Ray B.V. PC-APD, Diffraction software

Angle [x2i]	d-value '1 []	d-value '2 []	Peak width [x2i]	Peak int [counts]	Back. int [counts]	Rel. int [%]	Signif.
50.120	1.8186	1.8231	0.150	812	27	10.3	9.74
50.275	1.8133	1.8178	0.075	384	27	4.9	0.77
50.690	1.7994	1.8039	0.200	36	26	0.5	0.86
54.880	1.6715	1.6757	0.150	250	27	3.2	3.85
55.305	1.6597	1.6638	0.150	135	28	1.7	3.02
56.225	1.6347	1.6388	0.200	34	28	0.4	0.77
57.250	1.6079	1.6118	0.300	22	27	0.3	1.44
59.915	1.5425	1.5464	0.150	502	27	6.3	7.57
60.125	1.5377	1.5415	0.075	250	27	3.2	1.99
61.615	1.5040	1.5077	0.250	28	27	0.4	0.99
62.300	1.4891	1.4928	0.250	44	27	0.6	1.14
62.670	1.4808	1.4844	0.075	42	26	0.5	1.46
64.025	1.4531	1.4567	0.100	114	26	1.4	1.19
65.755	1.4190	1.4225	0.200	27	26	0.3	1.14
67.710	1.3827	1.3861	0.150	324	26	4.1	6.60
68.080	1.3761	1.3795	0.100	400	26	5.1	1.93
68.305	1.3721	1.3755	0.100	449	26	5.7	1.68
70.275	1.3384	1.3417	0.400	11	26	0.1	1.70

Philips Analytical X-Ray B.V. PC-APD, Diffraction software

Sample identification: 1392
Data measured at: Jan-29-2003 14:18:00

Diffractometer type: PW1710 BASED
Tube anode: Cu
Generator tension [kV]: 40
Generator current [mA]: 30
Wavelength Alpha1 []: 1.54056
Wavelength Alpha2 []: 1.54439
Intensity ratio (alpha2/alpha1): 0.500
Divergence slit: AUTOMATIC
Irradiated length [mm]: 12
Receiving slit: 0.2
Monochromator used: YES

Start angle [x2i]: 2.000
End angle [x2i]: 72.000
Step size [x2i]: 0.025
Maximum intensity: 918.0900
Time per step [s]: 1.000
Type of scan: CONTINUOUS
Intensities converted to: FIXED

Peak positions defined by: Minimum of 2nd derivative of peak
Minimum peak tip width: 0.00
Maximum peak tip width: 1.00
Peak base width: 2.00
Minimum significance: 0.75
Number of peaks: 29

Angle [x2i]	d-value '1 []	d-value '2 []	Peak width [x2i]	Peak int [counts]	Back. int [counts]	Rel. int [%]	Signif.
2.275	38.8015	38.8980	0.400	918	676	100.0	0.76
10.965	8.0622	8.0823	0.125	32	83	3.5	0.91
20.930	4.2408	4.2514	0.150	50	41	5.5	1.40
25.965	3.4288	3.4373	0.125	50	29	5.5	0.82
26.635	3.3440	3.3523	0.125	151	28	16.5	1.79
28.590	3.1196	3.1274	0.200	199	25	21.7	6.65
33.060	2.7073	2.7141	0.200	676	18	73.6	13.76
37.120	2.4200	2.4260	0.225	342	14	37.3	11.31
38.900	2.3133	2.3190	0.175	81	14	8.8	4.66
40.785	2.2106	2.2161	0.175	279	11	30.4	6.24
42.495	2.1255	2.1308	0.300	10	10	1.0	1.49
44.070	2.0531	2.0582	0.300	6	8	0.6	0.85
45.875	1.9765	1.9814	0.300	7	8	0.7	1.80
47.460	1.9141	1.9188	0.175	324	8	35.3	6.30
50.095	1.8194	1.8239	0.100	32	8	3.5	0.98
51.960	1.7584	1.7628	0.075	74	7	8.1	1.24
53.235	1.7193	1.7235	0.150	15	7	1.7	0.84
54.115	1.6934	1.6976	0.250	20	7	2.2	2.09
54.790	1.6741	1.6782	0.300	17	7	1.8	2.04
56.290	1.6330	1.6370	0.175	548	7	59.6	7.62

File: 1392.DI Jan-29-2003 15:06

Philips Analytical X-Ray B.V. PC-APD, Diffraction software

Angle [x2i]	d-value '1 []	d-value '2 []	Peak width [x2i]	Peak int [counts]	Back. int [counts]	Rel. int [%]	Signif.
56.465	1.6283	1.6324	0.100	296	7	32.2	1.29
57.720	1.5959	1.5998	0.100	34	7	3.7	0.78
58.990	1.5645	1.5684	0.150	77	7	8.4	2.31
59.975	1.5411	1.5450	0.100	32	7	3.5	1.19
61.705	1.5020	1.5058	0.150	104	6	11.3	3.20
64.295	1.4476	1.4512	0.150	123	6	13.4	2.47
65.165	1.4304	1.4339	0.075	19	6	2.1	0.76
68.205	1.3738	1.3773	0.200	13	6	1.4	1.16
68.635	1.3663	1.3697	0.075	19	6	2.1	1.35

APPENDIX G: Well Logs

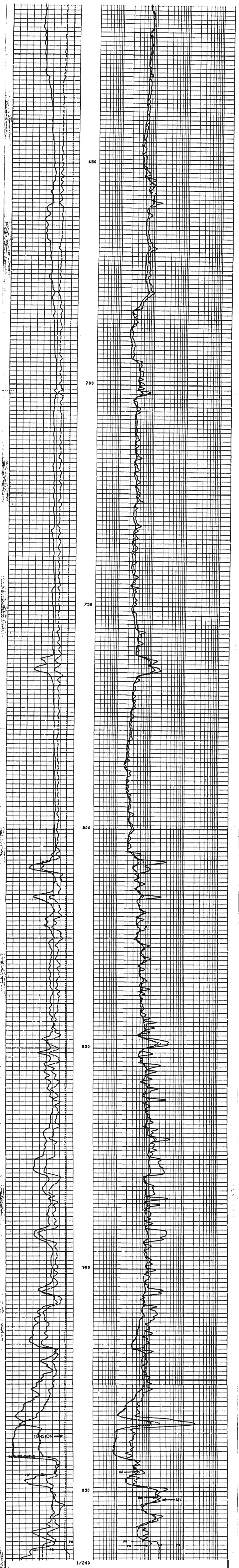
650
700
750
800
850
900
950
TENSION
1/240
CP 30.4
FILE 7
21-SEP-88 04:33
GR
-120.0
30.000
TENS(LB)
20000.
0.0
SP (MV)
-120.0
30.000
ILR (OHMM)
.20000
2000.0
ILM (OHMM)
.20000
2000.0
SFLU(OHMM)
.20000
2000.0
SENSOR MEASURE POINT TO TOOL ZERO
SRAT 10.54 METER
CBLS 10.97 METER
TT2 11.28 METER
TT4 9.83 METER
YT 11.28 METER
AMPL 11.28 METER
CBL 11.28 METER
TT1 10.97 METER
TT3 10.13 METER
TO 11.28 METER

3B

CP 30.4A FILE 18 21-SEP-88 07:29 SANDSTONE

TENS(LB)	20000.	0.0
C2 (MM)	125.00	375.00
BS (MM)	125.00	375.00
C1 (MM)	125.00	375.00
GR (GAPI)	0.0	150.00
DRHO(K/M3)	-250.0	250.00
DPHI	.60000	0.0
NPHI	.60000	0.0
PEF	0.0	10.000

SENSOR MEASURE POINT TO TOOL ZERO

MCAL 8.76 METER GR 15.01 METER

4A

1/240

CP 32.2 FILE 5 05-FEB-1989 14:36

TENS(LBF)	10000.	0.0
ILD (OHMM)	.20000	2000.0
ILM (OHMM)	.20000	2000.0
SFLU(OHMM)	.20000	2000.0
QLRA	-120.0	30.000
SP (MV)	-120.0	30.000

SENSOR MEASURE POINT TO TOOL ZERO

SRAT	12.67 METER	AMPL	13.41 METER
CBFS	13.11 METER	CBL	13.41 METER
TT2	13.41 METER	TT1	13.11 METER
TT4	11.96 METER	TT3	12.27 METER
TT	13.41 METER	TO	13.41 METER
CBSL	13.41 METER	TTSL	13.41 METER
CALI	9.70 METER	GR	19.68 METER
ILM	1.85 METER	ILD	3.02 METER
SP	.76 METER	SFL	2.08 METER
TENS	.76 METER	SPAR	.76 METER
NOIS	.76 METER		

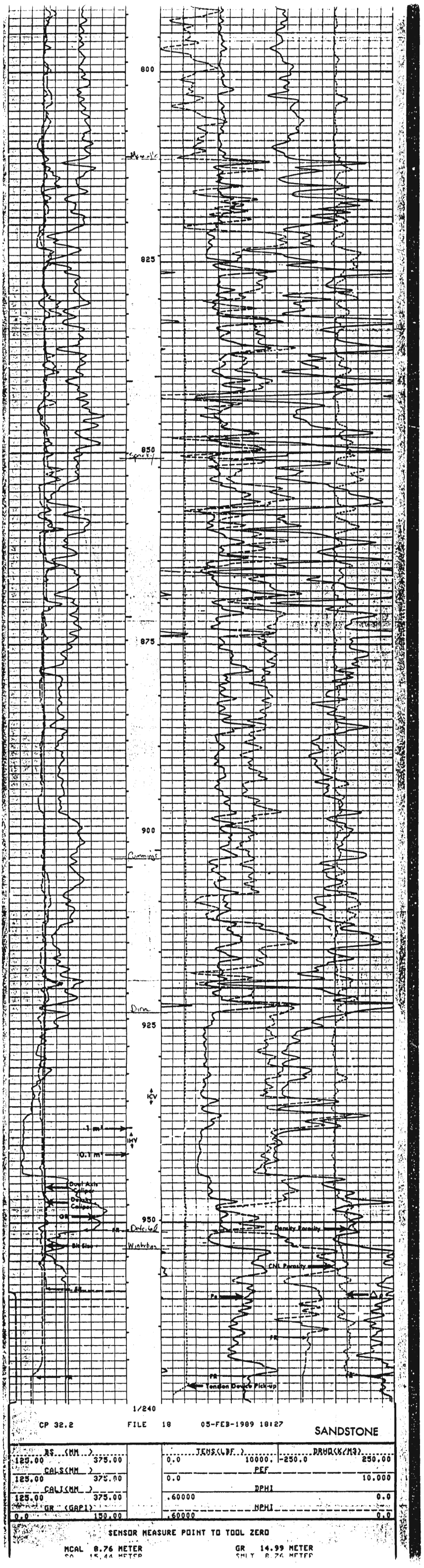
800
825
850
875
900
925
950
Cummings
Dina
Dakota
Winnipeg
ICV
IHV
1 m³
0.1 m³
Short Arm Caliper
Density Caliper
GR
Density Porosity
CNL Porosity
Tendon Device Pick-up
1/240
CP 32.2
FILE 18
05-FEB-1989 18:27
SANDSTONE
BS (MM) 125.00 375.00
CALS(MM) 125.00 375.00
CALI(MM) 125.00 375.00
GR (GAPI) 0.0 150.00
TENS(LBF) 0.0 10000.
PEF 0.0 10.000
DPHI .60000 0.0
NPHI .60000 0.0
DRHO(K/M3) -250.0 250.00
SENSOR MEASURE POINT TO TOOL ZERO
MCAL 8.76 METER
GR 14.99 METER